Analysis of the Structure of Phosphorylase Kinase by Mass Spectrometry

By

Mary Ashley Rimmer

Submitted to the graduate degree program in Biochemistry and Molecular Biology and the Graduate Faculty of the University of Kansas in partial fulfillment of the requirements for the degree of Doctor of Philosophy.

_____
Aron Fenton, Chairperson

_____
Gerald M. Carlson

_____
Antonio Artigues

_____
Thomas Yankee

_____
Michael Washburn

_____
Chad Slawson

Date Defended:
12/6/16

The Dissertation Committee for Mary Ashley Rimmer certifies that this is the approved version of the following dissertation:

Analysis of the Structure of Phosphorylase Kinase by Mass Spectrometry

_____

Aron Fenton, Chairperson

Date approved:

12/6/16

ABSTRACT

Phosphorylase Kinase (PhK) is a large, 1.3 MDa, regulatory enzyme in the glycogenolysis cascade, made up by four copies each of four different subunits, α, β, γ, and δ, giving 325 kDa of unique sequence. Three of the four subunits are regulatory (α, β, and δ), leaving the γ subunit to have the only known catalytic function. Likely due to the size and complexity of PhK, high resolution structures are only available for the smallest subunit, δ, and the catalytic domain of the γ-subunit. The structure of both subunits either in the complex or individually has proved difficult to study. To address some of the questions about the structure of PhK, we have employed three techniques (partial proteolysis, hydrogen/deuterium (H/D) exchange, and chemical footprinting), each in conjunction with mass spectrometry, to elucidate information about the solvent exposure and dynamics of the subunits in complex. In this search for more information about the location and disposition of the subunits in the complex, we have also produced models using a structural prediction program for the largest subunit, α, and of the regulatory domain of the catalytic subunit, γ. These models have been assessed using the H/D exchange results, and were found to be consistent with the experimental exchange data. Taking these three techniques together, we have been able to identify potential regions of inter-subunit contact on the α and γ subunits, identify regions on the α, β, and γ subunits that are surface exposed, even in complex with the other subunits, and produce experimentally consistent models of α and the γ regulatory domain.

ACKNOWLEDGEMENTS

"To learn to read is to light a fire; every syllable that is spelled out is a spark" – Victor Hugo

I first want to thank my Mom, who taught me not only how to read, but to love reading, and my Dad who taught me to search for the why and how behind things that I do; both of which led me here today.

I also want to thank my siblings, Cooper, Ben, Amy, Will, Elliot, Theresa, and Jake, who are always there to remind me not to take myself so seriously, an important thing to remember in graduate school!

I am also deeply grateful to my friends, who were my support system and beautiful people who have always believed in me – even when I didn't believe in myself, for having scientific discussions with me, for reading my papers and listening to presentations, for teaching me how to use software, and for listening to me: Mauricio, Stefanie, Taras, Victor, Phil, Carol, and Courtney. Gracias and Дякую, forever.

Thanks to the Biochemistry department for taking me in and committing to making me a scientist; in particular, Dr. Antonio Artigues and Dr. Maite Villar for fueling my love for mass spectrometry; my committee, Dr. Aron Fenton, Dr. Chad Slawson, Dr. Thomas Yankee, Dr. Antonio Artigues, and Dr. Michael Washburn for encouraging me and guiding me in my research, my career planning, and my soul searching; and Dr. Liskin Swint-Kruse for always being there to answer questions about science, graduate school, and for being such a positive female scientist role model.

Especially thanks to my lab for making me laugh and helping me keep track of all those many, many PhK facts: Jackie Thompson, Dr. Owen Nadeau, and Jessi Sage.

And last, but definitely not least, my eternal gratitude to Dr. Gerald Carlson, for always being my biggest advocate, for always pushing me to be more and do more, and for making me love wine and mac n' cheese.

"So much working, reading, thinking, living to do. A lifetime is not long enough!" –Sylvia Plath

CONTENTS

Abstract ... **iii**

Acknowledgements ... **iv**

Contents ... **vi**

List of Figures ... **ix**

List of Tables ... **x**

List of Abbreviations ... **xi**

Chapter 1 Introduction ... **1**

1.1 Overview ... 1

1.2 Subunit structure and function ... 2

1.2.1 The α and β subunits ... *4*

1.2.2 The δ subunit ... *5*

1.2.3 The γ subunt ... *6*

1.3 Genetics ... 7

1.4 Subunit Interactions ... 8

1.5 Quaternary Structure ... 11

1.6 Regulation and Activation of PhK ... 15

1.7 Changes upon Activation ... 17

1.7.1 Ca^{2+} Activation ... *17*

1.7.2 Phosphorylation Activation ... *19*

1.8 Partial Proteolysis ... 20

1.9 Hydrogen-Deuterium Exchange ... 20

Chapter 2 Analysis of PhK Structure Using Partial Proteolysis and Chemical Footprinting ... **24**

2.1 Introduction 24

2.2 Methods 26

2.2.1 Enzymes and Reagents. *26*

2.2.2 Partial Proteolysis. *27*

2.2.3 Chemical Footprinting. *28*

2.2.4 Mass Spectrometry. *31*

2.3 Results 32

2.3.1 Mapping exposed loops on non-activated PhK. *32*

2.3.2 Comparison of proteolytic cleavage sites in phospho-activated and non-activated PhK. *36*

2.4 Discussion 38

Chapter 3 Analysis of the α Subunit of PhK by Hydrogen-Deuterium Exchange 46

3.1 Introduction 46

3.2 Methods 48

3.2.1 Enzymes and Reagents. *48*

3.2.2 H/D exchange *48*

3.2.3 Tandem MS. *48*

3.2.4 Threading and structure modeling. *50*

3.3 Results and Discussion 50

3.3.1 Full-length Model of the α Subunit. *51*

3.3.2 GHL Domain (1-436). *52*

3.3.3 Domain 2 (437-624). *63*

3.3.4 Variable Domain 1 (625-750). *64*

3.3.5 CBL-1 Domain (751-965). *65*

3.3.6 Variable Domain 2 (966-1066). *66*

3.3.7 CBL-2 Domain (1067-1237). *66*

3.3.8 Structural comparisons of the homologous α and β subunits. *69*

3.4 Conclusions 70

Chapter 4 Analysis of the β and γ Subunits of PhK by Hydrogen-Deuterium Exchange.... 72

4.2 Methods..... 74

4.2.1 Enzymes and reagents...... *74*

4.2.2 H/D exchange..... *74*

4.2.3 Tandem MS. *75*

4.2.4 Data analysis. *75*

4.3 Results and Discussion 76

4.3.1 H/D Exchange of the β Subunit...... *76*

4.3.1.1 Comparison of H/D exchange results with models of β 78

4.3.1.1.1 GHL domain...... *79*

4.3.1.1.2 HRL domain. *83*

4.3.1.2 Site of intrasubunit crosslinking of β. 83

4.3.1.3 Exchange in regions of β surrounding sites previously indicated to be exposed: epitope and phosphorylation site...... **84**

4.3.2 H/D Exchange analysis of the γ subunit. *85*

4.3.2.1 N-Terminal insert: 1-20...... **86**

4.3.2.2 Catalytic domain: 21-298. 86

4.3.2.3 The C-terminal Regulatory Domain (γCRD): 299-386...... **95**

Chapter 5 Conclusions..... 99

5.1 Summary..... 99

5.2 Future Directions and Preliminary Data 101

5.3 Author Contributions 103

References..... 104

Appendix A..... 113

Appendix B..... 118

Appendix C..... 121

LIST OF FIGURES

Figure 1.1 The Subunits of PhK 3

Figure 1.2 CryoEM Reconstruction of PhK and Communication Network 14

Figure 1.3 Hydrogen-Deuterium Exchange Protocol 22

Figure 1.4 Example of Hydrogen-Deuterium Exchange Spectra Over Time 23

Figure 2.1 Proteolytic Patterns of Nonactivated PhK Subunits 33

Figure 2.2 Subunit Docking Site on PhK γ Subunit 45

Figure 3.1 Theoretical 3D Structure of the PhK α subunit 53

Figure 3.2 H/D exchange of the sub-domains of α 55

Figure 3.3 Model of α with H/D Exchange Results 60

Figure 3.4 Representative H/D Exchange Time Course Plots 61

Figure 3.5 The Proposed γ Subunit Binding Site of the Regulatory α Subunit 68

Figure 4.1 Model of β with H/D Exchange Results 77

Figure 4.2 H/D exchange analysis of the γ subunit catalytic domain. 87

Figure 4.3 I-TASSER threading model of the full-length γ-subunit 88

Figure A.1 Quantification of Peptide β1-15 116

Figure A.2 MS/MS of Peptide 1217-1224 of Phospho-Activated PhK subunit 117

Figure B.1 Percent Deuterium Incorporation Curves for α Peptides 118

Figure C.1 Percent Deuterium Incorporation Curves for β Peptides 121

Figure C.2 Percent Deuterium Incorporation Curves for γ Peptides 124

LIST OF TABLES

Table 1.1 Interactions of PhK Subunits 10

Table 2.1 Exposed Regions in Nonactivated and Phospho-Activated PhK[a] 29

Table 2.2 Identification of Carboxymethylated Cys in Non-activated and Phospho-activated PhK 35

Table 3.1 Domains of the α Subunit 54

Table 3.2 Data Consolidated Regions of the α Subunit 56

Table 4.1 Data Consolidated Regions of the β Subunit 80

Table 4.2 Data Consolidated Regions of the γ Subunit 91

Table A.1 Complete List of Partial Proteolysis Peptides 113

LIST OF ABBREVIATIONS

Ch, chymotrypsin; EM, electron microscopy; Fi, ficin; KC, endoproteinase LysC; mAb, monoclonal antibody; MS, mass spectrometer, -try, -tric; PhK, phosphorylase kinase; PKA, cAMP-dependent protein kinase; RC, endoproteinase ArgC; Th, thermolysin; Tr, trypsin; V8, protease V8; CaM, calmodulin; H/D, hydrogen/deuterium; TFA, trifluoroacetic acid; GP, glycogen phosphorylase; BKNR, β-karyopherin nuclear transport receptor family; CBL, calcineurin B-like; GH, glycosyl hydrolase; GHL, glycosyl hydrolase-like; IBL, importin α/β-like; HRL, Huntington-elongation-A subunit TOR (HEAT)-repeat like; CBD, CaM-binding domain; DAPK, death-associated protein kinase; CaMK, CaM-dependent protein kinase; PDB, Protein Data Bank.

Chapter 1
INTRODUCTION

1.1 Overview

Phosphorylation is an important type of cellular regulation involved in almost every cellular process, and is controlled by one of the largest protein families: protein kinases. There are two types of protein kinases, named after the substrate target: Ser/Thr and Tyr kinases;[1] however, there is a large amount of sequence conservation amongst all protein kinases, particularly in the catalytic region.

The first protein kinase to be purified and characterized was phosphorylase kinase (PhK; E.C. 2.7.1.38), a Ser/Thr protein kinase and one of the largest and most structurally complex protein kinases known.[2] PhK is made up of four copies each of four different subunits (α, β, γ, and δ), giving it an overall mass of 1.3 MDa (Figure 1.1). PhK is tightly regulated, both in the glycogenolysis cascade and within the complex itself, with three out of the four subunits in PhK being regulatory. PhK is regulated by diverse biological signals. In skeletal muscle, which will be the focus of this dissertation, PhK is coupled to muscle contraction through Ca^{2+} ions. Ca^{2+} binds to homologous subunits in both PhK and the troponin complex, activating both glycogenolysis and muscle contraction.[3] PhK is phosphorylated and activated by cAMP-dependent protein kinase (PKA), and then phosphorylates Ser14 on glycogen phosphorylase (GP) in the presence of Ca^{2+}, leading to the breakdown of glycogen to form glucose-1-phosphate.[2] Despite this large emphasis on regulation, PhK has only one currently known function, and only one biological substrate: GP, which is also activated only by PhK. Additionally, PhK is one of only three enzymes in muscle that is solely devoted to glycogen breakdown. This extreme specificity is highly unusual for protein kinases, although it is but one of the many unusual aspects of PhK.

PhK was first, and still predominately is, purified from rabbit fast-twitch skeletal muscle. This isoform is the most well characterized and will be the isoform discussed in this dissertation unless otherwise noted.

1.2 Subunit structure and function

Regulation of PhK has been studied extensively; however, little is known about its structure and the effect of activation on that structure. This is due to both the size and complexity of the complex, and its tendency to aggregate under many conditions. It is not possible to isolate the three largest subunits intact, or to reconstitute the hexadecamer from individual subunits. The established baculovirus system for producing PhK has a poor yield, and it is unknown if the correct post-translational modifications (PTMs) are included; therefore, the majority of protein studied must be purified intact, from rabbits. Because of these difficulties, studying PhK – in particular, its structure – remains very challenging, as many methods of structural studies typically used, such as NMR and X-ray crystallography, are not amenable to studying PhK. However, a variety of other methods have been employed, that have been useful in elucidating information about the structure of PhK, both of the complex and its individual subunits. Many of the methods that have been employed are not physiological or do not study the individual subunits in the context of the intact protein (e.g., two-hybrids and synthetic peptide binding studies). So while they provide information concerning the structure and function of certain subunits or regions and can guide other studies, full analysis of the intact complex under physiological conditions is still needed.

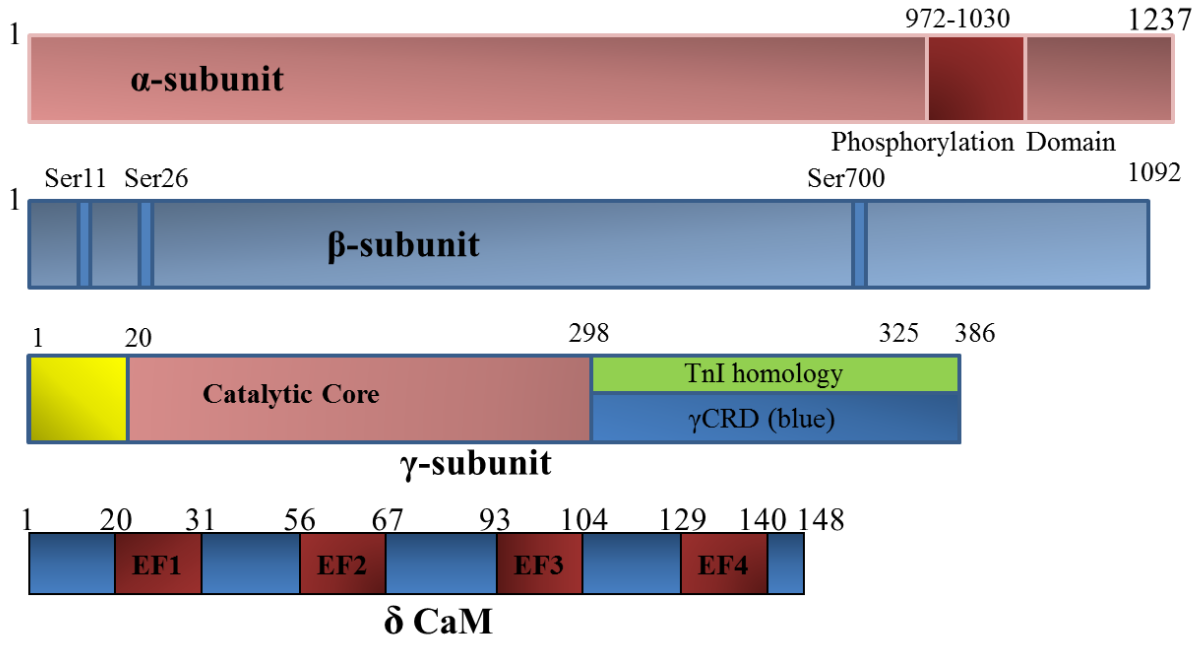

Figure 1.1 The Subunits of PhK

1.2.1 The α and β subunits

The two largest subunits in PhK, α and β, are regulatory. The primary form of α-subunit is made up of 1237 amino acids with a molecular mass of 138 kDa,[4] and the primary form of β of 1093 amino acids with a molecular mass of 125 kDa.[4] They are largely homologous, with 38% identity and 61% similarity, although the α subunit contains two regions that are unique. The β N-terminal region is also unique from α.[4] Activation of the complex by PKA occurs through phosphorylation on the β-subunit first, followed by phosphorylation on α, on regulatory phosphorylatable serines located in each of their respective unique regions.[5] Both subunits have been shown to have a glycoside hydrolase-like (GHL) domain,[6] which has been used to model the structures of both subunits,[7, 8] although the biological relevance of this domain is still being explored.[9] Similarly, both the α and β subunits have calcineurin B-like (CBL) domains.[10] CBL proteins are typically involved in regulation, but the role and physiological relevance of the CBL domains in PhK are still unknown. Epitopes for monoclonal antibodies (mAb) for each subunit have been determined (in α within the region of 1132-1237[11] and in β of 704-815[12, 13]), and have been useful in identifying the approximate subunit locations in the complex.[11, 12]

Farnesylation is a PTM of an isoprenyl group to a Cys at the C-terminal end of some proteins. This modification has been found on both the α and β subunits of PhK.[14] The motif for this isoprenylation is known as a CaaX box: Cys, two aliphatic amino acids, and a variable amino acid.[15] The Cys is farnesylated after translation, and the three terminal amino acids are typically cleaved, followed by carboxymethylation of the exposed Cys. Both the α and β subunits contain this motif, CAMQ and CLVS, respectively, and have been reported to be farnesylated; however, in the case of PhK, there is no cleavage event removing the terminal three residues, or the subsequent carboxymethylation.[14] Additionally, while farnesylation most commonly anchors

proteins to membranes, PhK, despite having the potential for eight farnesyl groups per complex, still purifies as water soluble. As such, the physiological function, and whether these subunits are in fact typically farnesylated, is still not understood. Additional indications that these subunits are not always, or perhaps even not often, farnesylated, was found through chemical footprinting studies on the intact complex, and are explained in detail in Chapter 2.[16]

Along with these features that are common between the two largest regulatory subunits, β has several unique aspects. While the N-terminus of α is unblocked, the β subunit is modified on its N-terminus by acetylation.[4] The unique N-terminal 31 residues of β make up its regulatory domain, where the main phosphorylatable Ser26 is located,[17] along with one of the secondary phosphorylatable sites, Ser11.[4, 13] While there is no crystal structure for either of the large regulatory subunits, a predicted structure has been generated for the β subunit, using threading, chemical crosslinking, mass spectrometry, and *ab initio* techniques,[8] and in Chapter 3 we have now modeled the α-subunit as well.

1.2.2 The δ subunit

The third regulatory subunit, δ, is the smallest subunit, with only 148 amino acids and a molecular mass of 16.7 kDa.[18] It is calmodulin (CaM); so, there are many crystal and NMR structures available for δ. What conformation δ adopts in the complex is still unknown, however. This subunit provides the Ca^{2+}-sensitivity of PhK, binding three molecules of Ca^{2+} per subunit, in three of its four EF hand domains, with the third domain forming a salt bridge with the γ-subunit.[3] Unlike CaM, which dissociates from CaM binding proteins in the absence of Ca^{2+}, the CaM subunit, δ, remains an integral part of PhK at all times, and can only be dissociated by the presence of urea with a Ca^{2+} chelator.[19] Like β, the N-terminus of δ is acetylated, and it has been

suggested through proteolysis studies that δ is protected from digestion in the complex. PhK is also able to bind extrinsic CaM in the presence of Ca^{2+}, further activating PhK.[20]

1.2.3 The γ subunt

The γ subunit is the catalytic subunit, with 386 amino acids giving it a molecular mass of 45 kDa.[21] Much more is known about the structure of this subunit, because of both its homology with other protein kinases and because the crystal structure of its catalytic domain (1-298) has been solved.[22] This catalytic domain makes up the first three-quarters of the protein, and is homologous with all other protein kinases, particularly PKA.[22] The last 88 residues of γ make up the regulatory domain (CRD) and have been shown to interact with the three other subunits, which puts physical constraints on γ, keeping it in the non-activated conformation.[13] The CRD has not been crystalized, although a predicted structure using I-TASSER has been modeled and is shown here in Chapter 4; however, it has not been as well characterized.

The catalytic domain of γ has a typical bilobal protein kinase structure, but contains four inserts that are not present in the homologous PKA: the first 20 residues, an acidic hexamer from 60-65, a hydrophilic hexamer from 196-201, and an acidic tetramer from 252-255.[22] Because these inserts are unique to γ, they most likely have functions that are unique to PhK and to γ itself. One possible function of these inserts is to communicate with the three other subunits, since PKA functions as a monomer, whereas γ functions in a complex, and the inserts are located on the periphery of the catalytic domain of γ.[22] The first 13 residues of γ that make up most of insert one lack electron density in the crystal structure, suggesting they are highly mobile. There is also a lack of density for insert two, suggesting it is part of an external loop.[22] This was further confirmed using both partial proteolysis (Chapter 2) and hydrogen-deuterium (H/D) exchange

(Chapter 4). Additionally, a mAb to the γ subunit has been developed, with the epitope lying in the C-terminus, residues 277-290.[12]

Although the crystal structure of the catalytic domain of γ has been solved, the γ structure is far from complete, lacking almost 100 residues, and it is not in complex. Therefore, it is possible that γ exists and behaves differently when complexed with the other three subunits. As such, modeling the remaining domain of γ and studying the dynamics and features of the subunit's structure in the intact complex is a key advancement in this dissertation (Chapter 4).

1.3 Genetics

Because the majority of PhK studies are done on the rabbit skeletal muscle, it is important to note that the rabbit, rat and human isoforms of each subunit share more than 90% identical amino acid sequences.

The α subunit is encoded by two different genes (α1 and α2),[23] but also has at least one known splice variant on α1 that is the predominant isoform found in slow twitch and cardiac muscle.[24] This isoform is known as α′ and has a deleted region of 59 residues compared to the fast twitch muscle α isoform.[24] Due to the tissue specific locations of these two isoforms, it is likely that this 59-residue deletion plays a role in tissue-specific regulation. Encoded by a separate gene there is also a liver isoform of the α subunit, which differs from the fast twitch muscle isoform: differences are located at regions in α that also differ from the β subunit.[24]

The β subunit is encoded by a single gene, although there are several splice variants that affect two different regions, creating tissue specific isoforms.[24] The γ subunit is encoded by two genes, and has at least two known isoforms: one expressed in both cardiac and skeletal muscle tissues,[25, 26] and one in the testis and liver.[27-29] The δ subunit is encoded by three different genes, although they all encode identical protein.[30] Isoforms of PhK other than those found in the fast

twitch muscle have not been well studied, meaning the majority of information on both regulation and structure available are for the fast twitch muscle isoform. As will be noted in this dissertation, several regions that present interesting results are isoform-specific regions, suggesting that these differences are important and play unique roles among the different tissues and species.

1.4 Subunit Interactions

With four copies each of four different subunits, the interactions within the complex are difficult to determine. Multiple techniques have been used to explore the quaternary structure of PhK, providing information about direct binding or associations of the subunits. Different techniques and applications of these techniques allow studies of PhK structure at different levels of resolution.

The lowest resolution data showing subunit interactions is obtained via crosslinking (a technique that uses small multifunctional reagents that are capable of covalently coupling protein side chains), yeast two-hybrid studies, and peptide binding. Results from studies on PhK employing any of the above techniques can indicate simply that two subunits are interacting or are proximal, but do not give us any indication about where the sites of interactions are. Summarized in Table 1.1 are the different interactions of PhK subunits that have been detected by low resolution techniques.

These same techniques with more detailed analysis can provide slightly higher resolution data by identifying the regions, but still not the exact residues, that are interacting. These types of experiments have shown that the α subunit N-terminal region binds β,[31] and the C-terminal region of α binds γ.[32] Yeast two-hybrid studies also narrowed the regions of α that self-associate to residues 833-854 and 1015-1237,[33] although this interaction could be from either two α

subunits interacting, or interactions within a single subunit. CaM binding domains have also been identified on α,[20] although these are believed to bind exogenous CaM, rather than δ.[20]

Using crosslinking in conjunction with mass spectrometry (MS) and search engine technologies, several individual residues on each subunit that interact with other residues have been identified. These interactions include β Arg18 crosslinking to the γ Lys303,[13] and δ Asp93 to γ Lys325.[3] All of these techniques taken together show that the interactions among α and β with γ take place within all three of their respective regulatory domains.

Another technique that has been used to study PhK is native MS. This technique permits the transmission of large, partially solvated, near native-like proteins, allowing the intact protein structure to be analyzed. Using either collision induced dissociation (CID) or solution disruption (denaturants prior to injection) to dissociate the PhK complex into sub-complexes and single subunits, it is possible to construct subunit interaction maps. Using native MS on PhK, Nadeau et al.[8] demonstrated that all subunits within the αβγδ protomer interact with one another, and by cross-linking and two-hybrid analyses that the regulatory α, β, and δ subunits appear to interact within the γCRD.[13]

Table 1.1 Interactions of PhK Subunits

Species	Cross-linking	Peptide binding	Two-hybrid	Native MS	Reference
αα	x		x		Nadeau *et al.*[34]
αβ	x			x	Ayers *et al.*[35]
αγ	x		x	x	Rice *et al.*[32] Nadeau *et al.*[36] Ayers *et al.*[35]
αδ	x			x	Jeyasingham *et al.*[3] Nadeau *et al.*[36]
ββ	x	x		x	Ayers *et al.*[35] Fitzgerald *et al.*[37]
βγ	x	x		x	Wilkinson *et al.*[12] Nadeau *et al.*[13]
βδ	x			x	Nadeau *et al.*[36, 38] Ayers *et al.*[35]
γδ	x	x	x	x	Jeyasingham *et al.*[3]

1.5 Quaternary Structure

In the first electron microscopy (EM) images of PhK from 1974, negatively stained particles showed a butterfly like structure: two "wings" connected by a bridge.[39] In 1985, also with negatively stained particles, a "chalice" form was observed, again containing two sections, termed the "stem" and "cup" in the chalice, though in these images the two sections lacked a connection between them.[40] A year later, the Carlson lab published EM structures of PhK, indicating a bilobal structure with two sections linked back to back by two narrow bridges, as opposed to the single bridge previously observed.[41] This "butterfly" form made up the majority of the structures observed by EM, and the "chalice" form only made up 4% of the structures. Additionally, there was a clear connection between the stem and cup in the chalice images. Scanning transmission EM was also used by the Carlson lab to study unstained images of PhK, and these were used to determine measurements for the complex: the lobes measured 16 by 17 nm and the bridges 1.5 by 3 nm.[41] In the same paper, it was also shown that selective proteolysis of the β subunit resulted in half-sized particles, which indicates that the integrity of the β subunit may be important for maintaining the butterfly structure, a hypothesis that was later confirmed by the same lab. These images indicate that the structure of PhK is likely a dimer of octamers. Another technique used to image PhK was scanning tunneling microscopy, which further confirmed the butterfly pattern with a bridge between the two wings.[42]

Later, a 3D plaster-of-Paris model of PhK was constructed from the EM images.[43] Tilting the model in different orientations, four views of the 3D structure were published, showing four identical αβγδ protomers that associate with D2 symmetry to form the two lobes. The two protomers are in a head-to-head arrangement to make up each symmetrical lobe,[11] with the lobes inverted and placed perpendicular to each other. The four protomers approximate a tetrahedron,

and each lobe of the model corresponds to a wing of the butterfly projection. This deduced model both accounted for and predicted all of the observed microscopic images. Additionally, this model of PhK contained four bridges, even though only two were seen in most EM images, because this was the most logical for the model.

Next, in 2002, a 3D reconstruction of PhK using more than 11,000 negatively stained particles in multiple orientations was published; an image that corroborated the previously deduced model, except for the number of bridges.[44] Because of the potential deformation from negative staining and the possibility of staining artifacts, cryoEM of frozen hydrated molecules was also used to image PhK. Using approximately 6000 particles, these cryoEM images were used to reconstruct a 3D model of the PhK complex (Figure 1.2).[45] When comparing the cryoEM image and the negatively stained image there were three important differences: 1) a dihedral angle between the two lobes of 90° instead of 68°, which confirms the tetrahedral model, 2) a compact rather than extended structure for the lobes, and 3) the four bridges that had been deduced were confirmed in these images. The four bridges were further confirmed using small angle X-Ray scattering (SAXS) - a technique that allows determination of the general shape of the complex.[46]

Using this information, it is possible to begin to hypothesize how the different subunits are situated within the complex. A mAb to the α subunit C-terminus was developed, and using undecagold labeled Fab fragments, the α subunit was visualized in scanning transmission EM of unstained PhK.[11] These images suggested a symmetrical arrangement of the carboxyl termini of the α subunits, indicating that the α-subunits are packed in a "head-to-head" arrangement within a lobe, as the C-termini of the α-subunits are all clustered on the wingtips of the lobes within the complex.

Using the mAbs for β and γ in conjunction with transmission EM, these subunits were labeled and their location identified on the EM image.[12] These images were then mapped onto the previously described plaster-of-Paris 3D model of PhK, providing locations for β and γ as well. Both the anti-γ and anti-β antibodies bind within the interior of the PhK molecule between its two lobes. The β subunit appears to be at, or near, the inter-lobal bridges, while γ is slightly further out and more central on the lobe face. Additionally, using native MS as was described earlier, Nadeau et al.[8, 47] found that all of the β-subunits interact, existing as a β_4 core. Using this information, along with intramolecular cross-linking of β, exposure of known surface accessible regions, phosphorylation sites, and the mAb epitope, they docked β into the cryoEM envelope of the PhK complex. They found that the only place in which the β-subunits fit as a β_4 complex was at the bridges and interior faces of both lobes. This explained the previous finding that proteolysis of β resulted in cleaving the PhK complex in half.

The δ subunit is different from the other three subunits, in that under conditions of low concentrations of urea in the absence of Ca^{2+}, a small percentage of δ can be exchanged for exogenous CaM.[19] Therefore, in order to visualize the location of this smallest subunit, mutated CaM to contain Cys was derivatized with Nanogold, and exchanged for δ.[48] This allowed the location of δ to be identified as being near the center of the molecule, just distal to the interlobal bridges, near the base of the catalytic core of γ, corroborating the previous data indicating that γ and δ interact.[32]

All of this information was combined and added to a model derived from cryoEM reconstructions (Figure 1.2) showing that the three regulatory subunits encircle the catalytic domain of γ, which is in keeping with the known interactions and regulatory mechanisms.

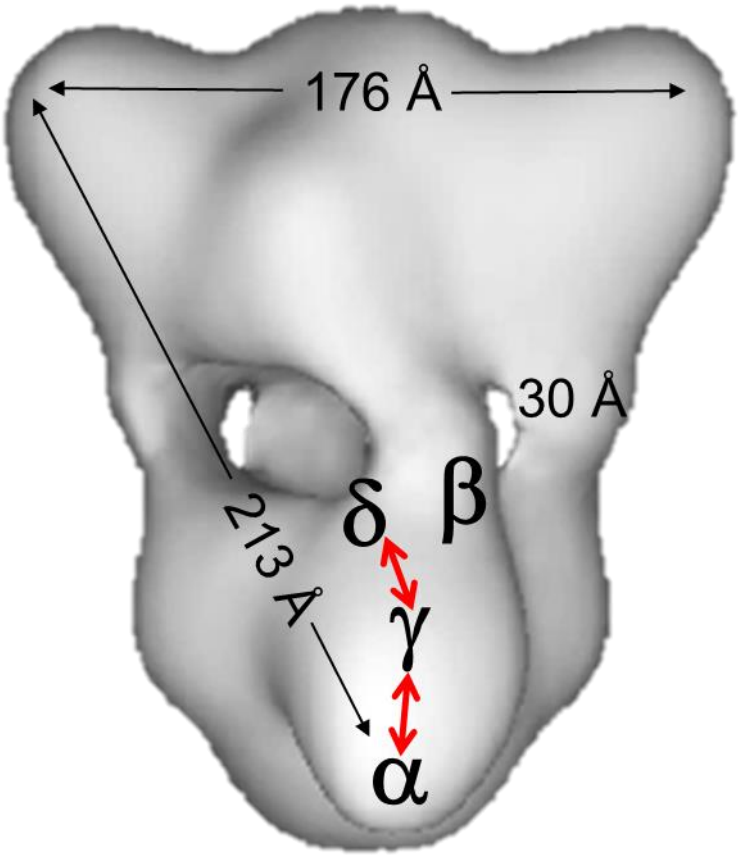

Figure 1.2 CryoEM Reconstruction of PhK and Communication Network

Modified from Nadeau et al.[45]

1.6 Regulation and Activation of PhK

Despite the seemingly simple and singular catalytic function of PhK known so far, the regulation of PhK is more complex. Three of the subunits, α, β, and δ, are regulatory and make up 86% of the complex's mass, with only γ having the known kinase catalytic role. Activation can occur by different effectors, both physiological and observed *in vitro*; but regardless of the method of activation, Ca^{2+} is absolutely required for activity.[49] As mentioned earlier, this Ca^{2+} sensitivity is through the δ subunit, where Ca^{2+} binds three of the four Ca^{2+} binding sites per δ.[50] Ca^{2+} activation is known to be physiological: in resting skeletal muscle, the Ca^{2+} intracellular concentration is 10-100 nM and rises to 1-10 μM upon stimulation of muscle contraction.[51, 52] These changes are in the appropriate range to allosterically regulate PhK. It has also been proposed that the binding of Ca^{2+} to δ results in a release of inhibition on the γ subunit, causing a conformational shift in the C-terminal domain of γ from an "off" to "on" formation, allowing γ to be activated and phosphorylate GP.[53]

This requirement for Ca^{2+} couples energy production glycogenolysis with muscle contraction in what is called the "excitation-contraction-energy production triad."[54] More specifically, the binding of Ca^{2+} to both the TnC subunit of the troponin complex and to the CaM (δ) subunit of the PhK complex – which are homologs – simultaneously triggers contraction and glyocgenolysis. Just as TnC and δ are homologous, so are TnI and γ. Multiple residues in the γCRD are the same as the inhibitory region of TnI, that binds to TnC and actin, depending on the concentration of free Ca^{2+}. Due to these similarities and the coupling of the two functions via Ca^{2+}, the ability to replace each other was investigated. TnC can replace its homologous subunit (δ) functionally, and activate isolated γ, and γ even binds TnC with a similar affinity as it does δ (CaM).[55] Additionally, it has been shown that γ can substitute for TnI in inhibiting actomyosin

ATPase,[55] and it has been suggested that the α subunit is functionally similar to actin. It was also shown that the γ subunit interacts with δ through a salt bridge involving this TnI-like domain in γ.[3] The residues in TnI that are homologous with the γCRD are encoded by a single exon. The location of this exon and the pattern of sequence similarity suggests co-evolution in skeletal muscle of Ca^{2+} regulation of both contraction and energy production.[3] This regulation is via the same recognition motif in TnI and the γ subunit in the two different complexes, involving their interactions with the homologous Ca^{2+}-binding proteins TnC and δ.[3]

Physiologically, PhK is also activated through phosphorylation by PKA on at least two subunits, α and β.[2] The phosphorylation of β occurs first at a rate 5-10 times greater than that of α, and this is the key activating step.[5] The most important phosphorylatable serine on β is Ser26,[17] although Ser11 and Ser700 are endogenously phosphorylated as well.[24] Phosphorylation of α amplifies the activity caused by β phosphorylation, but does not activate the complex itself.[5] The majority of phosphorylation sites in α is clustered in one area (972-1030), termed the phosphorylatable domain, where there are at least seven sites of phosphorylation. Ca^{2+} is required for the activity of phosphorylated PhK to be expressed, although the K_a for Ca^{2+} to activate is reduced $1/15^{th}$-$1/20^{th}$ by PKA phosphorylation of PhK.[49] This phosphorylation relieves inhibition placed on the γ subunit by the α and β subunits, allowing the kinase activity of γ to be expressed, similar to the release of inhibition by δ in the presence of Ca^{2+}.

In vitro, PhK can also be activated by an increase of pH from 6.8-8.2,[2, 56] and this is due to deprotonation of either the α or β subunits. The activation of PhK is measured using this in vitro alkaline pH activation method. At pH 6.8, the activity of PhK, i.e., its ability to phosphorylate its endogenous substrate, GP, is low, and at pH 8.2 it is far more active. However, PhK is also activated at pH 6.8 when phosphorylated. As such, the activation status of PhK can

be calculated by its pH 6.8 to 8.2 activity ratio. Non-activated PhK has a ratio of ~0.01-0.05 and when activated, by any means, this activity ratio increases to ~0.4-0.9.[56]

1.7 Changes upon Activation

In 1981, a paper by the Carlson lab was published in which they observed that there was a synergistic activation of PhK by Ca^{2+} and Mg^{2+}. Preincubation with Ca^{2+} and Mg^{2+} resulted in the abolition of the lag in autophosphorylation activation.[57] They proposed a conformational change induced by Ca^{2+} and Mg^{2+} that brings the complex into a favorable conformation for phosphorylation. Direct evidence for conformational changes induced by the activation of PhK has since been found, as will be described in the next two sections.

1.7.1 Ca^{2+} Activation

Ca^{2+} is the predominate and obligate activator of PhK. Furthermore, there is more structural information for conformational changes caused by this activator than any others. The first attempts to study structural changes were to use chemical crosslinking. The predominate observation was that Ca^{2+} causes an increase in the crosslinking of the α and γ subunits.[32, 35, 53] This was shown using formaldehyde, a near-zero-length crosslinker. This change in α-γ crosslinking by the addition of Ca^{2+} was also observed using a variety of different crosslinkers. Additionally, changes in α-δ, β-δ, and other subunit combinations were also observed by crosslinking in the presence of Ca^{2+}.[53]

Other techniques besides crosslinking were used to identify changes to PhK in the presence of Ca^{2+}. These include chemical footprinting,[53] which identified increased accessibility to γ; FRET, showing that Ca^{2+} perturbs δ;[58] and a variety of techniques demonstrating that the

stability of PhK is affected by Ca^{2+}.[54] All of these biochemical techniques point towards a Ca^{2+}-dependent network of communications among α,γ, and δ.

In reconstructions of PhK from 2D images of negatively stained PhK of the Ca^{2+} activated and non-activated complex, it is observed that the lobe tips, shown earlier to be made up of α, shift, and that the C-terminus of α collapses down into the lobe in the presence of Ca^{2+}.[44] Additionally, the bridges were affected by activation,[44] becoming more compact and going from parallel to oblique – final effects on the β subunit.[8] These changes to the β subunit were observed in the phosphorylated conformer as well, along with changes affecting the α and γ subunits. This suggests that Ca^{2+} and phosphorylation activation of PhK share many structural changes.[53]

Due to the complex being immobilized in EM on a grid after Ca^{2+} activation, these changes may not necessarily capture all that is going on in solution, although they confirm that changes do occur. In order to determine if these changes occur in solution as well, Ca^{2+}-activated and non-activated PhK were analyzed using SAXS.[46] SAXS allows for the determination of the general shape of the complex and for the detection of gross changes in the molecule, but in solution. These data also indicated that the bridges of the complex come closer upon activation, suggesting a rotation between the lobes.

When all the structural activation data are considered together and the biochemical data are mapped, structural changes are indicated among α, γ, and δ that correspond to the actual changes in density in the EM structures that were observed in the regions corresponding to these subunits.[44] These changes indicate a communication network: binding of Ca^{2+} to the δ subunit causes the C-terminus of α to meld into the complex, and these changes go down from the tip of the wings. It is known that the phosphorylation of α changes the affinity of δ for Ca^{2+}[59] which indicates that the changes are also going back down through the lobes, and based on the

interactions previously discovered, all of these changes are being mediated by the γCRD foming a communication network that goes both ways (Figure 1.2).

1.7.2 Phosphorylation Activation

Historically, the first evidence of conformational changes induced by phosphorylation was by crosslinking, where β-β dimers were detected by crosslinking in only the activated form of PhK.[37] More changes have been observed since then, using partial proteolysis, mAb binding studies, and additional crosslinking studies. Corroborating these changes to β and its interactions with other subunits are more biophysical techniques, most recently native MS.[47] When PhK is analyzed by native MS, it remains intact, with just minor amounts of smaller peaks appearing. These represent minor complexes. But when the phosphorylated complex is analyzed under identical conditions, subcomplexes containing multiple copies of the β subunit are observed, demonstrating increased association of β. Further, the phosphorylated complex becomes less stable upon phosphorylation. Crosslinking in combination with peptide mimetics has shown that the N-terminus of β binds to the C-terminus of γ,[13] and two-hybrid studies have shown that this interaction is disrupted by phosphorylation of the β subunit.[13]

Taking all of this information together, we can hypothesize locations, interactions, and conformational changes in the subunits of PhK. However, a more global analysis of the complex in solution that can identify exact residues and regions affected is still necessary in order to integrate all of the models, sequence information, and chemical information together. In order to do this, three separate MS-based techniques that allowed analysis or labeling of the entire complex, while still allowing for peptide or residue level results, were used: partial proteolysis

and H/D exchange, along with chemical footprinting performed by another student.

1.8 Partial Proteolysis

Partial proteolysis is a technique that is used to identify solvent exposed loops in a protein. Higher order protein structure inhibits proteases from reaching cleavage sites, regardless of the protease specificity for the primary structure, by either burial of the residues within the structure or by stereochemical constraints.[60] As such, when a protease is allowed but brief access to a protein, only regions that are exposed, accessible, and able to conform to the protease active site will be cleaved. Therefore, by introducing the protease to the protein for only a brief amount of time, one can identify those surface exposed regions in the complex. Coupling this technique with MS allows identification of the cleaved peptide – the loop – quickly and accurately.[61] We performed this technique on both the non-activated and the phospho-activated conformers of PhK. This approach identified multiple exposed loops in three of the four subunits (α, β, and γ), as well as several new loops that were exposed upon activation of the complex. For whatever reason, the δ subunit was not observed in these studies. Further exploration of this subunit will be necessary for any further explanation.

1.9 Hydrogen-Deuterium Exchange

The second technique used was H/D exchange. Hydrogens in a protein undergo continual exchange on the main and side chain groups, which are not noticeable until the hydrogen is replaced for a heavier isotope.[62-64] By incubating a protein in D_2O, rather than H_2O, the hydrogens exchange for deuterium, allowing the exchange to be measured easily by MS through the 1 Da mass shift (Figure 1.3 and Figure 1.4). The hydrogens on the amide backbone are the ones that are measurable, as the ones on the side chains are too highly exchangeable. Hydrogen-

bonding and burial within the protein or complex will occlude the hydrogens from exchanging.[65, 66] Exchange of amide hydrogens to deuterium can be used as a measure of solvent exposure[67], dynamics[68], and secondary structure.[69] For global analysis, H/D exchange allows labeling of the entire protein, yet peptide to residue resolution analysis. This technique is especially useful for large complexes such as PhK, as there is no size limit for the proteins studied. With larger protein, however, the data sets will be larger, and co-eluting peptides will be more common, making H/D exchange protocol set up and the data analysis the challenging steps. Despite these challenges, good coverage for three of the four subunits of PhK were obtained. For both the α and γ subunits (Chapters 3 and 4), H/D exchange was used to analyze homology models, and for the α, β, and γ subunits analysis of solvent exposure and dynamics was performed.

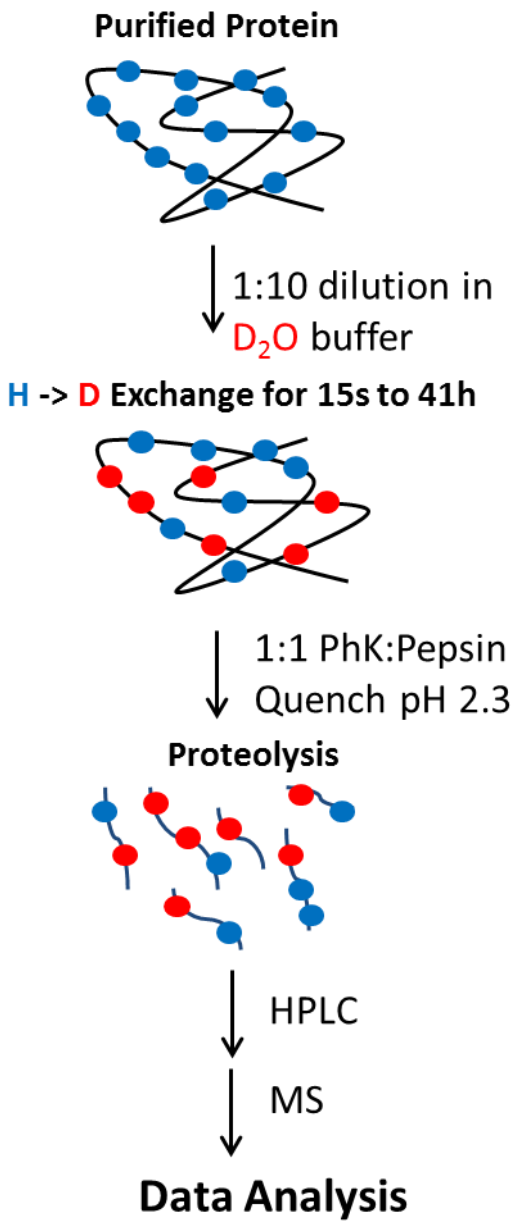

Figure 1.3 Hydrogen-Deuterium Exchange Protocol

Protocol for H/D exchange is as follows: purified protein is diluted into D_2O buffer and allowed to exchange at neutral pH for the desired amount of time. Quenching of exchange occured by lowering the temperature to 0 °C and the pH to 2.3. Addition of pepsin to this quench buffer allowed proteolysis of the protein to occur simultaneously. Following proteolysis, peptides were loaded onto the HPLC for subsequent analysis by MS. Data analysis follows.

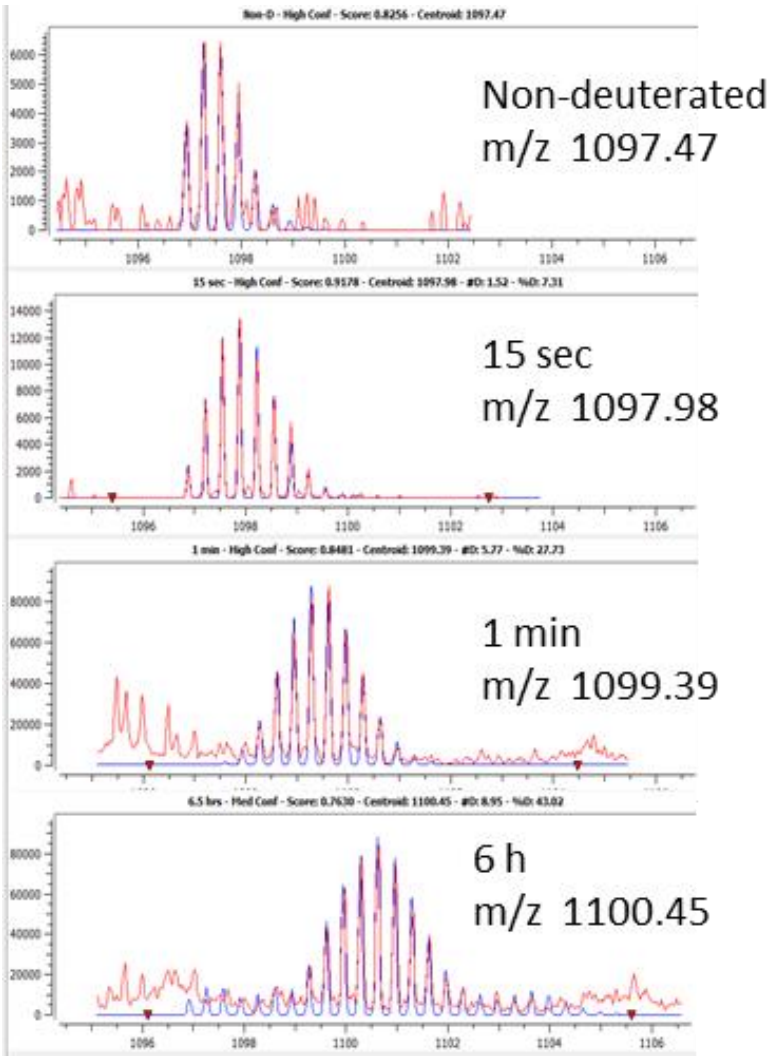

Figure 1.4 Example of Hydrogen-Deuterium Exchange Spectra Over Time

Representative mass spectra to illustrate the mass shift for an ion at m/z 1097.47 as more deuterium is being incorporated onto the peptide. Time spent in D_2O is indicated on the abscissa of the spectrum. The ordinate is the intensity of the peptide and the abscissa is the m/z.

Chapter 2
ANALYSIS OF PHK STRUCTURE USING PARTIAL PROTEOLYSIS AND CHEMICAL FOOTPRINTING

Reproduced with permission from Rimmer, M.A., Artigues, A., Nadeau, O.W., Villar, M., Vasquez-Montes, V., and Carlson, G.M. (2015) ***Mass Spectrometric Analysis of Surface-Exposed Regions in the Hexadecameric Phosphorylase Kinase Complex*** *Biochemistry 54(46):6887-95*

2.1 Introduction

PhK is a large, hexadecameric enzyme complex in the glycogenolysis cascade. The enzyme as isolated from fast-twitch skeletal muscle, as in this report, is made up of four copies each of four different subunits, $(\alpha\beta\gamma\delta)_4$, and has a mass of 1.3 MDa. The α (138.4 kDa, 1237 amino acids[4]), β (125.2 kDa, 1092 amino acids[4]) and δ (16.7 kDa, 148 amino acids[30]) subunits are regulatory, inhibiting the kinase activity of the catalytic γ (44.7 kDa, 386 amino acids[21]) subunit until β and then α are phosphorylated by PKA,[5, 70] which releases the inhibition and allows γ to phosphorylate GP in a Ca^{2+}-dependent reaction.[71] The δ subunit is an intrinsic CaM molecule, which accounts for the Ca^{2+}-sensitivity of the enzyme.[18]

Because of its large mass, the structure of PhK has been difficult to study; however, several methods have been employed that have produced low resolution 3D structures, including transmission EM,[43, 44, 72] cryoEM,[45, 73] and SAXS.[46] Structural evidence shows PhK to be tetrahedral, made up of two opposing lobes and four interlobal connecting bridges, with αβγδ protomers packed head-to-head in D2 symmetry.[43] The approximate locations of the subunits in EM structures of the complex have also been determined. The β subunits are located on the interior face of the lobes and make up the four connecting bridges,[8, 41] whereas the α subunits, which are homologous to β, are nevertheless positioned quite differently at the periphery of the lobes, with their known C-terminal epitope located at the distal ends of the lobes.[11] The γ subunits are proximal to the β subunits, although more central and distal on the interior lobe

face.[12] The δ subunits are located near the edge of the lobes,[48] and are known to directly interact with the γ subunit,[3, 74, 75,] although each subunit type directly interacts with the other three.[47]

Although the interactions and relative locations of the subunits within the PhK complex are beginning to be understood, much less is known regarding the exact disposition of the subunits in the complex, i.e., how they are actually situated. To make matters worse, high resolution structures are available only for δ[76] and the catalytic domain of γ,[22] the two smallest subunits. How those structures might be affected by their quaternary interactions within the complex is unknown, as are the portions of those structures exposed on the surface of the complex, instead of buried and shielded by subunit interfaces within the quaternary structure. In this study we have employed two complementary techniques, partial proteolysis and chemical footprinting, to map exposed regions of individual subunits in the hexadecameric $(\alpha\beta\gamma\delta)_4$ PhK complex. Both of these methods are useful for determining exposed regions of a protein and to examine conformational changes between different forms of a protein.[53, 60, 77-79] While there are numerous reasons why particular regions might be protected from protease cleavage, brief proteolysis of a protein will target regions that are most susceptible, which is highly indicative of surface exposed loops.[80, 81] Chemical footprinting also identifies solvent exposed regions, thus can corroborate partial proteolysis data. By using partial proteolysis and chemical footprinting in conjunction with MS, the released peptides can be sequenced to identify the exact residues that are cleaved or labeled, and thus, surface exposed. We have mapped exposed loops on the PhK holoenzyme in both its phospho-activated and non-activated conformers and were able to identify exposed loops in three of the four subunits (α, β and γ), as well as to observe changes in the sites of cleavage and iodoacetate labeling when PhK is activated by phosphorylation.

2.2 Methods

2.2.1 Enzymes and Reagents.

All proteases were from commercial sources: chymotrypsin (Ch), trypsin (Tr), and endoproteinase Arg C (RC) from Worthington Biochemical Corporation (Lakewood, NJ); ficin (Fi) and thermolysin (Th) from Sigma-Aldrich Corp. (St. Louis, MO); protease V8 (V8) from ICN Biomedicals (Irvine, CA); and endoproteinase Lys C (KC) from Promega Corporation (Madison, WI).

[^{3}H]Iodoacetic acid and its non-labeled counterpart were from American Radiolabeled Chemicals (St. Louis, MO) and Acros Organics (Morris Plains, NJ), respectively. All polyacrylamide gel reagents were from Bio-Rad Laboratories (Hercules, CA).

The catalytic subunit of PKA was purchased from New England Biolabs Inc. (Ipswich, MA).

Non-activated PhK was purified from New Zealand White rabbit psoas muscle as previously described[57] and stored at -80 °C. Phospho-activated PhK was prepared through phosphorylation of the non-activated enzyme by PKA, specifically by incubating non-activated PhK (1.2 mg/ml) with $Mg(CH_3CO_2)_2$ (1.5 mM), ATP (0.3 mM), PKA (2 μg/mL), NaF (50 mM), DTT (0.1 mM), EGTA (0.5 mM), and β-glycerophosphate (100 mM) at pH 6.8 for 10 min at 30 °C, which resulted in the incorporation of 0.35 and 0.37 mol phosphate per mol of α and β subunit, respectively. Phosphorylation was quenched with 200 mM EGTA. The phospho-activated PhK was dialyzed overnight at 4 °C in 50 mM Hepes buffer (pH 6.8) containing 10% sucrose and 0.2 mM EDTA, and was used immediately thereafter.

2.2.2 Partial Proteolysis.

To ensure that proteolysis reflected PhK's structure rather than protease selectivity, seven proteases with varying selectivities were used in partial proteolysis experiments. Because PhK's structure is affected by pH, temperature, and buffer conditions, it was important to maintain the same conditions throughout all of the proteolysis experiments; however, given that each protease has different conditions at which it performs optimally, maintaining the same conditions throughout would cause the proteases to hydrolyze at different efficiencies. To control for this, we determined the concentration for each protease that resulted in less than 10% of the α and β subunits being cleaved after an appropriate fixed time, ensuring roughly similar amounts of proteolysis for each protease. This standardization process was begun using concentrations of proteases that had been previously optimized using SDS-PAGE after a 10 min partial proteolysis of PhK at 30 °C and pH 6.8,[77] but with further optimizations of protease concentrations being made (Table 2.1) for use in the more sensitive MS analyses. The proteolysis time of 10 min was retained, as it allowed for sufficient proteolysis without significant loss of the activity of PhK and presumably, the structural integrity of the protein core. Measuring the maximal activity before and after proteolysis by all seven proteases under these standard conditions showed that only ficin digestion caused any significant loss of activity, and by only 20%.

The standard conditions for partial proteolysis were 30 °C and pH 6.8, conditions under which PhK is well characterized. Stock PhK (3.5 mg/mL) was diluted to 0.4 mg/mL in 50 mM Hepes containing 10% sucrose and 0.2 mM EDTA and equilibrated at 30 °C for 2.5 min. Protease was then added at the appropriate concentration (Table 2.1) and incubated for 10 min. Reactions were quenched by the addition of 80% acetonitrile with 0.8% formic acid, vortexed for 1 min, and centrifuged for 5 min at 14,000 rpm. The supernatant was removed to a fresh

Eppendorf tube, diluted in H_2O, and flash frozen in dry ice. Samples were lyophilized overnight, re-suspended in 0.1% formic acid, and analyzed by MS. If after repeated experiments, a peptide was observed in only one sample, and its presence could not be replicated, it was disregarded. Peptides were required to be present in a minimum of three independent reactions involving at least two different PhK preparations to be judged as high confidence peptides. Peptides with good MS/MS spectra that were also observed in two different PhK preparations, but only once in each, or peptides that were observed at least twice in a single preparation are both considered as moderate confidence peptides, and are denoted as such in Table 2.1.

2.2.3 Chemical Footprinting.

To map the surface-accessible thiol side chains of Cys in the individual subunits of the $(\alpha\beta\gamma\delta)_4$ complex, conditions were first optimized to ensure that the carboxymethylation of all subunits remained in the linear phase, as has been previously done.[77]

The optimized, standard reaction was carried out for 20 min at 25 °C and contained PhK (0.37 μM αβγδ tetramer), [^{3}H]iodoacetate (3.48 mM, 0.24 Ci/mole), Hepes (50 mM, pH 8.2), and EDTA (100 μM) and resulted in the linear incorporation of 0.08, 0.30 and 0.05 mol of carboxymethyl groups per α, β and γ subunit, respectively. For the mapping of modified residues by MS, non-labeled iodoacetate was substituted, and the reaction was quenched using a 100-fold molar excess of DTT over iodoacetate. The modified protein was then digested with Tr (26 PhK: 1 Tr; w/w) for 1 h at 37 °C. Aliquots (5% of the total volume) of acetonitrile were then added to the digest every h to a maximum of 30%, after which proteolysis was carried out for 16 h. The digest was quenched by addition of formic acid to 5% of total volume. Samples were prepared and analyzed by MS as described below. The procedure above was repeated with different preparations of PhK for both non-activated and phospho-activated forms of the complex.

Table 2.1 Exposed Regions in Nonactivated and Phospho-Activated PhK[a]

Protease	Abbr	Selectivity	Conc	Subunit	Non-activated	Phospho-activated
				α		627-662[c]
					663-690	663-748[d]
					708-748	
					972-1015	1000-1015
Trypsin	Tr	Arg and Lys	0.08 μg/mL	β	1-18[1]	1-18
					24-32	24-32
					683-694[b]	
				γ	1-27	1-27
						68-78[d]
						276-296[d]
					367-386	367-386
				α	699-741	699-741
					967-1013	967-1013
Protease V8	V8	Asp and Glu	4.0 μg/mL			1103-1113
				β	1-16	1-9
						713-725
				γ	1-17	1-23
					45-68[d]	45-73
						184-196
					281-294	280-294
				α	677-721[d]	677-683
						708-721
					997-1010	997-1006
Lys C	KC	Lys	0.4 μg/mL	β	1-32	1-13
					683-696	683-694
					791-807[d]	

				γ	**360-386**	
Chymotrypsin	Ch	Aromatic, acidic, hydrophobic	0.2 μg/mL	α		**703-709**
					718-733	718-733
					1006-1017	1006-1014
						1217-1224[d]
				β	1-15	1-15
					779-811[d]	784-811[d]
				γ		**1-16**
					277-298	277-298[d]
					371-386[d]	371-386
Thermolysin	Th	Hydrophobic	15 μg/mL	α	677-688	
					699-746	
					984-1013	
					1017-1040	
					1156-1170	
				β	1-22	
				γ	1-23	
Ficin	Fi	Non-specific	0.04 μg/mL	α	194-210	
					718-748	
					988-1012	
					1033-1041	
				β	1-22	
					26-32	
				γ	1-26	
					367-386	
Arg C	RC	Arg	8 μg/mL	β	1-20	

[a]Sequence numbers correspond to either a single peptide or a series of overlapping peptides for any given protease.
[b] Bold indicates a difference that is observed with but a single protease.
[c] Grey shading denotes regions that are different overall between non-activated and phospho-activated conformers.
[d] Region includes moderate confidence peptides. See Table A.1 for more details.

2.2.4 Mass Spectrometry.

All samples were lyophilized overnight and brought up to a final volume of 10 μL in 0.1% formic acid. They were loaded onto a C18 reversed-phase peptide trap (100 μm inner diameter fused silica) packed in house with 3 cm of 100 Å, 5 μm, Magic C18 bioparticles (Michrom Bioresources, Auburn, CA). Following a wash with 0.1% formic acid for 30 min at 1.5 μL/m, peptides were eluted into the connected reversed-phase C18 resolving column (75 μm inner diameter, packed to a length of 12 cm with the same bioparticles used for the peptide trap) at a flow rate of 350 nL/m over a 90-min period using a gradient of 10-40% acetonitrile (buffer A = 0.1% formic acid; buffer B = acetonitrile, 0.1% formic acid). The column was mounted on the electrospray stage of a hybrid linear ion trap Fourier transform ion cyclotron resonance MS (LTQ FT, Thermo-Finnigan, San Jose, CA) equipped with a 7 tesla magnet and controlled by Xcalibur software packaged to continuously perform mass scan analysis on the FT. This was followed by MS/MS scans on the ion trap for the six most intense ions, using dynamic exclusion of two repeats of the same ion, 30 sec repeat duration, and 90 sec exclusion duration. Normalized collision energy for all MS/MS scans was set to 35%. LC MS data were collected with the source operated at 2.0 kV, with the ion transfer temperature set to 200 °C.

For data analyses all MS/MS scans were searched using the Sequest algorithm included in Proteome Discoverer (ThermoFinnigan) using an in-house built protein database containing the sequences of PhK and common contaminants. The mass range for spectrum selection was 350 to 5000 Da. A minimum of 6 and a maximum of 144 amino acid residues were used to generate the peptide library to be searched. The ion mass tolerances were 20 ppm for parent ions and 0.6 Da for fragment ions. Protease selectivity was defined as indicated in Table 2.1. A maximum of two missed cleavages was allowed per peptide. The following variable

modifications were selected: phosphorylation of Ser, Thr and Tyr, deamidation of Asn and Gln, and oxidation of Met, and a maximum of three modifications per peptide were allowed. Additionally, for the chemical footprinting experiments, carboxymethylation of Cys was considered as a variable modification. The results of the searches were filtered using the following set of criteria for high statistical confidence: minimum cross-correlation score of (Xcorr) of 1.5, 2.0 and 2.5 (partial proteolysis) and 1.5, 2.0 and 2.25 (chemical footprinting) for 1, 2 and 3 charged ions, respectively, and a delta correlation score (Δcorr) greater than 0.08. The amino acid sequence assignment of all peptides of interest was subsequently inspected manually. Supplementary Table A.1 provides details for all observed peptides.

2.3 Results

2.3.1 Mapping exposed loops on non-activated PhK.

Partial proteolysis was used to detect surface exposed loops on the individual subunits of the PhK complex (Table 2.1 and Figure 2.1), and when possible, the solvent exposure of those regions was verified through chemical footprinting by carboxymethylation (Table 2.2). Proteolytic cleavage patterns of non-activated PhK by proteases with different specificities revealed common cleavage sites, indicating the presence of exposed loops in the complex's quaternary structure (Figure 2.1).[a]

[a]It should be noted that throughout this chapter the amino acid residue numbers correspond to their actual positions in the parent subunit polypeptide chain, as opposed to their codon positions in the cDNA for that subunit, i.e., the final presence (α subunit[4]) or absence (β[4] and γ[21] subunits) of an N-terminal Met is taken into account.

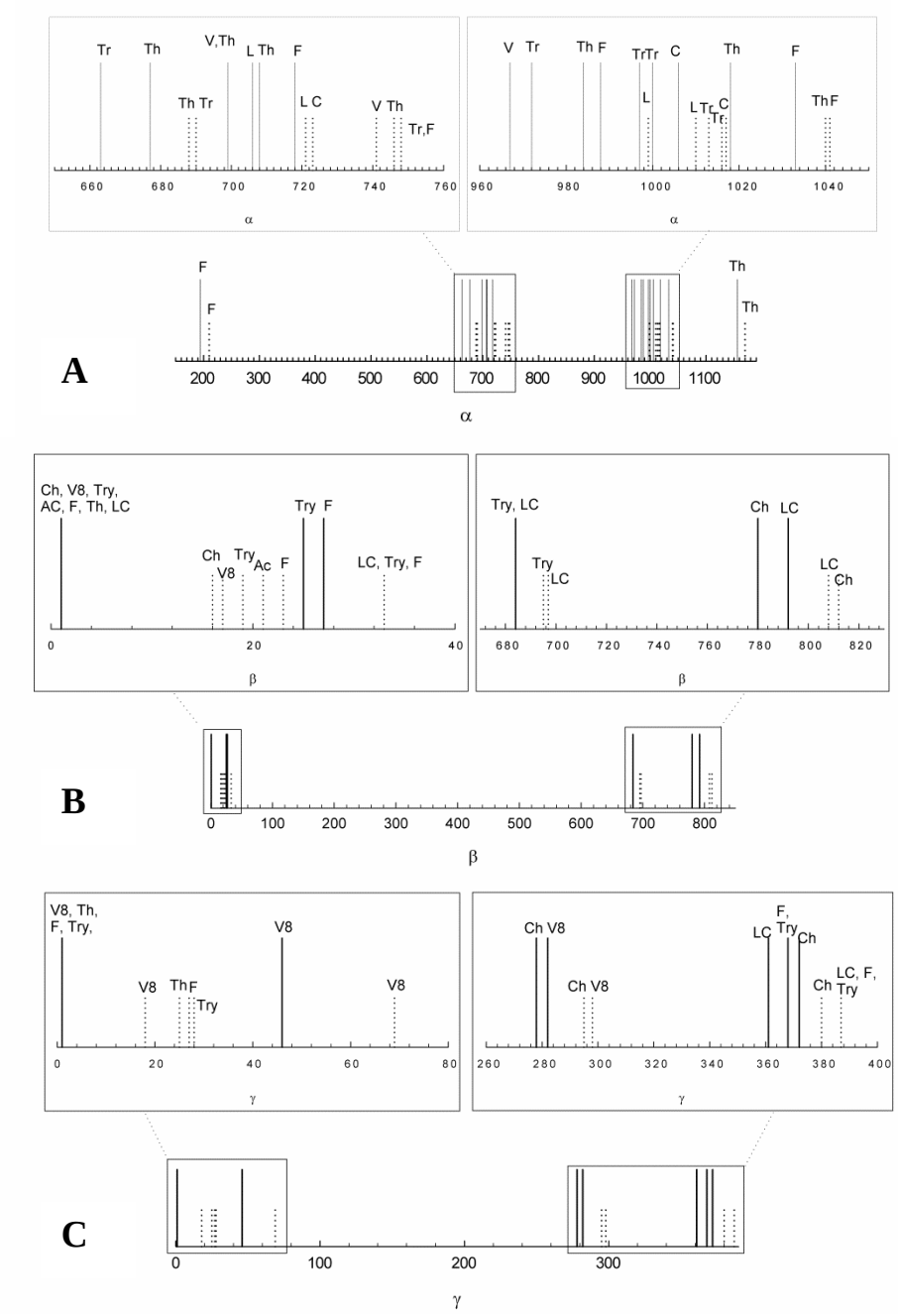

Figure 2.1 Proteolytic Patterns of Nonactivated PhK Subunits

Proteolytic patterns of non-activated PhK subunits (A) α, (B) β, and (C) γ. Non-activated PhK was incubated as described in materials and methods with the seven different proteases at the concentrations listed in Table 2.1. Residue numbers and sites of cleavage for each protease are shown, with the solid lines indicating the N-terminus for each released peptide and its corresponding C-terminus shown by dotted lines. Boxed regions of extensive proteolysis are shown expanded above the parent subunit. Despite the largely different selectivities of the various proteases, they cleave in mainly the same regions of the subunits, showing clearly defined areas of surface exposure. No peptides were observed from the δ subunit.

With the exception of RC, all proteases targeted the α subunit, and Th did so relatively selectively (Table 2.1). Two regions of the α subunit were observed with all of the proteases that cleaved it: 663-748 and 967-1041. These entire regions were not observed with any specific protease, but at least one or more peptides were cleaved by each protease, spanning varying lengths within each region. Correspondingly, two Cys side chains (656 and 697), either proximal or within the first observed loop, were carboxymethylated. The second loop is from 967-1017, and likely extends to residue 1041, based on peptides detected after digestion with Th (1017-1040) and Fi (1033-1041). Additionally, the region 194-210 was observed only in the Fi samples, whereas the stretch from 1156-1170 was observed in Th proteolysis only.

The β subunit was cleaved by all seven proteases, with KC targeting β selectively. One region was especially susceptible to proteolysis: the N-terminal regulatory domain 1-32 (Table 2.1),[13] which has a quite different sequence in other isoforms of β.[24] Peptides from within this region were seen during proteolysis by all seven proteases. Two additional spans in the β subunit that were observed in digests with multiple proteases include residues 683-696 (Tr, KC) and 779-811 (KC, Ch). The latter stretch completely overlaps a region (779-806)[24] that is different in the nonmuscle isoform of β. Portions of the intervening sequence between 696 and 779 are also exposed, as indicated by carboxymethylation of Cys733 and 735 (Table 2.2), which happen to be the only two cysteines in that stretch.

The catalytic subunit of PhK, γ, does have a crystal structure solved for its catalytic core, composed of residues 1-298.[22] The first 13 residues are likely to be highly mobile, as they are not observed with satisfactory electron density in the crystal structure. This region (1-27) was also observed after partial proteolysis by four of the six proteases that cleaved the γ subunit (Table 2.1). Just C-terminal to this region, another loop (45-68), or an extension of the first, was

Table 2.2 Identification of Carboxymethylated Cys in Non-activated and Phospho-activated PhK

		Non-activated		Phospho-activated	
	Cys #	Trial 1	Trial 2	Trial 1	Trial 2
α	24	+	+	+	+
	121	+	-	-	-
	238	+	+	+	+
	326	+	-	-	-
	488	+	+	+	+
	551	+	+	+	-
	656	+	+	+	+
	697	+	+	+	+
	844	+	-	+	+
	1096	+	+	+	+
	1199	+	+	+	+
	1234	-	-	+	+
β	75	+	+	-	+
	89	+	+	-	-
	259	+	-	-	-
	279	+	+	+	+
	298	+	-	+	+
	362	+	-	-	-
	433	+	+	-	-
	558	+	+	-	-
	574	+	+	-	-
	733	+	+	+	+
	735	+	+	+	+
	922	+	+	+	-
	1065	+	+	+	+
	1089	-	+	-	+
γ	36	+	+	+	+
	42	+	+	+	+
	138	+	-	+	-
	172	+	+	+	+
	308	-	-	-	+

revealed by partial proteolysis with V8 and modification of two proximal Cys residues (36 and 42, Table 2.2). As shown in Figure 2.1C, the C-terminal region also contains two exposed loops that include residues 277-298 (Ch, V8) and 360-386 (Tr, KC, Fi, Ch, V8).

2.3.2 Comparison of proteolytic cleavage sites in phospho-activated and non-activated PhK.

In order to observe phosphorylation-induced conformational changes that may affect surface exposed loops, PhK was phosphorylated by its physiological activator PKA (described under Materials and Methods), and partial proteolysis was performed under the same conditions used for the non-activated enzyme, but with only four proteases (Tr, KC, V8, Ch). We identified common regions that were cleaved from either form of PhK, regardless of protease specificity, although some peptides represented slightly different cleavage points (Table 2.1). Thus, activation of the enzyme did not greatly affect most of the exposed and flexible regions on the complex; however, there were nevertheless several differences in the proteolytic patterns. We also compared the carboxymethylation of the two PhK conformers (Table 2.2).

When PhK is phosphorylated, the α subunit is cleaved at the same loop regions (656-748 and 967-1015) observed for the non-activated conformer; however, a new region (627-662, Tr) proximal to the former loop was observed. Additionally, two new regions near the C-terminus of α appear as well: a peptide corresponding to residues 1103-1113 (V8) and one from residues 1217-1224 (Ch). Correspondingly, we observed that Cys1234 was modified only in the phosphorylated complex (Table 2.2), suggesting that the entire C-terminus from residues 1217 to 1237 may be more exposed in the phospho-activated conformer.

In the β subunit, the N-terminal region contains a Ser (26) that is targeted by PKA,[4, 17, 82, 83] and we have shown previously that this region of β is susceptible to chemical modification in the PhK complex.[13] Correspondingly, we find that this region is exposed in both the phospho-

activated and non-activated conformers of PhK (Table 2.1). Previous studies have shown that the β subunits not only undergo conformational changes in the phosphorylated PhK complex,[12, 37, 77] but also interact preferentially with themselves in that complex.[8, 47] Phosphorylation of the complex is known to alter the accessibility of residues and/or regions of the β subunits. [12, 77] Corroborating these findings, we detected only in digests of phospho-activated PhK a new peptide comprising residues 713-725 (V8), just C-terminal to Ser700, another target for PKA.[4] In contrast to new regions being observed in the phospho-conformer, a proximal loop of β, namely 683-694 (Tr), was detected only in non-activated PhK, again suggesting conformational changes in this part of the subunit. A similar putative burial of certain regions upon phosphorylation is observed upon moving nearer toward the N-terminus, as chemical footprinting suggests that the solvent accessibility of Cys433, 558 and 574 is altered in the phospho-conformer. These three residues were observed to be carboxymethylated in non-activated PhK, but not in its phosphorylated counterpart (Table 2.2).

The chemical footprinting and partial proteolysis patterns of the γ subunit were quite similar in the phospho-activated and non-activated forms of PhK. There were, however, two peptides, 68-78 (Tr) and 184-196 (V8), formed by cleavage of phospho-PhK that were produced by no other proteases with either PhK conformer. There were also some slight changes in proteolysis patterns for all four proteases with the phospho-activated complex.

To gain more information on the relative exposure of the various loops in the two PhK conformers, a time course of proteolysis was performed at 1, 3 and 10 min with three proteases: Tr, V8 and Ch. The most salient observation from these experiments was the rapid cleavage by all proteases of both conformers at both termini of the γ subunit (data not shown) and of the N-terminus of the β subunit (Supplementary Figure A.1).

2.4 Discussion

Previously, it has been shown that partial proteolysis[77] and chemical footprinting[53] can be used as conformational probes to detect structural differences between non-activated and activated forms of PhK. In that footprinting study only the subunits modified were identified; and in the partial proteolysis study, SDS-PAGE was used as the method of detection for proteolytic patterns. As such, exact sites of cleavage were not identified, and sensitivity for smaller released peptides was low. In the current study, peptides released by proteolysis were detected by MS, which is able to identify the exact site where cleavage occurred. The use of MS has allowed us to map exposed loops on the intact complex of PhK using both partial proteolysis and chemical footprinting, and has provided us with detailed information about specific regions that was not previously available. As such, we are able to use these regions to not only learn more about the disposition of the subunits within the structure, but also to enhance and corroborate previously determined information about those subunits.

That the α subunit is readily degraded by a wide variety of proteases in this and previous work[77] suggests a peripheral location for this subunit in the PhK complex. The more N-terminal major exposed loop in α (663-748; Table 2.1 – Tr, KC, Fi, Th, Ch, V8) identified in this study ends at the residue, Arg748, previously shown to be targeted by the HIV protease.[84] This loop coincidentally overlaps with most of the region (654-713) that is deleted in the α' isoform of PhK found in slow-twitch and cardiac muscle.[24] The second major loop in α (967-1041; Table 2.1 – Tr, KC, Fi, Th, Ch, V8) encompasses its entire phosphate-rich region (970-1030)[23] containing seven phosphorylated residues. This loop also includes one of two regions in α that is tissue-specific (1012-1062), differing from its largely homologous liver-specific isoform, αL,[85] and there are two regions of alternative splicing within this loop: 1012-1024 and 1025-1041.[86]

Both of these major loops in α overlap with its only two regions (676-766 and 967-1064) that are unique compared to its homologous β subunit.[4] That both of these regions are relatively hydrophilic prompted speculation that they may be surface exposed and play a role in mediating PhK's interactions with the environment.[4] One potential interaction may be with PhK's protein substrate, as yeast two-hybrid screening identified the region of α from 864-1014, which overlaps with the second loop, as containing a site that interacts with glycogen phosphorylase.[87] Our current work certainly indicates a surface exposure for both unique regions. That the C-terminal region of α is surface exposed is further supported by immuno-EM using a mAb against an epitope within this region.[11] Affinity labeling of the PhK complex with exogenous CaM, an activator termed δ', provided even more evidence for C-terminal surface exposure, as only the α subunit was labeled and within a peptide from 1080-1114.[20]

Although the identification of the four β subunits as the four bridges of the PhK complex[8] places it more precisely than the other three subunits, which areas of it are surface exposed is less understood. Partial proteolysis of the β subunit revealed three exposed loops, one of which was cleaved by all seven proteases and represents the N-terminus from 1-32. As with the phosphorylation loop of α, this region of β is unique (i.e., not found in α) and contains the major phosphorylation site, Ser26, that accounts for activation of the complex by PKA.[83] This Ser, as well as Ser11, is also autophosphorylated.[4] A second loop in β from 683-696 (Table 2.1 – Tr, KC) is directly adjacent to a region (697-719) reported to have the highest PEST score (6.2) of any sequence in the PhK complex.[88] Such a score is suggested to signal a high rate of *in vivo* turnover of a protein.[89] The third loop from 779-811 (Table 2.1 – KC, Ch) overlaps with a sequence (770-794) that has been shown to tightly bind (as a synthetic peptide) to isolated CaM.[90] This loop also overlaps a partially defined epitope (704-815)[8] for a mAb against β. Both

the first and third loops correspond to regions of β that are different in isoforms produced by alternative RNA splicing in tissues other than skeletal muscle.[24] All three exposed loops described above are also on the surface of a recently published atomic model of β derived from intra-subunit chemical crosslinking, threading, MS and *ab initio* approaches,[8] further corroborating that model.

Not only are the α and β subunits homologous, but both have a CaaX box for polyisoprenylation at their extreme C-termini, CAMQ and CLVS, respectively,[4] and both have been reported to be farnesylated on the Cys in the CaaX box.[14] In the case of α this is Cys1234; however, we observe the carboxymethylation of this residue in phospho-activated PhK (Table 2.2), meaning that it was not farnesylated prior to treatment with iodoacetate. We do, however, observe farnesylated peptides in MS spectra from both the α and β subunits, but we also observe non-farnesylated C-termini, as well.[b] Although it is likely that some of the non-farnesylated peptides arise from instability of the farnesylthioether bond in MS,[91] some clearly represent incomplete post-translational modification within purified PhK.

High resolution structures are available only for the two smallest subunits of PhK, γ (catalytic) and δ (CaM[76]), and for the former, only the catalytic domain (1-298).[22] In the crystal structure, the first 13 residues of the free γ subunit are likely to be highly mobile, as they have poor electron density,[22] and this region (1-27; Table 2.1 – Tr, Fi, Th, V8) was also readily cleaved during partial proteolysis, indicating that the N-terminus of γ is mobile and exposed in the solvated, hexadecameric PhK complex as well.

[b] In the initial report of farnesylation of α and β, good yields of recovery (75 and 50%, respectively) for farnesylated peptides were interpreted as both subunits being fully farnesylated in the PhK complex.[14] In agreement with that previous study, however, we did observe that the final three residues of both subunits were neither removed nor carboxymethylated in farnesylated peptides (data not shown)

A second exposed loop (45-68; Table 2.1 – V8) observed in our data corresponds to another region in γ's crystal structure that also lacked electron density (53-63).[22] A third loop region of γ occurring between 277-298 (Table 2.1 – Tr, KC, Fi, Ch, V8) completely encompasses two short helices[22] and contains the epitope (277-290) for an anti-γ mAb raised against intact PhK.[12] The final loop between 360-386 (Table 2.1 – Tr, KC, Fi, Ch) is consistent with a previous study showing that an antibody raised against a synthetic peptide corresponding to residues 362-386 strongly interacts with the PhK complex.[92] This region of the γ subunit overlaps significantly with its C-terminal CaM-binding domain (332-371) identified using overlapping synthetic peptides.[74] This finding suggests that the interaction between the γ and δ subunits within the PhK complex may be predominantly through the N-terminal CaM-binding domain of γ (287-331)[74], which matches our finding of zero-length crosslinking between δ and Lys325 of γ in the PhK complex.[3] Partial proteolysis revealed no exposed loops for the δ subunit, which is not surprising given its small size and compact crystal structure of two Ca^{2+}-binding lobes connected by a central helix.[76] Chemical footprinting showed no modification of the δ subunit because it contains no Cys.[30]

Besides the interaction of the C-terminal regulatory domain of γ with the δ subunit discussed above, the γ subunit also directly interacts with α and β.[13, 32, 36, 47] Information on which regions of the catalytic domain of γ might be interacting with the remainder of the PhK complex can be gained by mapping the surface accessible sites of proteolysis, carboxymethylation, mAb binding, and the known sites of substrate interaction[93] onto the crystal structure of the catalytic domain[94] and determining the regions omitted. These omitted regions, lacking evidence for surface exposure, are potential sites of interaction between the catalytic domain and the complex proper. Such a map of surface accessible regions covers several large

areas that include the entire N-lobe, part of the interconnecting chain between the lobes, as well as the E (C-terminal 3/4th)- and I-α helices, activation loop, substrate binding sites, and catalytic residues of the C-lobe. The region omitted is at the bottom, backside (opposite the active site cleft) of the C-terminal lobe of γ and includes three stretches of residues. Progressing toward the C-terminus, the first stretch includes residues 116-126, which form a loop connecting the D and E α-helices. The second stretch includes the C-terminus of helix F and part of the loop connecting it to helix G. The third comprises helix H and the two connecting loops bracketing helix H. The overall omitted region forms two connected perpendicular surfaces with a total area of ~ 507 Å^2. Given their location and potential function as subunit-interaction sites, these surfaces could anchor part of the C-lobe of γ on the interior lobe face of the PhK complex, as if this derriere region of γ is sitting upright on a short chair composed of the remaining subunits (color coded red in Figure 2.2) with the N-lobe and catalytic cleft of γ exposed to solvent.

Based on previous work, we thought the β subunit would be the one most likely to show conformational changes resulting from phospho-activation. For one thing, it is the subunit whose phosphorylation is key for activation of the complex.[5] Moreover, chemical crosslinking of the PhK complex has shown the amount of conjugates formed between β and other subunits to be significantly affected by phosphorylation.[35, 36, 38] Also, native MS of phospho-PhK shows a large increase in the self-association of β subunits.[47] Finally, the exposure of a β epitope (within 704-815) in the complex is greatly increased by phosphorylation.[12] The only specific region of β previously known to be involved in these conformational changes was that broadly defined epitope; but we can now identify a short loop (713-725, Table 2.1 – V8) within that broad region as becoming more exposed. Moving further toward the N-terminus of β, cysteines 574, 558 and

433 also may become less exposed upon phosphorylation, as they no longer become carboxymethylated (Table 2.2).

Phosphorylation also brought about several changes in the C-terminal half of the α subunit, one being a newly hydrolyzed loop between residues 627-662 (Table 2.1 – Tr), which contains the caspase-3 cleavage site of α, Asp 646.[95] Further toward the C-terminus, new peptides were observed from 1103-1113 (Table 2.1 – V8) and 1217-1224 (Table 2.1 – Ch), as well as new carboxymethylation of Cys1234 (Table 2.2). The last three conformational changes occurring in the terminal 135 residues of α coincident with activation by phosphorylation are in the same general region (1060-1237) of that subunit within the PhK complex that has been shown to participate in a Ca^{2+}-sensitive α↔γ↔δ communication network[32] and to undergo a Ca^{2+}-dependent redistribution of mass near the lobe tips, [44] where an anti-α mAb (epitope within 1132-1237) binds.[11] Even though they occur in the same general region of the α subunit, the observed conformational changes associated with activation by phosphorylation and by Ca^{2+} are probably not the same because the activity of phospho-activated PhK remains Ca^{2+}- dependent,[96] albeit with an altered affinity for Ca^{2+}.[49, 96, 97]

Results from these two simple techniques of partial proteolysis and chemical footprinting implicate specific regions of three of PhK's subunits as being surface accessible in the complex. More importantly, they corroborate and expand previous studies of the complex that characterized specific regions or amino acids, including sites of mAb binding, affinity labeling, phosphorylation, and single cleavage by several proteases. Further, they suggest roles as sites of target interactions for the distinct regions of variation among the different isoforms of α and β, as well as the unique regions in their otherwise homologous sequences. They also suggest how the catalytic domain of the γ subunit might be anchored to the remainder of the PhK complex.

Finally, they give the first indication of regions of conformational change throughout the complex upon phospho-activation.

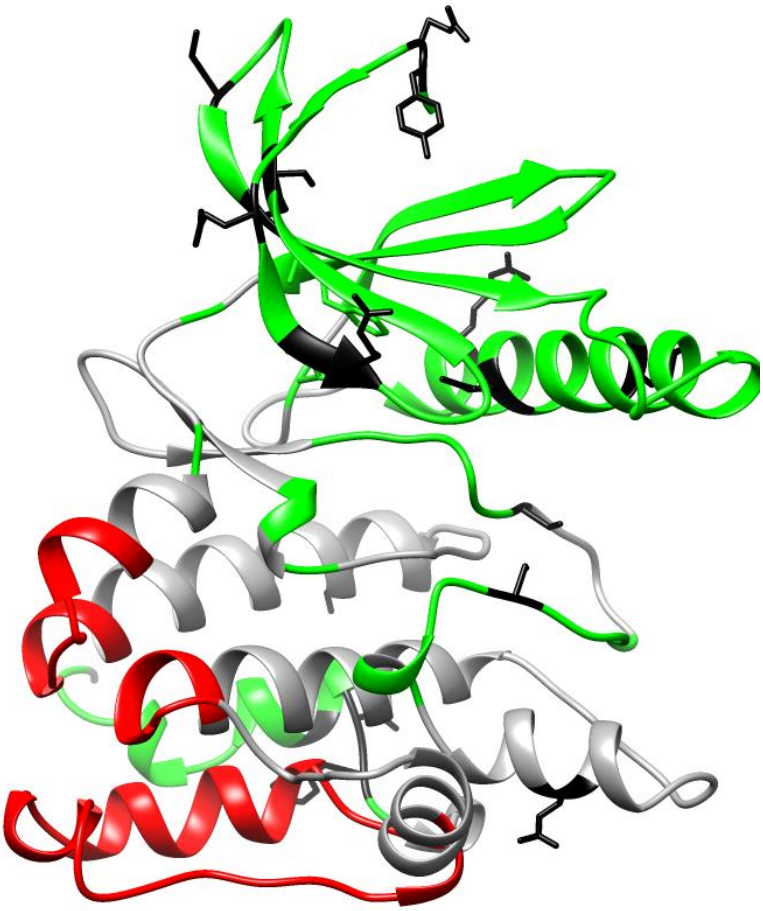

Figure 2.2 Subunit Docking Site on PhK γ Subunit

Crystal structure (Protein Data Bank (PDB) entry 1PHK) of the catalytic domain of PhK γ, with surface accessible regions colored green, based on known substrate-binding, ligand-binding, and antibody-binding sites. Carboxymethylated cysteines and protease cleavage sites detected herein are colored black with corresponding amino acid side chains. The potential subunit-docking site in the contect of the $(\alpha\beta\gamma\delta)_4$ complex is colored red. Note that the C-terminal region of γ known to bind δ (CaM) is not present in this γ construct.

Chapter 3
ANALYSIS OF THE α SUBUNIT OF PHK BY HYDROGEN-DEUTERIUM EXCHANGE

 Rimmer,M.A., Nadeau,O.W., Yang, J., Artigues, A., Zhang,Y., and Carlson, G.M. ***The Structure of the Large Regulatory α Subunit of Phosphorylase Kinase as Determined by Hydrogen-Deuterium Exchange and Modeling.***

3.1 Introduction

In the cascade activation of glycogen utilization leading to energy production in mammalian skeletal muscle, PhK phosphorylates and activates GP, which then degrades glycogen.[2] The $(\alpha\beta\gamma\delta)_4$ PhK complex is among the largest and most complex enzymes known, with 90% of its 1.3 MDa mass involved in its regulation (i.e., the integration of activating signals). The activity of PhK, catalyzed by its γ subunit, is markedly enhanced by various metabolic, hormonal and neural stimuli, which it integrates through allosteric sites on its three regulatory subunits, α, β and δ. The δ subunit is an endogenous molecule of tight-binding CaM,[18] which accounts for PhK's activation by Ca^{2+} ions. The enzyme is also activated by phosphorylation of its α and β subunits,[5, 83] although the β subunit predominates in this form of activation, because it is the first subunit to be phosphorylated and its phosphorylation parallels activation of γ.[5] Much less is known about the function of α. Apart from its secondary role in activation by phosphorylation,[5] the α subunit has been shown to be part of a Ca^{2+}-dependent subunit communication network in PhK that also involves the γ and δ subunits.[32]

Crystal structures for the δ subunit and the catalytic domain of γ are available,[22, 76] but not for the large α (138.4 kDa) and β (125.2 kDa) subunits. These last two subunits are homologous, and are likely products of an early gene duplication event.[4] From sequence analysis, Pallen first reported that both the α and β subunits possess N-terminal GHL domains.[6] These domains were later modeled using threading and additional informatics approaches,[7] using as templates related

glycosyl hydrolase-15 (GH-15) family members, which are predominately starch degrading enzymes that contain $(\alpha/\alpha)_6$ barrel catalytic domains.[98] The actual presence of such a domain in PhK was later indicated by its tight binding of the glucoamylase inhibitor acarbose, which perturbs PhK's structure and stimulates its kinase activity.[9] In addition to the N-terminal GHL domains in α and β, Callebaut and coworkers predicted that both subunits contain two C-terminal CBL domains,[10] suggesting a similar overall domain structure for both regulatory subunits; however, structural predictions for remaining domains in these proteins remained elusive. Nadeau *et al.*[8] first predicted a structure for the full-length β subunit using an integrated structural approach, combining multiple threading, chemical crosslinking, MS, CD spectroscopy, cryoEM and bioinformatics to analyze the structure of this subunit and locate it in the quaternary structure of the PhK complex. In that report, multiple threading of the complete subunit indicated a two-domain structure, containing an N-terminal GHL domain and a C-terminal HEAT-repeat, protein phosphatase 2A subunit PR65/A-like domain.[8] Here we report the first atomic model of the full-length α subunit and evaluate that structure using H/D exchange, coupled with high-resolution MS.

In H/D exchange, amide backbone exchange of protons with deuterons provides information relating to a protein's secondary and tertiary structure, as well as dynamics. We have measured H/D exchange for the α subunit while part of the $(\alpha\beta\gamma\delta)_4$ PhK complex to evaluate its structure and compare that to our predicted model and the previously predicted domains.[10] Although theoretically there are no size limitations for proteins using H/D exchange-MS, very large complexes such as PhK, which has 325 kDa of unique sequence, pose significant challenges in the use of this technique. Arguably, the greatest challenge is to design a protocol that reduces potential proton back-exchange through the use of shorter gradients, but without

negatively affecting peptide coverage due to co-eluting peptides from overly-short gradients. We have successfully addressed these difficulties in our analysis of PhK using H/D exchange, and report significant coverage of exchange throughout its regulatory α subunit.

3.2 Methods

3.2.1 Enzymes and Reagents.

PhK was purified from New Zealand White rabbit psoas muscle as previously described[57] and stored at -80 °C. Deuterium oxide, pepsin, and trifluoroacetic acid (TFA) were from Sigma-Aldrich Corp. (St. Louis, MO), ammonium phosphate from Thermo Fisher Scientific (Pittsburgh, PA), and MS grade acetonitrile from J.T. Baker Chemical (Center Valley, PA).

3.2.2 H/D exchange

PhK stock (3.5 mg/mL) was diluted to 0.4 mg/mL in 90% D_2O Hepes buffer (10 mM Hepes, 10% sucrose, 0.2 mM EDTA, pD corrected for equivalent pH of 6.8) and incubated at 30 °C. At various times of incubation between 15 sec and 6 h, 10-μL aliquots were removed, and exchange was quenched by the addition of 10 μL of cold 0.12 M ammonium phosphate buffer (pH 2.0) containing 0.4 mg/mL pepsin, for a final pH of 2.3. Each sample was immediately loaded onto the HPLC loop and kept at - 2 °C for a 3-min digestion using a custom-built cooling chamber to reduce back exchange,[99] after which the resulting peptides were analyzed by on-line reversed-phase HPLC MS.

3.2.3 Tandem MS.

Initial peptide identification was performed using non-deuterated protein samples. Following pepsin digestion, as above, with H_2O Hepes buffer and incubation at 30 °C for 2.5 min, the

resulting peptides were loaded onto a reversed-phase C18 column and desalted for 4 min at a rate of 75 μL/min with solvent A (0.1% TFA). The peptides were then eluted at a flow rate of 25 μL/min with the following gradient: 20-70% solvent B (0.1% TFA in acetonitrile) over 30 min, followed by 70-90% solvent B for 3 min. The peptides eluted between 18 and 34 min. The MS (LTQ FT, Thermo Fisher Scientific) was operated in data-dependent mode to perform one MS scan on the FT, followed by six MS/MS scans on the six most intense ions in the ion trap. Peptide identification was performed by Proteome Discoverer (Version 2.0, Thermo Fisher Scientific) using the Sequest HT algorithm to search a database containing the sequences of all four PhK subunits and common contaminants. Peptide map protein coverage was 88% for the α subunit, 94% for β, 90% for γ and 91% for δ.

Deuterated samples were analyzed in a similar manner, with the omission of the tandem mass analysis; only ICR FT scans were used. H/D exchange data were analyzed using HDExaminer (Sierra Analytics), and manual analyses were performed using Qual Browser (Thermo-Finnigan). All peptides could not be analyzed in the deuterated samples, and the final coverage of the α subunit fell from 88% in the non-deuterated to 74%; however, despite the large size of α, many of these peptides were overlapping, providing good data for amino acid level resolution in many regions. H/D exchange kinetics in Figure 3.4 were fit using OriginPro version 9.2 to a two-parameter exponential

$$D = N_1(1 - e^{-k_1 t}) + N_2(1 - e^{-k_2 t})$$

where D is the deuterium content at time t, N_1 and N_2 are the number of fast and slow exchanging hydrogens, respectively, and k_1 and k_2 are the respective rate constants.[100] The data

points for the exchange time courses of the individual peptides shown in Figure 3.4 and Supplementary Figure B.1 represent a minimum of two, but up to four, individual exchange experiments.

3.2.4 Threading and structure modeling.

The theoretical atomic model of the α subunit was constructed using I-TASSER.[101, 102] With the rabbit muscle α subunit sequence (Accession # = P18688) as query, multiple sequence-template alignments were initially generated by the meta-server LOMETS.[103] Domain boundaries were delimited by ThreaDom,[104] and the α subunit sequence was divided into two domains, based on the threading alignments and the template structures. The first, corresponding to a GHL domain, matched well with several high scoring templates, with a TM score of 0.63 and RMSD of 8.5 Å. The second, corresponding to an IBL domain, had lower scoring templates, and a TM score and RMSD of 0.34 and 17.1 Å, respectively. The domains were constructed by I-TASSER, with spatial restraints (Cα distance map and side-chain contacts) extracted from the templates being used to guide replica-exchange Monte Carlo assembly simulation, with sparse distance and contact restraints from short template fragments used as additional restraints to assist the simulations.[102] Decoys generated during the structural assembly simulations were clustered by SPICKER,[105] and the cluster centroid models were further refined by REMO to build the full-atomic model.[106] The entire α subunit model was constructed by connecting both domain models together with the domain orientation repacked based on the I-TASSER energy potential.

3.3 Results and Discussion

The $(\alpha\beta\gamma\delta)_4$ PhK complex has 325 kDa of unique sequence, 138.4 kDa of which is accounted for by the regulatory α subunit. Our initial peptide mapping of non-activated PhK identified 192

unique peptides corresponding to the α subunit, providing overlapping coverage for 88% of its sequence. To analyze the structure of this subunit in the context of the intact complex, H/D exchange was carried out on the non-activated PhK for different time intervals up to 6 h. Peptides with either overlapping envelopes or low-intensity peaks were then excluded, the latter because the intensity and quality of the spectrum peaks decreased further with the incorporation of deuterium. A total of 69 peptides with well-defined, non-overlapping envelopes were selected, resulting in accurate mass measurements of H/D exchange for 74% of the α subunit. The time-course of exchange for 64 of these peptides is presented in Supplementary Figure B.1, with the remaining five shown in Figure 3.4.

H/D exchange was used to evaluate the multi-domain structure and functional regions of the α subunit, either predicted[6, 7, 10] or determined experimentally.[4, 11, 16, 20, 24, 32, 33, 90] Analyses of the deuterium content for peptides that overlapped specific regions in the primary structure of the α subunit allowed us to further resolve the extent incorporation occurring at multiple or even single amino acids at discrete sites within these regions. To simplify comparison of the amount of exchange in different regions of α, the extent of incorporation in each region was converted to percent of the total possible exchange, with the relative amount of exchange for a given region arbitrarily being classified as low (< 33%), medium (33-62%) or high (> 62 %). The relative exchange rates in the various regions were then used to evaluate the previously predicted domain structures for α,[10] as well as our following current model.

3.3.1 Full-length Model of the α Subunit.

A 3D model of the complete α subunit was generated using the I-TASSER hierarchical structural modeling approach.[102] Multiple threading alignments of the α sequence were carried out to identify template structures from the PDB library,[103] followed by structural assembly and

refinement steps, with subsequent reconstruction of atomic models.[106] In the best fit structure (Figure 3.1A), two major domains comprising residues 1 – 436 (GHL) and 437 – 1237 (IBL: importin α/β-like) were predicted and modeled, using as templates members of the GH-15 family (blue-grey trace) and IBL nuclear transport receptors of the β-karyopherin (BKNR) family of proteins (yellow trace).[107, 108] Although the thread content and coverage for the GHL domain in our model are in agreement with previous results,[7] our threading templates differ significantly for the remainder of the subunit. The tertiary structure calculated for the IBL domain in our model is, however, consistent with the overall domain structure previously predicted for this region of the subunit.[10] Thus, our model will be directly compared to that of Carrière *et al.*[10] using the regions of α that were initially delineated in their model (Figure 3.1B and **Table 3.1**).

3.3.2 GHL Domain (1-436).

As discussed above, predictions of the structures of the α and β subunits suggested both subunits to have multiple domains, with the first being an N-terminal GHL domain,[6, 7] our current multi-domain model derived from threading is consistent with these previous reports. The GH-15 thread coverage of α shown in Figure 3.1 (blue-gray trace) displays the canonical $(\alpha/\alpha)_6$-barrel fold for the catalytic domains found in bacterial and archaeal glucoamylases and glucodextranases.[109] Thirteen α-helices are proximal to the active sites in these enzymes with two groups of six internally and externally packed α-helices forming the $(\alpha/\alpha)_6$-barrel.[109] GH-15 enzymes commonly contain a general acid-base pair of catalytic Glu residues spaced approximately 200 residues apart;[109] for the α subunit, but not β, Carrière *et al.*[7] noted that two such Glu residues were appropriately situated in the active site funnel to effect catalysis. We

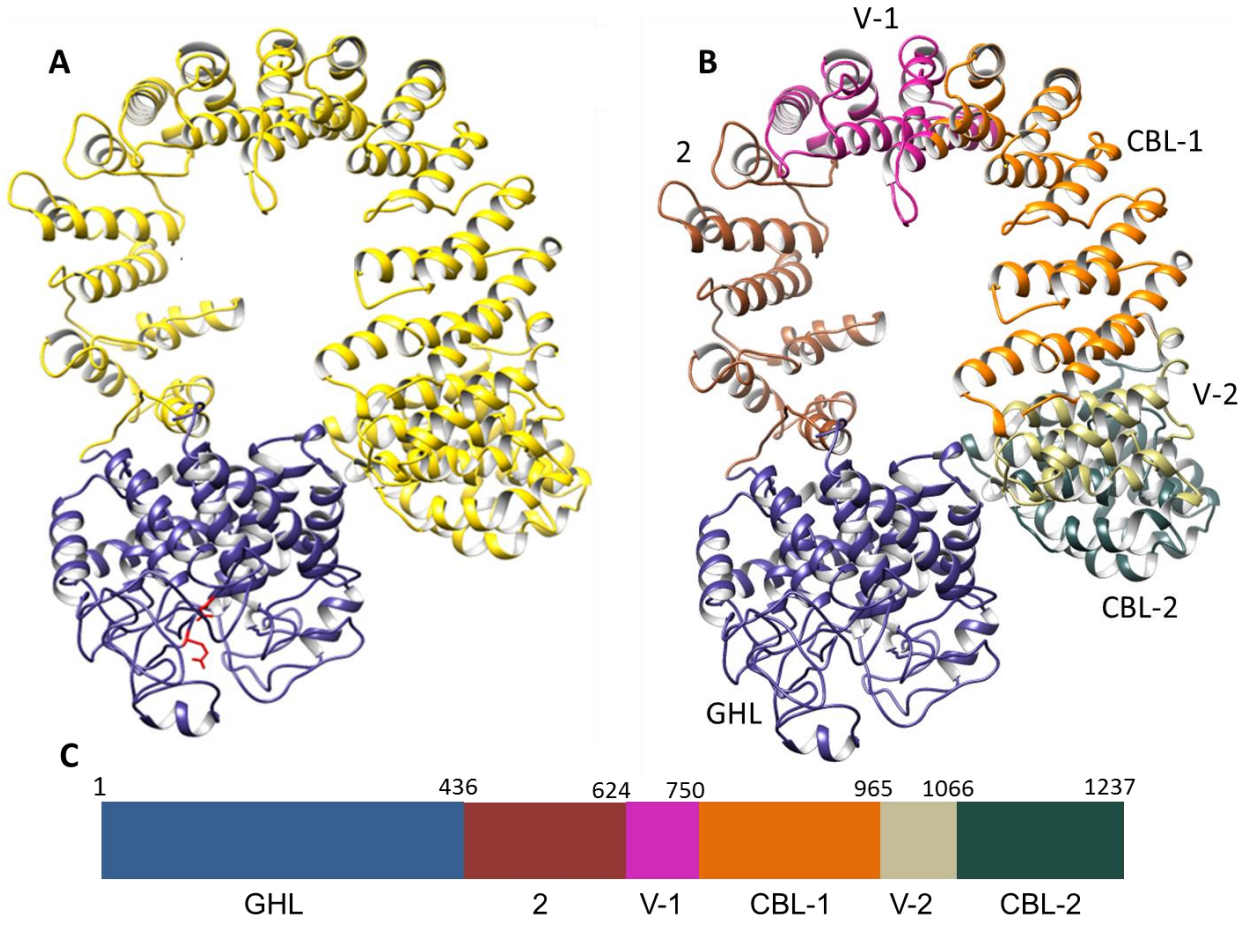

Figure 3.1 Theoretical 3D Structure of the PhK α subunit

(A) Hierarchical protein structural modeling of the α subunit carried out using I-TASSER.[102] X-ray crystal structures of glucodextranase (PDB ID: 1ULV) from *Anthrobacter globiformis* bound to acarbose (not shown) and importin β (IBL)(PDB ID: 4C0O) from human were used to thread, respectively, residues 1-436 (blue-gray ribbon trace) and 437-1237 (gold trace) of the multi-domain α sequence. Putative catalytic Glu residues 185 and 371 shown in red. (B) Subdomains of the large IBL domain labeled and color coded to match the schematic of the linear structure of α shown in (C). Further modeling details of the GHL domain and IBL subdomains are listed in Table 3.1.

Table 3.1 GHL domain and IBL subdomains of the α subunit as described in this paper and shown in Fig 3.1.

Domains	Subdomains	Residues	Template/threading Structures	
			Previous Modeling	Our Model
GHL		1-436	Glycoside hydrolase	Glycoside hydrolase
IBL	2	437-624	No previous model	BKNR
IBL	Variable-1	625-750	No previous model	BKNR
IBL	CBL-1	751-965	Calcineurin B-like proteins	BKNR
IBL	Variable-2	966-1066	No previous model	BKNR
IBL	CBL-2	1067-1237	Calcineurin B-like proteins	BKNR

GHL Domain and IBL subdomains of the α subunit as described in this paper and shown in Fig 3.1. Previous modeling templates from Carrière *et al.*[10] are listed for comparison to our modeling templates.

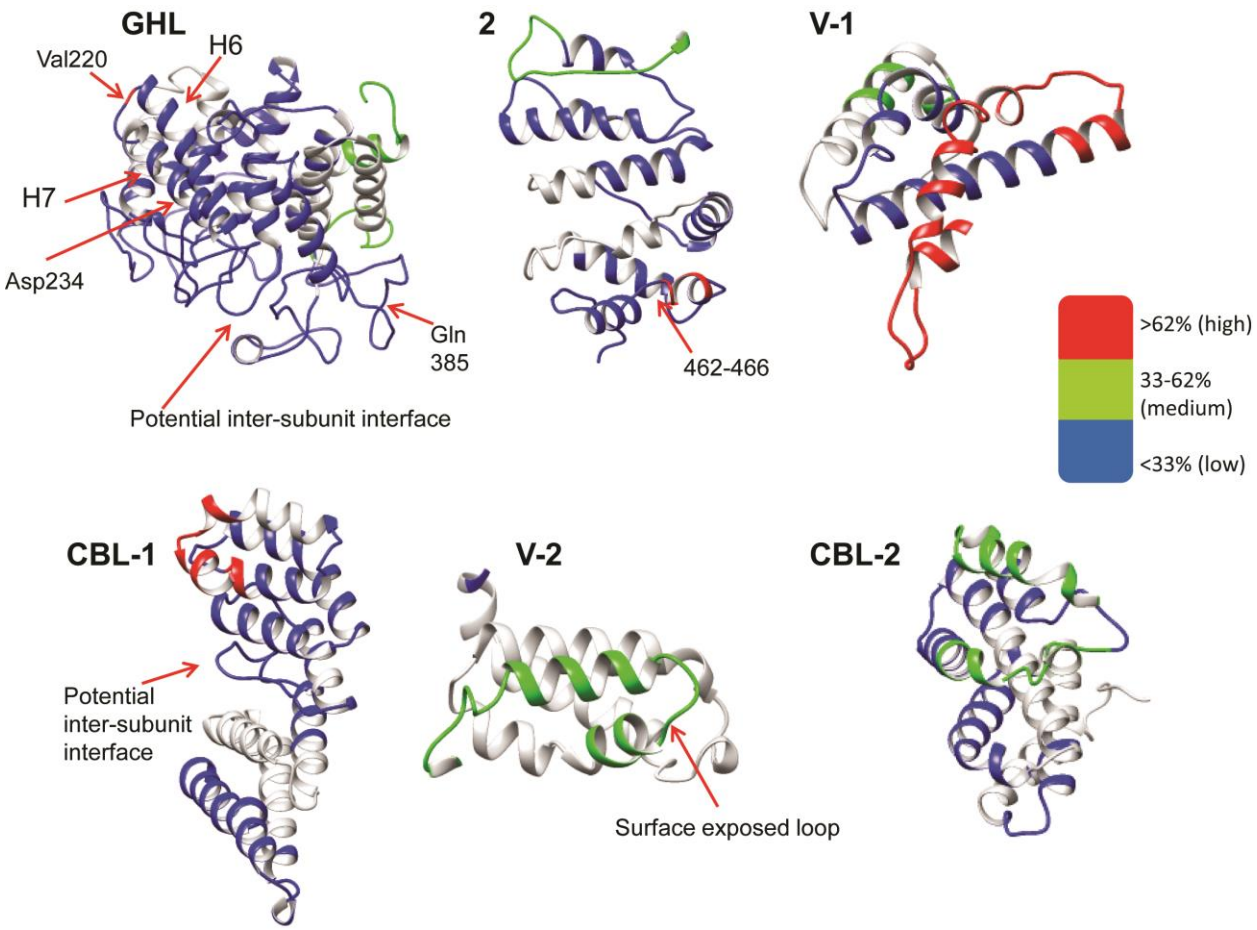

Figure 3.2 H/D exchange of the sub-domains of α

H/D exchange after 30 sec of the α subunit GHL domain and IBL subdomains. The locations of the domain/subdomains are outlined in Figure 3.1 and details of modeling are in Table 3.1. Specific regions of interest discussed in the text for the domain/subdomains are labeled.

Table 3.2 Data Consolidated Regions of the α Subunit

Data Consolidated Regions[a]	15 sec[b] (%D)		10 min[b] (%D)		90 min[b] (%D)		6 h[b] (%D)	
3-17	48	Medium	61	Medium	66	High	65	High
26-43	19	Low	28	Low	33	Medium	36	Medium
44-49	2	Low	0	Low	5	Low	5	Low
50-52	0	Low	0	Low	0	Low	0	Low
55-60	2	Low	2	Low	2	Low	2	Low
61-81	9	Low	11	Low	16	Low	17	Low
82-91	0	Low	0	Low	0	Low	0	Low
94-112	11	Low	19	Low	26	Low	31	Low
113-122	0	Low	7	Low	23	Low	24	Low
125-135	24	Low	39	Medium	42	Medium	45	Medium
136-144	0	Low	0	Low	4	Low	18	Low
173-181	1.5	Low	--	Low[c]	8	Low	11	Low
184-199	12	Low	42	Medium	51	Medium	52	Medium
200-217	3	Low	5	Low	7	Low	7	Low
220	100	High	100	High	100	High	--	High[c]
221-233	15	Low	20	Low	48	Medium	--	Medium[c]
234	40	Medium	80	High	90	High	100	High
235-242	10	Low	15	Low	23	Low	45	Medium
245-259	17	Low	32	Low	40	Medium	40	Medium
262-264	0	Low	0	Low	0	Low	0	Low
265-275	23	Low	29	Low	36	Medium	77	High
278-294	3	Low	6	Low	7	Low	11	Low
295-296	5	Low	10	Low	20	Low	15	Low
299-311	13	Low	30	Low	38	Medium	41	Medium
312-325	9	Low	43	Medium	51	Medium	58	Medium
362-372	35	Medium	39	Medium	37	Medium	37	Medium
375-384	13	Low	18	Low	29	Low	42	Medium
385	0	Low	20	Low	80	High	90	High

386-406	13	Low	21	Low	32	Low	37	Medium
408-412	0.7	Low	0.9	Low	1.4	Low	2	Low
415-445	8	Low	21	Low	30	Low	37	Medium
448-461	16	Low	28	Low	42	Medium	50	Medium
462-466	100	High	--	High[c]	100	High	88	High
513-531	21	Low	36	Medium	42	Medium	52	Medium
545-571	12	Low	27	Low	36	Medium	44	Medium
573-585	32	Low	38	Medium	39	Medium	46	Medium
586-607	10	Low	24	Low	32	Low	39	Medium
610-614	30	Low	68	High	74	High	68	High
615-627	39	Medium	50	Medium	48	Medium	47	Medium
634-639	49	Medium	60	Medium	55	Medium	52	Medium
662-699	24	Low	28	Low	--		33	Medium
702-704	80	High	80	High	83	High	77	High
705-722	65	High	64	High	62	Medium	60	Medium
725-732	71	High	71	High	68	High	66	High
733-749	55	Medium	61	Medium	57	Medium	56	Medium
750-763	49	Medium	51	Medium	51	Medium	50	Medium
773-798	18	Low	30	Low	38	Medium	45	Medium
789-825	1.5	Low	6	Low	6	Low	7	Low
850-876	14	Low	24	Low	27	Low	32	Low
877-879	20	Low	67	High	73	High	70	High
930-966	7	Low	11	Low	15	Low	20	Low
1037-1078	41	Medium	47	Medium	47	Medium	46	Medium
1081-1087	21	Low	39	Medium	50	Medium	54	Medium
1088-1103	6	Low	13	Low	19	Low	26	Low
1106-1121	46	Medium	68	High	65	High	64	High
1124-1131	4	Low	6	Low	28	Low	35	Medium
1132-1143	1.4	Low	15	Low	16	Low	18	Low
1167-1176	1.3	Low	3	Low	6	Low	7	Low
1178-1189	19	Low	38	Medium	46	Medium	51	Medium

1204-1215	4	Low	7	Low	15	Low	16	Low

[a]Regions showing the deuterated coverage of the entire α-subunit, with the percent deuterium incorporated and the resulting classification of that region listed for each time point. Data consolidation[110] has been applied to all regions, and the number of deuterons incorporated has been converted to percentages. Overlapping peptides used for further resolution are not included. Redundant peptides (same peptide, with different charge) are also excluded; entire time courses for every peptide can be found in the supplementary material.
[b]Four time points, out of the nine, are shown here to represent early, middle and late exchange.
[c]If no data were available for a specific time point, the classification for the peptide that could be reasonably extrapolated from the prior and subsequent time point is listed for that point.

found that the protein structurally closest to the best model for this region of α is *Anthrobacter globiformus* glucodextranase (GDase; PDB # 1UG9),[109] with a TM score of 0.77 and a RMSD of 2.04 Å, indicating a good topographical match.[111] The best of the top 10 templates for the GHL domain from the PDB was a crystal structure of glucodextranase in complex with the pseudo-tetrasaccharide acarbose, a potent transition state inhibitor of glucoamylases.[112] Correspondingly, we have found that PhK also binds acarbose, stabilizing a conformation of the complex that stimulates its kinase activity, indicating communication between the acarbose binding site(s) and the kinase catalytic site.[9]

As expected for a highly helical structure, the majority of the GHL domain (Figure 3.1 and **Table 3.1**) is protected from exchange (Figure 3.2D). At 15 sec, over 80% of the domain undergoes low exchange, with only the N-terminal 17 residues (Figure 3.4A) and peptide 360-372 exhibiting medium exchange and residue 220 high exchange (Figure 3.2D). The extent incorporation measured for residue 220 (resolved using overlapping peptides covering residues 182-242) is consistent with its location in a short loop in our model that was previously suggested by partial proteolysis.[16] This short loop connects two helices (residues 199-218 and 224-241) that correspond to helices 6 and 7 in GH-15 structures (Figure 3.2D). Helix 6 is packed internally, and peptide 198-217, corresponding to this helix, shows very low exchange, even after 6 h (Figure 3.4B); helix 7 is external in the GHL $(\alpha/\alpha)_6$ barrel fold and correspondingly shows medium exchange (Table 3.1). These exchange data parallel results from a recent report showing that thermal denaturation of the GH-15 catalytic domain from *A. awamori* undergoes a predicted pattern of unfolding, in which helices 6 and 7 are among the last and first, respectively, of the 12 barrel helices to unfold.[113]

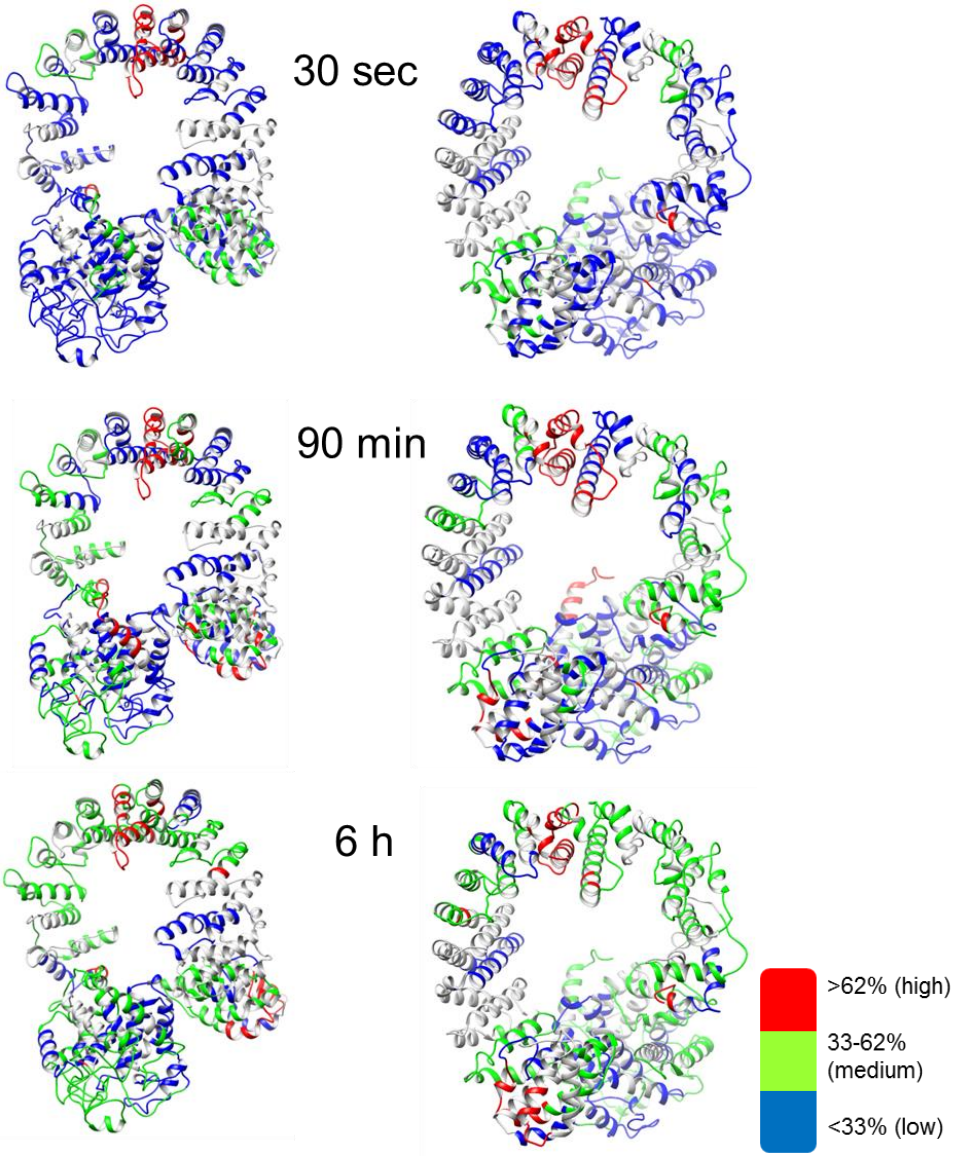

Figure 3.3 Model of α with H/D Exchange Results

The deuterium level of the α subunit from non-activated PhK is mapped onto the model of α at three different time points in the front and back orientation, with the lowest deuterium levels in blue, medium levels in green, and the highest deuterium incorporation in red, as indicated by the inset.

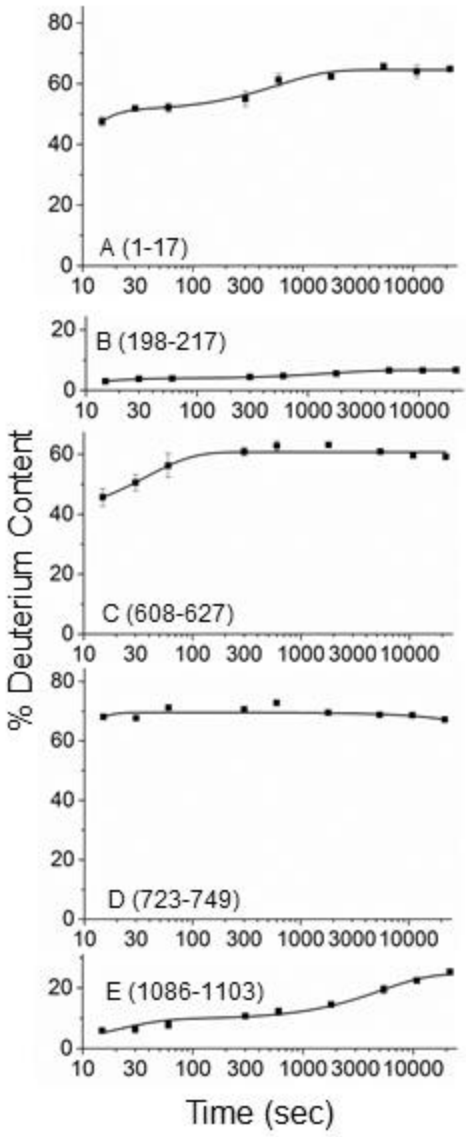

Figure 3.4 Representative H/D Exchange Time Course Plots

Percentage of deuterium incorporated for peptide graphed over time. Peptides corresponding to residues 1-17 (A), 198-217 (B), 608-627 (C), 723-749 (D), and 1086-1103 (E). Error bars are the average deviation of independent exchange experiments as described under methods and materials. Time course graphs of exchange for all remaining peptides can be found in Figure B.1.

Moreover, from overlapping peptides we observed a residue (234) within helix 7 that exhibited high exchange within 10 min (Figure 3.2D), suggesting that this helix may be partially melted in the PhK complex. One other residue, 385, also progresses from low to high levels of exchange by 30 min; however, the residues surrounding it (373-384 and 386-406) are part of a large extended loop that undergoes only medium levels of exchange by 3 h. The surprisingly slow exchange observed for this long loop structure and several others along one face of the GHL domain (Figure 3.2D) suggests that it might occur at an inter-subunit interface in the PhK complex, which would be consistent with crosslinking[9, 34, 38] and other known interactions of the α subunit within the complex.[33]

Even after 5 min, greater than 80% of the GHL domain undergoes only low or medium levels of exchange, again consistent with a largely helical structure (Figure 3.3). One of the medium exchanging peptides, 360-372, rapidly reaches that extent, followed by regions 123-135, 243-256 and 297-325, with all plateauing at medium levels of exchange. Peptides covering the majority of the regions 24-43, 263-275 and 373-461 also slowly reach medium levels of exchange. These measurements are consistent with a simulation demonstrating that the catalytic domain of a related GH-15 member glucoamylase unexpectedly underwent thermal denaturation at moderate temperatures, suggesting that regions of the $(\alpha/\alpha)_6$ barrel may be moderately dynamic,[113] which could apply to both glycosyl hydrolase (GH) monomers and the GHL domain of α within the PhK complex. All other regions of the α-GHL failed to reach more than low levels of exchange, even after 6 h (Figure 3.3).

3.3.3 Domain 2 (437-624).

Following the GHL domain, our structural model differs from the domains predicted by Carrière *et al.*,[10] which is to be expected given that we modeled the entire region from 437- 1237 using members of the BKNR family. The predicted large IBL structure for the C-terminal 65% of the α model was a good topographical match (TM score = 0.922; RMSD = 2.01Å) with an importin-β complex in the protein data bank (PDB # 3EA5),[114] and its predominately helical HEAT repeat structure corresponded well with the high helical content estimated previously for the α subunit by CD spectroscopy.[8] In addition to the structural similarities between the α model and importin-β, both proteins share additional functional and structural features, including self-association,[33, 108] alternative splicing in different tissues to form isoforms with large internal deletions,[24, 107] and multiple protein interaction sites.[2, 20, 32-34, 108]

To facilitate comparisons, throughout the remainder of this paper, our predicted large IBL structure for α will be discussed in terms of the smaller, individual domains previously predicted to lie within it,[10] which are denoted in **Table 3.1**. Thus, we begin working toward the C-terminus of the IBL structure by first examining the sequence from 437-624, which was referred to by Carrière *et al.*[10] as Domain B; but for consistency in terminology within our discussion, we refer to as Domain 2.

Our model shows the region of the IBL corresponding to Domain 2 to be primarily an anti-parallel α-helical structure, which is consistent with the low H/D exchange rates generally observed at short times for this region (Figure 3.2A). In fact, the majority of the domain undergoes low levels of exchange until later time points, and still has only medium levels of exchange by 6 h, indicating that it is relatively well protected. Only two exceptions to the observed low levels of exchange were found, residues 462-466 (Figure 3.2A) and 608-627

(Figure 3.4C), with high and medium exchange, respectively, at 15 sec. These peptides overlap with two loop structures identified in the model (458-463 and 607-622).

3.3.4 Variable Domain 1 (625-750).

At the beginning of Variable Domain 1 (Figure 3.2B), a small loop (residues 627-628) is predicted to connect two small 1- and 5-turn helices. Peptides from this region (608-627 and 632-639) undergo medium levels of exchange, in agreement with minimal levels of secondary structure. The α subunit of PhK is mostly homologous with β, but has several regions that are unique, one of them being 676-766.[4] Residues 654-712 from within this region are deleted in the splice variant isoform (α′) found in cardiac PhK,[24] and as a whole this α-unique region has been reported to be highly variable among different species.[10] We observed a high level of exchange for a large stretch (residues 700-763) of Variable Domain 1 merging into CBL-1, consistent with the model's large loop structures connecting several small helices. Likewise, Variable Domain 1 was also hypothesized to be a hinge region by Carrière *et al.*[10]

Our model, with its highly ordered helical structure of Domain 2 contrasting significantly with the more random helix-(large loop)-helix structure of Variable Domain 1, agrees well with the previous prediction[10] that these two regions would have distinctly different structures. Certainly, the generally low level of deuterium incorporation observed for Domain 2 compared to the high levels for Variable Domain 1 indicates two distinct structural domains.

Regarding residues 654-712, which are deleted in the α′ splice variant, our model predicts that they are predominantly helical. For example, the stretch from 660-699 is largely helical, and correspondingly very slowly deuterated, exhibiting low levels of exchange even after 6 h. In contrast, the remainder (700-712) of the alternatively spliced region is part of a peptide that undergoes rapid and high exchange by 15 sec; our model shows these residues to occupy the

last two turns of a helix and extend into a long loop. The remainder of Variable Domain 1 also exhibits high levels of exchange, in agreement with its predicted structure of a series of small helices connected by large loops.

Based on its high content of hydrophilic amino acids, the region from 676-766 was suggested to be predominantly on the surface of the PhK complex where it could influence interactions of the kinase with its environment.[4] This hypothesis of surface exposure is supported by our high exchange data (peptide 723-749 is shown in Figure 3.4D), as well as partial proteolysis of the complex,[16] which exposed a loop (699-748) overlapping this region. This loop was the most rapidly proteolyzed region of α in the PhK complex, and was targeted by a variety of proteases having different specificities.

3.3.5 CBL-1 Domain (751-965).

The first 13 residues of this region, proximal to the high exchanging hinge region of Variable Domain 1, likewise rapidly exchange (30 sec) at high levels, and in our model comprise a small connecting loop between, and in the initial turns of, two helices (Figure 3.2C). The CBL-1 Domain was predicted by Carrière *et al.*[10] to contain two EF hand motifs, which are helix-loop-helix structures. Although our model does not predict a calcineurin-like structure for this region of α, it does show a high overall helical content, with the exception of a relatively large loop (850-870). Both the helices and the loop, which is located on the inner face of the molecule, showed low levels of exchange at less than 30 min. Protection of this large loop from exchange is consistent with its being at an interfacial contact site between subunits (Figure 3.2C). The loop is proximal to a leucine zipper (833-854) that was previously implicated in the self-association of α subunits in two-hybrid assays;[33] and in fact, zero-length crosslinking of PhK by

transglutaminase has been shown to form an α–α dimer,[34] although the specific location of the crosslink has yet to be determined.

3.3.6 Variable Domain 2 (966-1066).

This 101-residue domain is highly helical in our IBL threading model, with distorted helix-loop structures occurring at its predicted N- and C-termini. All but three residues at the termini of Variable Domain 2 (Figure 3.2F) constitute a region (967-1064) that is unique to α (i.e., not present in β), and which contains the regulatory phosphorylatable region (970-1030). Adjacent to the N-terminus of this domain, residue 967 has been identified as an exposed loop end by partial proteolysis, which is consistent with our model. The C-terminus of this domain, residues 1035-1066, occurs within a peptide (1035-1078) that rapidly undergoes exchange to a medium level (15 sec), which is maintained through 6 h; our model shows this stretch to be a loop-short helix-loop structure. The previous identification of an exposed loop end by partial proteolysis at residue 1041[16] occurs at a distorted helix-loop (1037-1041) in the model.

3.3.7 CBL-2 Domain (1067-1237).

This second of the two CBL domains (Figure 3.2E) predicted by Carrière *et al.*[10] represents the remainder of the α subunit and contains three known functional regions: 1) a region that binds to the γ subunit's apparent master allosteric activation switch for the PhK complex;[13] 2) a site that binds exogenous CaM;[20] and 3) an epitope for a mAb specific for the α subunit.[11] The first of these regions, the α-γ interaction site, which was determined by two-hybrid screening and near-zero-length chemical crosslinking with formaldehyde,[32] is likely to be protected against exchange by PhK's quaternary structure. The last two sites, which are targeted by exogenous CaM and the anti-α antibody, are by definition surface accessible, and therefore susceptible to

exchange at levels dictated by the overall secondary structure of each binding site. This information was applied to our model and used in conjunction with our H/D exchange data to evaluate and refine our predictions regarding the location and structure of the three functional regions within the CBL-2 domain. The γ binding site (colored in cyan in Figure 3.5A) is known to occur somewhere between residues 1060 and 1237,[32] which includes the last seven residues of variable domain 2 and all of the CBL-2 domain. As shown in Figure 3.5A, this cyan region occurs within a single structural domain that projects perpendicularly from the plane bisecting the large toroid formed by the remainder of the subunit. A blow-up of the structural domain with H/D exchange levels shown in Figure 3.5B reveals extended exchange surfaces that face primarily either the interior or exterior of the toroid. Several low exchange regions (1086-1103 and 1122-1144) along the inner face with both helical and loop (1094-1103 and 1131-1134) secondary structures suggest the presence of an inter-subunit contact site, consistent with our previous mapping of the γ interaction site to CBL-2.[32]

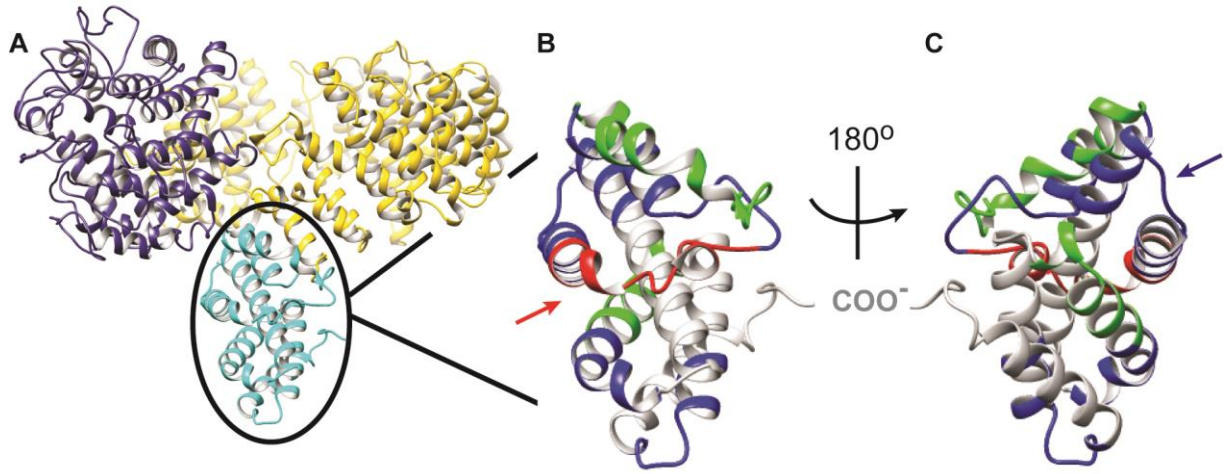

Figure 3.5 The Proposed γ Subunit Binding Site of the Regulatory α Subunit

(A) The atomic model of the α subunit shown in Fig. 2A is rotated 90°, placing the toroid perpendicular to the plane of the page. The GHL and IBL domains are shown in the same color scheme as in Fig. 3.1A (blue and yellow, respectively), with the C-terminal 178 residues (1060-1237, now in cyan instead of yellow) of the latter domain projecting from the toroid. Opposite sides of this projection, enclosed by an ellipse, are shown blown up with their 90-min H/D exchange heat maps in Panels B and C. The low exchanging surface of Panel C (blue arrow) reveals the putative binding area for the γ subunit, whereas the opposite high exchanging surface (Panel B, red arrow) overlaps the known binding site for exogenous calmodulin.

Medium and high exchange at later time points was observed in CBL-2 for residues with primarily helical structure along the outer face (1067-1086 and 1104-1121), suggesting exposure of this region in the complex. This exposed region overlaps with a CaM-crosslinked α peptide (1080-1114) that was isolated from a digest of PhK after chemical crosslinking in the presence of exogenous Ca^{2+}/CaM.[20] That the region between 1086 and 1103 only slowly exchanges over a 6-h period (Figure 3.4E) argues that the residue crosslinked to CaM lies in one of two stretches, 1080-1085 or 1104-1114.

Previously, the epitope for a mAb against the alpha subunit was mapped to within the last 106 residues (1132-1237) of CBL-2.[11] H/D exchange results identified four peptides covering three regions within this epitope, the majority of which undergo only low exchange. However, residues 1176-1189 undergo medium levels of exchange by 5 min, and are proximal to a previously identified exposed loop (1156-1170), suggesting that the actual epitope is centrally localized within the 1132-1237 stretch.

3.3.8 Structural comparisons of the homologous α and β subunits.

In a previous report we modeled the full-length β subunit (1092 residues) and demonstrated that two major domains of that subunit were good topographical fits with GH and HEAT-repeat proteins from the PDB.[8] However, our results for α indicate that the extent of GH and HEAT–repeat thread coverage for the two subunits is significantly different. For example, thread coverage of the β-GHL spanned the first 629 residues, which included the $(\alpha/\alpha)_6$ GH-15 catalytic domain and auxiliary B and C domains found in bacterial and archaeal GH-15 members; in contrast, GH-15 templates for α primary structure extending beyond residue 436 produced models with low TM scores (data not shown), suggesting structural differences between α and β immediately C-terminal to the conserved $(\alpha/\alpha)_6$ domain structures for regions

of these subunits corresponding to Domain 2 of α. As discussed above, Domain 2 in α is best modeled by HEAT-repeat template structures, and thus has a greater percentage of helical composition than its counterpart region in the β subunit.[8] The highest ranking templates for the α- and β-HEAT-repeat domains and their extent coverage in each subunit also differed, with the best template for β corresponding to protein phosphatase 2A subunit PR65/A.[8] The differences in the modeled structures for α and β likely reflect not only their different functions,[5, 13, 32] but also regions that are unique to α, namely two large inserts that comprise both its Variable Domains.[4] These domains, which have been modeled successfully for the first time in this report, demonstrate the presence of a hinge region and several helix-loop-helix structures that were not previously observed in the full[8] and partial[7, 10] models of the β subunit.

3.4 Conclusions

The H/D exchange coverage of the α subunit in the PhK complex allowed us to evaluate for the first time an atomic model of the full-length subunit, showing it to be a multi-domain structure comprising both GHL and IBL folds. Previous predictions for the domain structure of α[10] corresponded reasonably well with distinct subdomains in the IBL fold, as did known functional sites on the subunit. Our results also provide for the first time a structural rationale for previous two-hybrid screens involving the α and γ subunits,[32] localizing an intramolecular γ-binding site to the CBL-2 domain, which in our model has additional potential interfaces for interactions with exogenous Ca^{2+}/CaM and a subunit specific anti-α mAb.[11, 20] The previous structural analysis predicted C-terminal CBL-1 and CBL-2 domains to be EF-hand-like structures;[10] but, although we observed similar helical content for these domains, our results showed them to be structurally different, with our best topographical match being importin-β. These results do not rule out,

however, the possibility that the predicted CBL domains may function similarly to EF-hand Ca^{2+}-binding proteins.

Chapter 4
ANALYSIS OF THE β and γ SUBUNITS OF PHK BY HYDROGEN-DEUTERIUM EXCHANGE

4.1 Introduction

PhK is an $(\alpha\beta\gamma\delta)_4$ hexadecameric enzyme complex of 1.3 MDa that phosphorylates and activates GP in the cascade activation of glycogenolysis. The γ subunit (44.7 kDa, 386 amino acids) is the catalytic protein kinase,[21] and its activity is controlled by the three regulatory subunits: α (138.4 kDa, 1237 amino acids[4]), β (125.2 kDa, 1092 amino acids[4]) and δ (16.7 kDa, 148 amino acids[30]). The major forms of regulation of PhK are its activation by PKA, predominantly through phosphorylation of Ser26 on its β subunit,[17] and its activation by the binding of Ca^{2+} to its δ subunit, which is tightly bound, endogenous calmodulin.[18] Of these two types of activation, that by Ca^{2+} is the most fundamental, in that the phosphorylated enzyme still requires Ca^{2+} for the kinase activity of the γ subunit to be expressed.[115] Although binding of the CaM (δ) subunit within the PhK complex seems to occur largely through interactions with the γCRD,[3, 74, 75] the binding of Ca^{2+} to δ induces large structural changes throughout the entire PhK complex,[44] and an $\alpha\leftrightarrow\gamma\leftrightarrow\delta$ Ca^{2+}-dependent communication network has been observed within the complex.[32] Also within the PhK complex, the γCRD has been shown to interact with the N-terminal region of the β subunit near its PKA phosphorylation site,[13] and regions of the β and γ subunits that are proximal within the complex have been shown to be structurally coupled to each other and with PhK activation.[12] Moreover, a model has recently been formulated in which non-activated PhK is characterized by an interaction between the γCRD and the nonphosphorylated N-terminus of β, with phosphorylation of the latter weakening that interaction and giving rise to activation of γ.[116]

Subunit interactions within the PhK complex have been characterized through chemical crosslinking[31, 32, 35, 36, 38, 53] and native MS[8, 47], and it has been found that every type of subunit interacts with every other type within the $(\alpha\beta\gamma\delta)_4$ complex.[47] Reconstructions of EM images show that the hexadecamer is actually arranged as a dimer of $(\alpha\beta\gamma\delta)_2$ octamers perpendicular to each other, but separated by four bridges, i.e. a pseudotetrahedron.[11, 43] Portions of all four subunits have been localized within the complex by EM,[11, 12, 48] and the four bridges at the core of the complex are known to be composed of β subunits.[8] Less is known, however, about the atomic structures of the individual subunits, particularly within the context of the hexadecameric complex. High resolution structures of CaM (δ) and the catalytic domain of the γ subunit (minus the γCRD) have been solved,[22, 117] but in the absence of PhK's other subunits. The α and β subunits are homologous, with two unique regions in α and one in β,[4] and a structural model for each has been generated (Chapter 3).[8] Both models show highly helical, two-domain structures, but only the α structure has been evaluated in the context of the hexadecameric complex (Chapters 2 and 3).[16] In this current study the structural model for β is also now evaluated in the context of the entire complex, with attention paid to the β_4 core.

As indicated above, within PhK the β and γ subunits are associated with each other near the N-terminus of β and the C-terminus of γ. The γ subunit is a typical CaM-dependent Ser/Thr protein kinase in which its C-terminus is thought to bind the δ subunit through one or both of two previously identified high- affinity calmodulin-binding sites.[3, 74] Because the structure of the 87-residue γCRD has not been previously characterized, we have modeled its structure as part of the full-length γ subunit and evaluated the structure of the complete subunit as part of the PhK complex.

The structures of the β and γ subunits as part of the $(\alpha\beta\gamma\delta)_4$ PhK complex are evaluated herein by H/D exchange on non-activated PhK. In this technique, the amide backbone hydrogens exchange for deuterium when a protein is incubated in a D_2O buffer. This provides information concerning the secondary and tertiary structure of the protein, as well as surface exposure of specific regions, and dynamics. The multiple subunits of PhK result in 325 kDa of unique sequence, making H/D exchange challenging, though not impossible. We have developed a protocol that allows us to run a sufficiently long gradient to reduce the number of co-eluting peptides, while maintaining a short enough gradient to reduce back-exchange of the deuterons as well. This protocol has provided significant coverage of the α, β and γ subunits, the latter two being the subjects of this report.

4.2 Methods

4.2.1 Enzymes and reagents.

PhK was purified from the psoas muscle of New Zealand White rabbits as previously described[57] and stored at -80 °C. MS grade acetonitrile was from J.T. Baker Chemical (Center Valley, PA); ammonium phosphate was from Thermo Fisher Scientific (Pittsburgh, PA); and TFA, deuterium oxide, and pepsin were from Sigma-Aldrich Corp. (St. Louis, MO).

4.2.2 H/D exchange.

H/D exchange was performed as previously described (Chapter 3). Briefly, PhK stock was diluted to 0.4 mg/mL in 90% D_2O buffer (10 mM Hepes, 10% sucrose, 0.2 mM EDTA, pD corrected for equivalent pH of 6.8) and incubated at 30 °C. Aliquots of 10 μL were removed after 15 sec, 30 sec, 1 min, 5 min, 10 min, 30 min, 90 min, 3 h and 6 h and quenched with 10 μL of cold 0.12 M ammonium phosphate buffer (pH 2.0) containing 0.4 mg/ml pepsin. Each sample

was then immediately loaded onto the HPLC loop for a 3-min digestion at -2 °C[99] and analyzed by on-line reversed-phase HPLC MS.

4.2.3 Tandem MS.

MS analysis was performed as previously described (Chapter 3). Briefly, peptide identification was performed using non-deuterated protein samples treated as described above, but with H_2O Hepes buffer, and proteolysis at 30 °C for 2.5 min. Peptides were then loaded onto a reversed-phase C18 column for desalting prior to elution by a gradient of 20-70% acetonitrile containing 0.1% TFA. One MS scan was performed on the FT, followed by six MS/MS scans on the six most intense ions in the ion trap (LTQ FT, Thermo Fisher Scientific). Peptides eluted between 18 and 34 min, and peptide identification was performed by Proteome Discoverer (Version 2.0, Thermo Fisher Scientific). Peptide map subunit coverage was 88% for the α subunit, 94% for β, 90% for γ and 91% for δ. Deuterated samples were analyzed using only the ICR FT scans.

4.2.4 Data analysis.

H/D exchange data were analyzed using HDExaminer (Sierra Analytics) and manual analyses were performed using Qual Browser (Thermo Finnigan). Final coverage for the β subunit was 76%, and γ was 87%, as all peptides could not be analyzed in the deuterated samples. H/D exchange kinetics were fit using OriginPro version 9.2 to the following equation:

$$D = N_1(1 - e^{-k_1 t}) + N_2(1 - e^{-k_2 t}),$$

where D is the percent deuterium content at time t; N_1 and N_2 are the percentage of the total exchangeable hydrogens associated with the fast and slow rates, respectively; and k_1 and k_2 are the respective rate constants.[100] Each time course data point represents a minimum of two, but up to four, individual, independent exchange experiments.

4.3 Results and Discussion

Of the 325 kDa of unique sequence in the PhK complex, the regulatory β subunit accounts for 125.2 kDa, and the catalytic γ subunit 44.7 kDa. In order to analyze the structures of these subunits in the complex, H/D exchange was performed on intact, non-activated PhK. The H/D exchange was performed over a time course from 15 sec to 6 h. For analysis of the exchange results and to facilitate comparison of different regions of the subunits, the extent of incorporation into each peptide was converted to a percent of the total possible exchange. These percentages were arbitrarily classified as low (≤ 30%), medium (31-60%) and high (> 60%), which is the terminology that will be used to discuss the relative exchange in specific regions of the subunits. Table 4.1 and Table 4.2 employ this terminology, with color coding, in presenting the percent exchange into specific regions of the β and γ subunits, respectively, at early, mid, and late times of exchange. The complete time courses of exchange into all of the specific peptides used to construct these two data consolidation tables are shown in the Supplementary Material C.

4.3.1 H/D Exchange of the β Subunit.

Although the peptide map of the β subunit yielded 94% coverage, when deuterated peptides with overlapping envelopes or low-intensity peaks were excluded, 72 good peptides remained, resulting in a slightly reduced coverage of 76%. Despite the size of β, there were enough remaining peptides covering overlapping regions of the protein for data consolidation to narrow the location of exchange to within a few residues (Table 4.1).

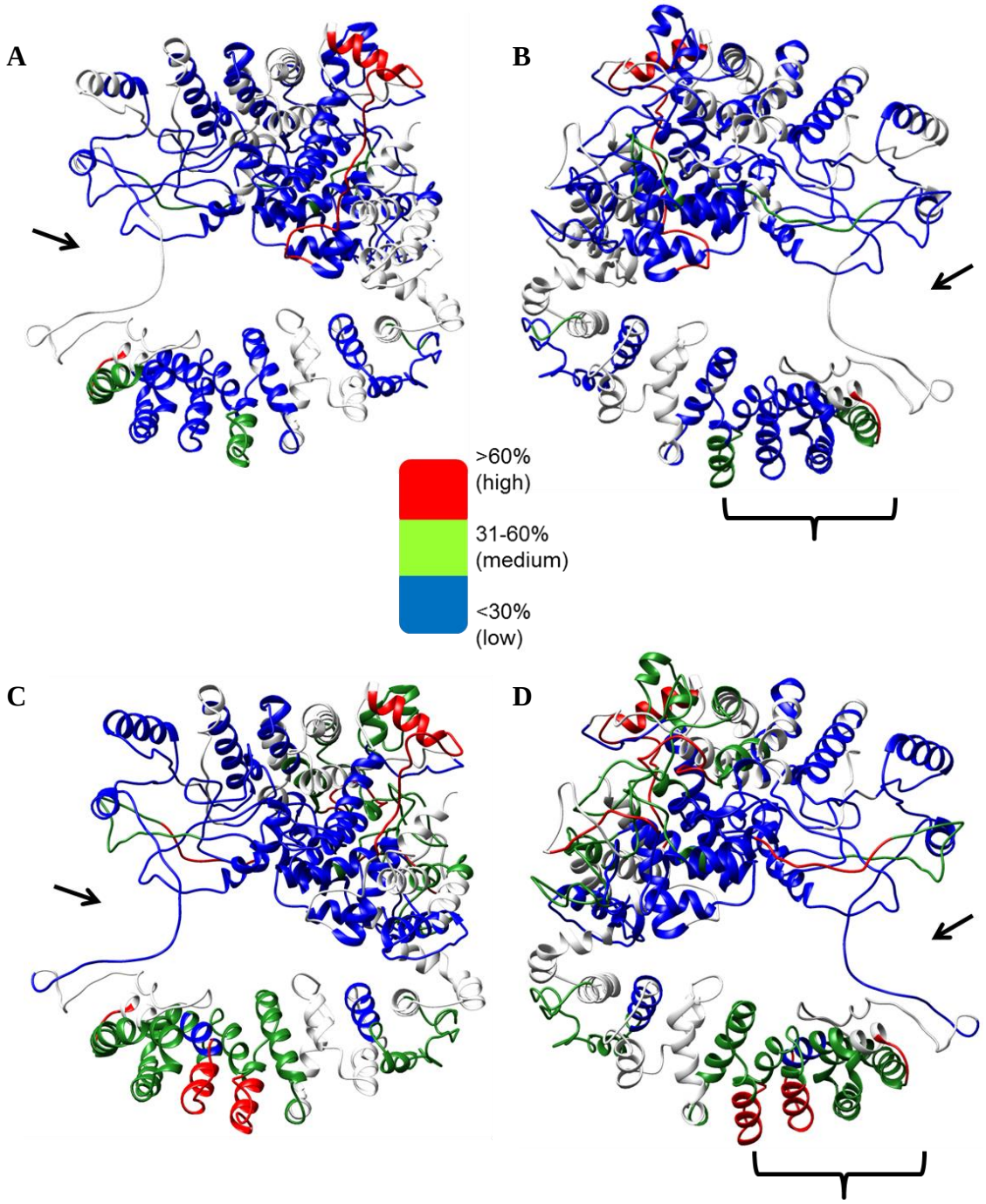

Figure 4.1 Model of β with H/D Exchange Results

The exchange results from the non-activated PhK β subunit are mapped onto the theoretical model of β, with low levels of exchange in blue, medium levels in green, and high levels of exchange in red, as indicated by the inset. (A) 15-sec time point front view, (B) 15-sec time point back view, (C) 90-min time point front view and (D) 90-min time point back view. Arrows indicate β-βinteraction region as suggested by β-docking studies[8] and H/D exchange results. Brackets show mAb epitope.

4.3.1.1 Comparison of H/D exchange results with models of β

Although there currently are no high resolution structures for the β subunit, a 3D atomic structure of the subunit has been predicted by hierarchical modeling using I-TASSER.[101, 102, 118] The predominately helical (69%)[8] β subunit structure comprises three separate domains: an N-terminal phosphorylatable domain (residues 1-40) that is unique to this subunit,[4] a glycosyl hydrolase-like (GHL) domain (residues 41-670),[6-8] and a Huntington-elongation –A subunit TOR (HEAT)-repeat like (HRL) domain (residues 671-1092).[8] These three domains together form a toroid-like structure with the subunit's N- and C-termini proximal to each other.[8] The β model was docked successfully into a 3D cryoEM envelope determined for non-activated PhK[8] using as reference information a β_4 complex observed by native MS, known phosphorylation sites, and the approximate location of the subunit in the complex determined by immunoEM with a β subunit-specific mAb.[12] As determined by cryoEM, PhK is a large bilobal structure with four interconnecting bridges.[44] Four β models packed as a dense D2 symmetrical core in the EM envelope, forming numerous contacts with one another in orientations in which the GHL domain of each model occupied the interior region of one lobe and the HRL domain occupied a single connecting bridge and part of the interior of the second lobe.[8] The H/D exchange results support the predicted structure and its packing in the complex, with the vast majority of residues observed in the deuterated peptides undergoing low exchange after 15 sec and only 5.7% attaining high levels of exchange in the same time period. Even after 6 h, the percentage of residues undergoing high exchange increased to only 15; however, regions of the subunit experiencing higher exchange were consistent with the secondary (2°) and tertiary (3°) structures predicted and described below for the major domains.

4.3.1.1.1 GHL domain.

The best matches for the GHL domain in the PDB database were from bacterial and archaeal glucoamylases and glucodextranases, which have a catalytic domain (β residues 41-485) with an $(\alpha/\alpha)_6$ barrel fold and apparent starch-binding domains (β residues 486-671) with mixed 2° structure.[109] The catalytic domains of these enzymes are α-helical toroids composed of 12 helices with interconnecting loops that alternately pack to form two groups of six helices, with one group arranged externally and the other internally to form a deep active site pocket.[109] Experimental evidence supporting the existence of these domains was revealed in a report demonstrating that PhK tightly binds the GH-15 transition-state inhibitor acarbose, which stimulates PhK's kinase activity and alters cross-linking of its β subunits.[9] Recently we demonstrated that helices in the GHL catalytic domain of the homologous PhK α subunit exchanged moderately (Chapter 3) in a pattern that was consistent with the simulated unfolding of a related GH-15 family member that unexpectedly underwent thermal denaturation at moderate temperatures,[113] suggesting the α subunit $(\alpha/\alpha)_6$ barrel to be moderately dynamic. Similarly we observed that several helices transitioned from low to medium levels of exchange in the β subunit barrel. With the exception of helix 5 and all but one turn of helix 6, exchange coverage of the β subunit $(\alpha/\alpha)_6$ subdomain included all of the remaining helices. Levels of deuterium exchange were low for helices 1-3 (residues 45-62, 84-100 and 108-130, respectively), 8 (293-298), 11 (385-391) and 12 (441-454), and all but the first three residues of helix 10 (371-379) (Table 4.1). Medium levels of exchange were observed for helices 4 (126-137), 7 (235-253), and 9 (310-323), but only at extended times (≥90 min). Medium exchange was observed in several regions within loops (63-83, 138-170, 212-234 and 324-370) connecting helices, but high exchange was observed in regions of two loops only (324-370 and 395-440).

Table 4.1 Data Consolidated Regions of the β Subunit

Data Consolidated Regions[a]	15 sec[b] (%D)		10 min[b] (%D)		90 min[b] (%D)		6 h[b] (%D)	
9-33	67.5	High	69.4	High	69.9	High	66.3	High
36-44	65.0	High	74.7	High	--[c]	High	64.1	High
49-52	1.7	Low	7.7	Low	21.7	Low	26.7	Low
53-60	0	Low	0.9	Low	3.8	Low	8.8	Low
61	10	Low	7	Low	30	Low	50	Med
64-87	27.4	Low	42	Med	45.6	Med	43.8	Med
88-99	0	Low	0	Low	0	Low	0	Low
102-125	4.4	Low	4.0	Low	5.8	Low	7.1	Low
128-148	12.6	Low	26.1	Low	38.8	Med	43.6	Med
151-160	4.1	Low	19.2	Low	24.3	Low	28.4	Low
209-220	21.7	Low	40.6	Med	49.2	Med	57.1	Med
223-245	12.5	Low	29.6	Med	33.3	Med	34	Med
248-261	9.4	Low	21.5	Low	24.7	Low	25.7	Low
281-311	10.0	Low	14.9	Low	15.4	Low	17.5	Low
314-332	5.7	Low	11.5	Low	21.5	Low	32.8	Med
333-341	13	Low	51	Med	73	High	72	High
354-371	31	Med	36	Med	42	Med	44	Med
372-373	5	Low	35	Med	35	Med	40	Med
374-392	7	Low	12	Low	17	Low	19	Low
395-408	19.5	Low	29.9	Low	36.1	Med	41.9	Med
409-414	12	Low	25	Low	30	Med	37	Med
415	10	Low	0	Low	20	Low	30	Low
418-439	26.4	Low	45.8	Med	53.1	Med	53.3	Med
442-446	2.6	Low	6.7	Low	18.3	Low	23.8	Low
449-469	10	Low	1	Low	3	Low	6	Low
470-480	52.5	Med	73	High	76	High	75.1	High
483-498	24.4	Low	38.4	Med	45.8	Med	49.4	Med
501-533	4.5	Low	3.6	Low	5.6	Low	3.7	Low

541-575	12.2	Low	23.0	Low	30.1	Low	37.3	Med
596-617	8.8	Low	13.9	Low	14.9	Low	14.7	Low
622-634	--	Low	14.1	Low	11.5	Low	12.4	Low
639-662	14.0	Low	26.7	Low	48.6	Med	41.6	Med
665-669	2.9	Low	0.4	Low	0	Low	0	Low
717-727	26.6	Low	48.1	Med	51.6	Med	50.4	Med
728-732	12	Low	32	Med	42	Med	54	Med
733-736	68	High	68	High	70	High	75	High
745-754	9.2	Low	24.2	Low	46.5	Med	47.3	Med
757-779	17.9	Low	36.6	Med	53.0	Med	56.2	Med
780-786	0	Low	6	Low	10	Low	21	Low
789-802	25.2	Low	56.6	Med	72.5	High	72.5	High
805-819	18.4	Low	36.9	Med	53.8	Med	54.6	Med
822-835	33.7	Med	66.6	High	79.1	High	78.3	High
838-852	16.2	Low	22.2	Low	31.7	Med	34.1	Med
855-866	8.1	Low	25.5	Low	--	Med	46.2	Med
925-933	3.6	Low	11.0	Low	23.0	Low	33.8	Med
936-948	12.5	Low	25.9	Low	33.4	Med	34.3	Med
951-970	16.5	Low	38	Med	45.5	Med	48.1	Med
971-973	43	Med	63	Med	66	Med	73	Med
1012-1043	--	Low	12.3	Low	17.8	Low	22.7	Low
1056-1067	11.8	Low	30.3	Low	--	Med	42.7	Med

[a]Regions showing the deuterated coverage of the entire β-subunit, with the percent deuterium incorporated and the resulting classification of that region listed for each time point. Data consolidation[110] has been applied to all regions, and the number of deuterons incorporated has been converted to percentages. Overlapping peptides used for further resolution are not included. Redundant peptides (same peptide, with different charge) are also excluded; entire time courses for every peptide can be found in the supplementary material C.
[b]Four time points, out of the nine, are shown here to represent early, middle and late exchange.
[c]If no data were available for a specific time point, the classification for the peptide that could be reasonably extrapolated from the prior and subsequent time point is listed for that point.

Helices 1, 8, 11 and 7 are predicted to be the first to unfold upon thermal denaturation of the GH-15 $(\alpha/\alpha)_6$ barrel;[113] however, exchange for the first three of these helices was very low for the β subunit barrel. Additionally, exchange for helix 7 in the β subunit was predominately low, whereas in α its exchange varied from low to high, consistent with its partial melting in the complex (Chapter 3). Despite being packed for the most part internally within each lobe in our model, several helices in the β subunit barrel underwent medium exchange, suggesting it also to be moderately dynamic. These results are consistent with a large body of evidence demonstrating that the β subunit undergoes significant conformational changes in the PhK complex.[8, 12, 37, 44, 77] Differences in the H/D exchange for the $(\alpha/\alpha)_6$ barrels for the homologous α and β subunits provide additional evidence supporting differences in the modeled structures generated by us (Chapter 3)[8] and others,[7] with the barrel for α conserving more residues critical for GH catalytic function and that for β containing a small C-terminal insert.[7]

The secondary structure content of the starch binding sub-domain of the GHL differs significantly from the $(\alpha/\alpha)_6$ sub-domain, in that the majority of residues (65%) in the former subdomain compose six large extended loops that connect six helices ranging from 2-6 turns. The level of exchange for regions in four of the loops (501-529, 568-589, 611-629 and 662-671) was for the most part low, with medium exchange occurring only after prolonged times for two of the loops (54-563 and 644-653). Given these H/D exchange results, most of the loops are presumably protected from exchange either through subunit interactions or limited exposure to the solvent interface, both consistent with the positions predicted for these loops in the lobe interiors of PhK from docking the β models in the PhK cryoEM envelope.[8]

4.3.1.1.2 HRL domain.

In docking the atomic model of β in the PhK cryoEM envelope, the N-terminus of the HRL domain connects to the GHL domain through an extended loop that passes through a region of low density in the center of PhK to the interior face of the opposing lobe, where it transitions to a highly helical structure that occupies roughly half of the interior lobe face and one of the interlobal connecting bridges.[8] With the exception of several regions discussed below, most of this domain underwent low exchange, progressing to medium exchange at extended times, consistent both with its docking in PhK's quaternary structure and its predicted secondary structure.[8] High levels of exchange were observed for four regions (733-736, 789-802, 822-835 and 971-973) containing predicted loops, with residues 779-811 being previously identified as a loop by partial proteolysis.[16] The high exchange in these loop regions is consistent with their surface exposure in our docking of β within PhK's quaternary structure.[8]

4.3.1.2 Site of intrasubunit crosslinking of β.

Previously we demonstrated that the N- and C-termini of the β subunit were proximal in PhK by chemically cross-linking Lys1025 to residues Tyr51 and Lys53 with 1,5-difluoro-2,4-dinitrobenzene in the $(\alpha\beta\gamma\delta)_4$ complex.[8] The potential physical interaction between these regions is consistent with the short spacer (3-5Å) afforded by this particular crosslinker. H/D exchange within regions containing these residues (49-52 and 1012-1043) revealed extremely low extents of exchange throughout the entire time course, supporting the crosslinking results, and providing additional evidence for the interaction of these two regions of β within the PhK complex.

4.3.1.3 Exchange in regions of β surrounding sites previously indicated to be exposed: epitope and phosphorylation site.

Using truncation mutants to determine the cross-reactivity of a monoclonal antibody against the β subunit that had been previously developed,[12] Nadeau *et al.*[13] narrowed the region in which the epitope likely occurs to residues 704-815 (4.1B, bracket), and went on to use this information to aid in the docking of the β subunit within the cryoEM envelope.[8] Within this stretch, H/D exchange analysis indicated residues 733-736 to be one of the highest exchanging regions identified in the entire β subunit, even at the shortest times of exchange. Moreover, these four residues (733-736) are the only ones in this stretch to lack secondary structure, making up a small loop between two helices. Consequently, this short stretch becomes a strong candidate as the epitope in question.

The key residue targeted by PKA in its activation of PhK and glycogenolysis is Ser26 of the β subunit,[17] which lies within the N-terminal regulatory domain of β, residues 1-31.[4] This domain appears to mediate an important interaction with the γCRD, which keeps the activity of γ from being expressed in non-activated PhK, and upon phosphorylation the inhibitory function of this region is released, resulting in activation of the PhK complex.[119] Due to the requirement for the β regulatory domain to be exposed and accessible to PKA to allow the phosphorylation of Ser26, it was expected that this region should undergo a high level of exchange. Indeed, the stretch from 9-33 and the adjacent 36-44 are among the highest exchanging regions in the β subunit at short times. Besides being the regulatory domain, the first 31 residues of β are unique from its largely homologous α subunit, and were initially hypothesized as being surface exposed based on a relatively large percentage of hydrophilic residues.[4] Later, partial proteolysis

suggested that this region was on the surface of PhK,[16] which is confirmed by these high levels of exchange.

4.3.2 H/D Exchange analysis of the γ subunit.

The catalytic γ subunit of PhK is a Ser/Thr calmodulin-dependent protein kinase (CaMK). The CaMK family comprises over 70 members,[120, 121] making it one of the largest families in the vertebrate kinome. CaMKs have autoregulatory domains, CRDs, that are located C-terminal to their catalytic domains and that range between 40 and 50 residues in length.[122, 123] In most members, the CRD interacts with the catalytic domain in the absence of Ca^{2+}, either blocking or distorting the kinase active site. This inhibitory interaction is generally relieved by phosphorylation of, and/or CaM-binding to, the CRD.[122] The γ subunit has three domains, an N-terminus (20 residues) that is unique to this kinase,[21] a catalytic domain (residues 21-289) that shares ~ 38% homology with the catalytic domains of other CaMKs, including CaMKIIδ[123] and death-associated protein kinase (DAPK).[122] In contrast, the CRD is unique with respect to other CaMKs, based both on its large size (96 residues) and multiple subunit interaction sites.[13] High resolution structural information is available only for the catalytic domain; thus, H/D exchange results will be discussed in reference to both the crystal structure of the catalytic domain (Figure 4.2) and a model of the full-length subunit (Figure 4.3) constructed by a multiple threading approach using I-TASSER.[102] As with β, analysis of the deuterated samples resulted in slightly reduced coverage of this subunit, with 37 good peptides providing 87% coverage of γ.

4.3.2.1 N-Terminal insert: 1-20.

In two different crystal structures of the isolated catalytic domain of γ containing the intact N-terminal insert of 20 amino acids with respect to PKA,[22, 93] the first 13-14 residues of the N-terminus lacked sufficient density for structural determination.[22] On the basis of the position and orientation of the remaining residues in the N-terminus, showing them to project into the solvent, it was hypothesized that these residues were mobile.[22] Our H/D exchange analysis of this region of γ in the context of the entire PhK complex is consistent with this hypothesis, showing a region (residues 3-25) that includes the N-terminus to undergo medium exchange (31-42%) throughout the entire time course (Figure 4.2A). These results suggest this region to be relatively solvent accessible and unlikely to be a subunit interaction site in the non-activated conformer of PhK.

4.3.2.2 Catalytic domain: 21-298.

A comparison of the crystal structures of the catalytic domains of PKA and PhK γ,[22] which are 33% sequence similar,[22] show γ to have the typical bilobal protein kinase fold, comprising an N-terminal lobe with mixed α-helical, β-sheet secondary structure, connected through a flexible hinge to a large primarily helical C-terminal lobe. A large catalytic cleft is at the interface between the lobes, with nucleotide and protein substrate binding occurring primarily at sites in the N- and C-terminal lobes, respectively.[93] Active site accessibility is determined by the positions of the lobes with respect to each other, and a translation of approximately 9Å, progressing from an open to a closed conformation, occurs when ATP is bound in the active site cleft.[124] The catalytic domains of protein kinases are dynamic structures, in which conformational transitions are controlled by a flexible network of hydrophobic residues, termed

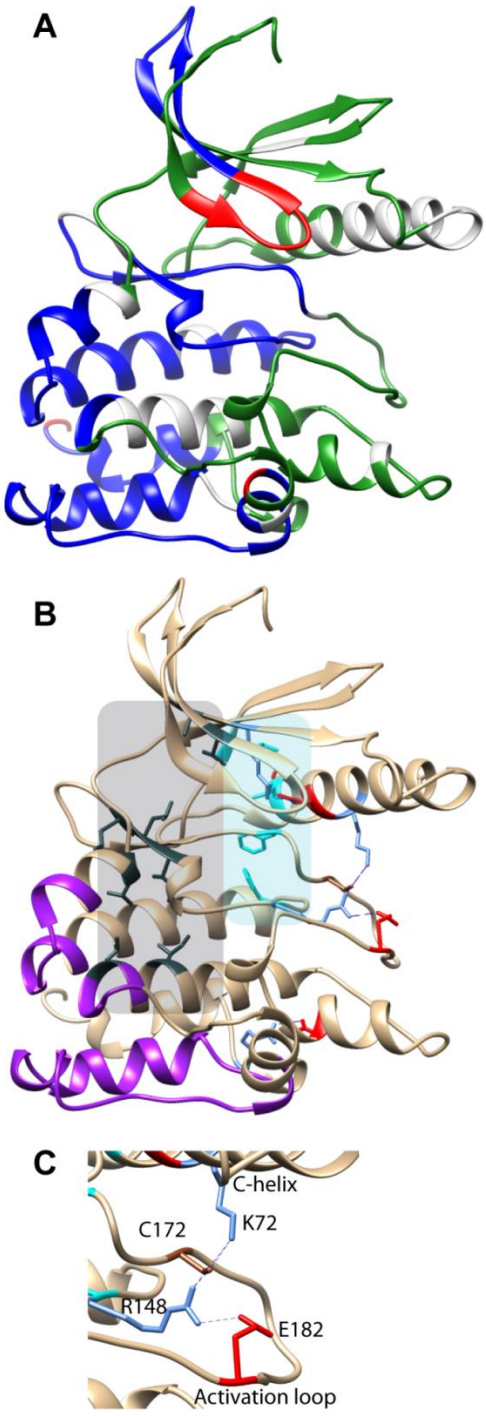

Figure 4.2 H/D exchange analysis of the γ subunit catalytic domain.

(A) Crystal structure (PDB entry 1PHK) of the catalytic domain of PHK γ [22], with HDX results (10 min) mapped onto the structure as indicated in Fig 1. (B) Structural features of the catalytic domain, including hydrophobic residues composing the R (cyan) and C (slate gray) spines, with the side chains colored and shaded as indicated. The region of this domain implicated as a subunit contact region [16] is indicated by the purple ribbon structure. (C) Magnified view of the stabilizing interaction network between the C-helix and activation loop of the catalytic cleft.

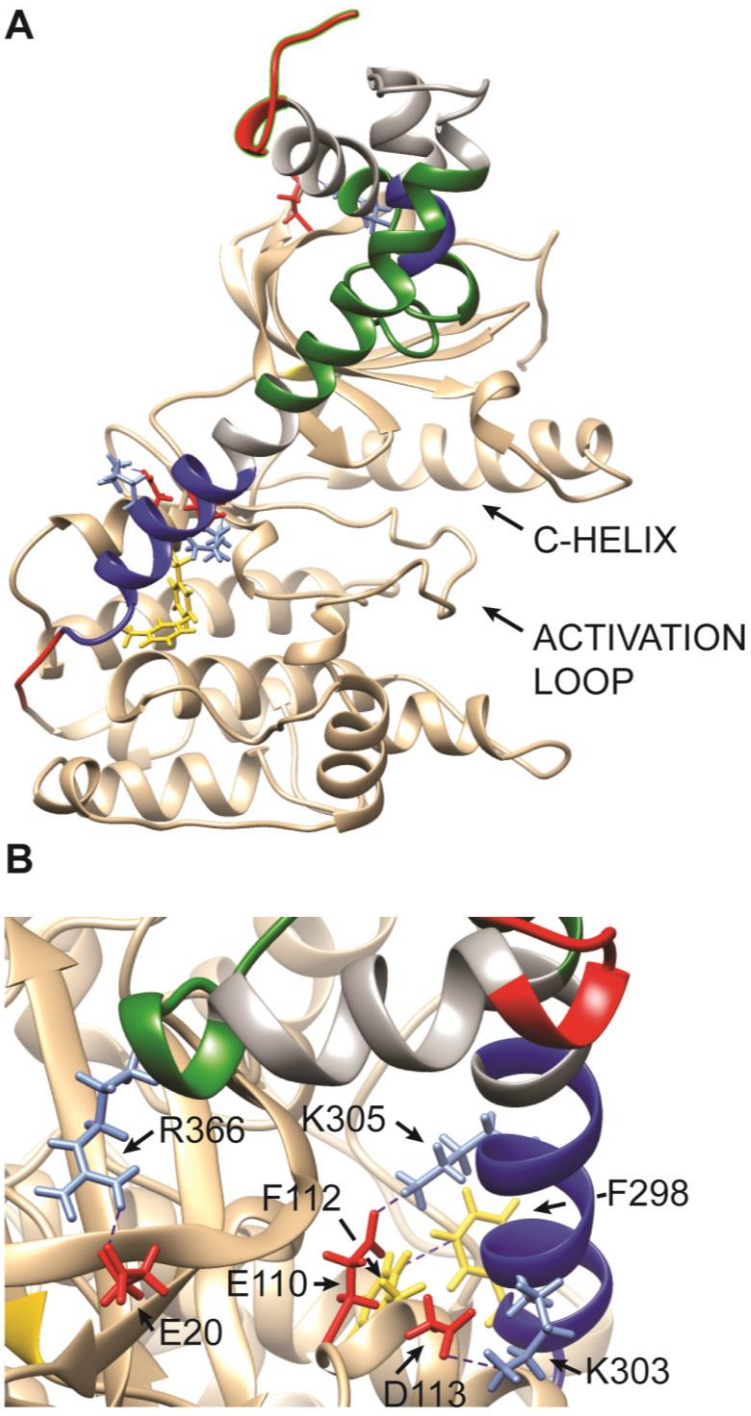

Figure 4.3 I-TASSER threading model of the full-length γ-subunit

(A) Catalytic domain (tan) with CRD (grey) overlaid with the exchange results (10 min) as indicated under Fig 1. (B). Expanded view of side chain contacts between residues from the catalytic domain and the γCRD.

spines,[125-127] that form a 3D network of interactions[124] that traverse the kinase core from the F-helix in the C-lobe to the extended β sheet of the N-lobe (Figure 4.2B). Two distinct groupings of hydrophobic residues have been characterized, the regulatory (R) and the catalytic (C) spines, both of which are conserved in eukaryotic protein kinases.[124] Full assembly of the R spine is a characteristic of activated kinase structures, as observed in crystal structures of the catalytic domain of γ, which is constitutively active as a free truncated subunit.[75] Disruption of this spine leads to kinase inactivation.[124] The R spine comprises four residues (His147, Phe168, Leu77 and Leu89) in the γ subunit of PhK. H/D exchange in regions containing His147 and Phe169 was low through 90 min (Table 4.2), with the former region remaining at this level for 6 h and the latter increasing to medium exchange. The region (residues 74-99, Table 4.2) containing Leu77 and Leu89 (Table 4.2) comprises approximately 1.5 turns of a helix (74-80), a connecting loop (81-88) and part of a β-sheet (89-99), with both residues occupying positions near the loop junctions. In PKA, two residues in β5 (Met120 and Met118) form part of a shell that surrounds the R spine that is important for kinase regulation.[128] Mutation of Met120 to Phe in several kinases leads to activation,[129] and in the γ subunit of PhK,[21] the Met120 equivalent is Phe103. The low to moderate exchange observed for these regions in γ suggests the presence of a fully or nearly intact spine. The C-spine, which comprises residues Ala26, Val33, Leu156, Leu157, Leu111, Ile155, Leu222 and Ile218 in γ, is assembled in the presence of adenine analogs, and couples β2 and β3 in the N-lobe with helices D and E in the C-lobe through contacts with the adenine and ribose rings.[124] H/D exchange coverage was measured for all but two of these residues, with low levels of exchange observed for the majority of residues detected. Despite the absence of ATP, the exchange levels for these residues are consistent with low solvent exposure in the complex or full/partial assembly of the spine.[124]

The activation loop for the active site of γ, residues 178-185, is part of a long extended loop (167-193) that begins and ends with two highly conserved motifs, DFG and APE, respectively.[21] Glu193 in the APE motif forms a salt bridge with Arg275 in the loop between the H and I helices.[22] In PKA disruption of this interaction by mutation leads to significant decreases in its activity.[130] We observed that regions containing these loops were initially low exchanging, transitioning to medium exchange at later time points, consistent with the presence of the stabilizing salt bridge. Typically, the activation loops of kinases in active conformers are phosphorylated, resulting in the formation of an ion pair between the phosphorylated residue and a positively charged residue at the N-terminus of Helix C. In PKA, the former and latter are phospho-Thr197 and His87. This key phosphorylated residue is replaced in γ with Glu182, which is another marker of activation in the γ kinase core.[22] Unlike phospho-Thr187 in PKA, Glu182 does not form any direct contacts with the C-helix, rather it is indirectly linked to the C-helix through a previously described network of interactions that includes residues Arg148 and Cys172 in loops proximal to the active site and Lys72 in Helix C (Figure 4.2C). Glu182 forms an ion pair with Arg148, which is proximal to Cys172 (3.47Å), and Cys172 is within H-bonding distance (2.73Å) with Lys72 in the C-helix,[22] mimicking the stabilizing interaction between the activation loop and helix C in PKA. Despite Arg148, Cys172 and Glu182 being in loops, we observed that the regions containing them exchange at low levels initially, followed by medium exchange through the time course. Further, although exchange for Lys72 was not measurable, regions bracketing it underwent low or low to medium exchange. The culmination of exchange data for all four of these residues support the stabilizing interaction network described above and the constitutive activity observed for the isolated γ subunit in solution.[75]

Table 4.2 Data Consolidated Regions of the γ Subunit

Data Consolidated Regions[a]	15 sec[b] (%D)		10 min[b] (%D)		90 min[b] (%D)		6 h[b] (%D)	
3-25	31	Med	42	Med	41	Med	42	Med
26-30	56	Med	70	High	70	High	70	High
31	70	High	70	High	70	High	70	High
32	30	Low	100	High	90	High	100	High
33-44	4	Low	14	Low	28	Low	37	Med
45-58	24	Low	31	Med	24	Low	24	Low
74-99	19	Low	32	Med	39	Med	45	Med
102-111	19.1	Low	51	Med	53.9	Med	55	Med
114-134	5.4	Low	15.1	Low	29	Low	36	Med
137-141	0	Low	0	Low	0	Low	0	Low
142-156	9	Low	14	Low	22	Low	30	Low
160-170	8.8	Low	30.4	Low	39	Med	47	Med
172-196	23	Low	34	Med	34	Med	36	Med
199-212	19	Low	37	Med	41	Med	42	Med
222-233	15	Low	15	Low	5	Low	8	Low
224-236	25	Low	31	Med	31	Med	28	Low
237	100	High	100	High	100	High	100	High
238	0	Low	20	Low	80	High	100	High
240-267	14	Low	30	Low	41	Med	44	Med
270-279	25	Low	46	Med	49	Med	55	Med
280-289	8	Low	12	Low	20	Low	28	Low
290-295	73	High	79	High	78	High	79	High
296-309	17	Low	26	Low	32	Med	32	Med
317-330	23	Low	55	Med	61	High	61	High
353-369	32	Med	34.6	Med	39	Med	42	Med
381-386	61	High	69.9	High	65	High	62	High

[a]Regions showing the deuterated coverage of the entire γ-subunit, with the percent deuterium incorporated and the resulting classification of that region listed for each time point. Data consolidation[110] has been applied to all regions, and the number of deuterons incorporated has

been converted to percentages. Overlapping peptides used for further resolution are not included. Redundant peptides (same peptide, with different charge) are also excluded; entire time courses for every peptide can be found in the supplementary material C.
[b]Four time points, out of the nine, are shown here to represent early, middle and late exchange.

The C-helix is a structural integrator whose spatial position influences the dynamics and activity of protein kinases.[131] It contains one of the spine residues, which in γ is Leu77, and any movement of the helix that displaces this residue from the spine leads to inactivation.[132] Similar to the interaction in PKA, helix C in γ is stabilized by a conserved salt bridge (3.6 Å) between Lys48 and Glu76 and the loop connecting this helix to β4; regions containing both residues predominately undergo low exchange, suggesting the presence of this stabilizing interaction in γ.

However, many of the contacts between helix C and the remainder of the core that are observed for PKA are missing in γ. As discussed above, stabilization of the C-helix through interactions with the activation loop appears to occur through contacts that are unique to γ. Taken together, our results indicate for the first time that the γ subunit is catalytically competent in the non-activated $(\alpha\beta\gamma\delta)_4$ complex, i.e., activation results from deinhibition caused by the release of quaternary constraints.

Besides its N-terminus and residues 60-66, there are two other inserts in the catalytic domain of γ that do not correspond to the sequence of the homologous PKA, namely residues 196-201 and 252-255. In the γ crystal structure, the former comprises one turn of a helix and connecting loop, which project directly into the solvent just below the activation loop.[22] Several residues (196, 199-201) of this region and residues directly flanking it undergo low levels of exchange at 15 sec, increasing to medium levels at 5 min and for the remainder of the time course. The region encompassing residues 252-255 shows similar levels of exchange, remaining at low extent until 90 min and increasing only to medium after that. This latter region includes one-half turn of a helix and part of a connecting extended loop that also project out into the solvent in the γ crystal structure.[22] The level of exchange for both of these inserts and their

solvent-exposed positions in the crystal structure suggests the possibility that they may be near subunit interaction sites in the $(\alpha\beta\gamma\delta)_4$ complex.

Using EM in conjunction with a mAb against the γ subunit, the epitope, identified as being somewhere within the stretch from 277-290, was shown to be located centrally on the interior lobes of the PhK complex.[12] To be accessible to the antibody, this region must be surface exposed, and we find that residues 270-279 rapidly undergo medium levels of exchange. In contrast, residues 280-289, immediately adjacent to this region, remain low exchanging throughout the entire time course, suggesting the actual epitope is located N-terminally in the 277-290 stretch.

From mapping partial proteolysis loops, carboxymethylation footprinting, the mAb binding site, and known sites of substrate interaction onto the crystal structure of the γ subunit, we identified a region on γ that showed no overlap with any of these experimentally identified surface exposed regions. This region was hypothesized to be a site of interaction of the γ subunit with the remainder of the PhK complex.[16] In the tertiary structure of γ, this proposed anchoring region comprised three stretches of residues in the C-terminal lobe, on the opposite side of the active site near the "bottom" of the subunit: 1) a loop connecting the D and E helices, 2) the C terminus of helix F and a portion of the loop connecting it with helix G, and 3) helix H and the two loops that bracket it. In our H/D exchange data, all three of these regions undergo low levels of exchange at 15 sec, and the majority of the residues remain at low levels of exchange throughout the time course. A few of the residues reach medium levels of exchange, but even those do not get above low levels until at least 10 min or later in the time course. These data are consistent with the hypothesis that these three regions of γ do, in fact, represent an area in which it interacts with other subunits within the complex.

4.3.2.3 The C-terminal Regulatory Domain (γCRD): 299-386.

The γCRD has no sequence homology with other protein kinases, and there is no high resolution structural information for this domain. It has, however, been previously shown to interact with all three of the regulatory subunits in PhK.[13] To gain further insights into the binding interactions of the γCRD with other subunits, we constructed an atomic model (Figure 4.3) of the full length γ subunit using the I-TASSER multiple threading approach.[102] The top 10 templates in the PDB database that corresponded to the final predicted structure for γ included two other CaMKs complexed with Ca^{2+}/CaM: DAPK and CaMKIIδ. The modeled structure of the γCRD and its position with respect to the catalytic domain most closely matched the DAPK CRD in complex with Ca^{2+}/CaM; however, a number of stabilizing contacts between the CRD and the catalytic domain observed for CaMKIIδ were also conserved in the γ model. For example, disruption of hydrophobic interactions between Phe98 and Phe292 in CaMKIIδ by mutating either residue leads to activation of the kinase,[123] and similar interactions between the corresponding residues in the homologous γ subunit (Phe112 and Phe298) are suggested by their proximity (3.6 Å). CaMKII residues Glu96 (PhK γ Asp113) and Arg297 (γ Lys303) form a salt bridge, which is mirrored by an ion pair between these corresponding residues in γ at a distance of 2.7 Å. Two additional non-conserved stabilizing contacts between the γCRD and catalytic domain are formed between Lys305 and Glu110 (2.8 Å), as well as Arg366 and Glu20 (1.83 Å). H/D exchange is low, especially at early time points, for most of the peptides containing the eight residues indicated above (Table 4.2), which is consistent with their proposed intra-subunit interactions. Although both Arg366 and Glu20 are located on peptides that undergo medium exchange, they are bracketed by high-exchanging peptides, consistent with their supplying a

stabilizing salt-bridge. Such a salt bridge would connect the N-lobe of the catalytic domain of γ with its CRD, mimicking the known stabilizing salt-bridge observed between the same domains in the crystal structure of DAPK complexed with Ca^{2+}/CaM.[122]

A large body of work has demonstrated a direct linkage between the γCRD and the δ subunit. The region of the γ subunit that interacts with the δ subunit was initially localized to its C-terminal one-quarter (residues 290-386) by truncation,[75, 133] synthetic peptides[74] and crosslinking.[3] The truncated γ subunit missing the γCRD is active, but insensitive to Ca^{2+}/CaM.[75, 133] Screening of the C-terminal quarter of γ for potential high affinity CaM-binding sequences through the use of overlapping synthetic peptides revealed two distinct, non-overlapping CaM-binding domains (CBDs).[74] The more N-terminal CBD (N-CBD) stretches from residues 297-331 and the more C-terminal CBD (C-CBD) from 337-366. Although it is not known whether only one, or both, of these CBDs interact with the δ subunit within the PhK complex, we previously gained direct evidence of an Asp-Lys salt-bridge between δ and the N-CBD of γ through the zero-length crosslinking of δ Asp93 and γ Lys325 within the complex.[3] The exchange coverage we observed for the two CBDs (Table 4.2) was 77% for the N-CBD (both termini covered similarly, but with a seven-residue gap in middle) and 47% for the C-CBD (the C-terminal half). The least exchange observed within the CBDs was for the N-terminal portion of the N-CBD, with peptide 296-309 showing low exchange for up to 30 min (28% exchange; Figure C.1) and only 32% exchange after 6 h (Figure C.1). Thus, as with zero-length crosslinking, our exchange results support the binding of δ to the N-CBD of γ within the PhK complex. We cannot, however, rule out the participation of the C-CBD in the binding of δ, inasmuch as we did not observe peptides from within the N-terminal half of the C-CBD. Moreover, it should be noted that the binding of δ within the PhK complex is likely to be

relatively dynamic, in that single molecule trajectory analyses of PhK containing δ subunit labeled at its N- and C-termini with a fluorescent donor-acceptor pair showed that subunit to repeatedly jump back-and-forth between extended and compact conformational substates under constant conditions.[134] The repeated alternate binding of δ to first a single CBD and then to two could produce such a result. Multiple non-contiguous interactions between CaM and several of its protein targets have been characterized,[135, 136] e.g., small conductance Ca^{2+}-activated potassium channels.[135] Unlike most CaM targets, both the potassium channel and PhK bind CaM in the absence of Ca^{2+}, but are activated only in its presence.[18, 137] This form of CaM binding is atypical with respect to other CaMK members, which bind and are activated by CaM only in the presence of Ca^{2+}.[120, 122] Moreover, unlike any other CaMK, the γ subunit of PhK functions as part of a large complex with three additional regulatory subunits, including the β subunit, which is predominate in the activation of PhK through phosphorylation.[5, 17]

As discussed above, the structural and functional coupling of the β and γ subunits in the $(\alpha\beta\gamma\delta)_4$ complex has been characterized by multiple methods.[12, 13, 116] Although crystal structures of the isolated catalytic domain show it to contain all the structural elements of an activated kinase,[22] the H/D exchange results herein suggest a catalytically competent conformation of γ in the non-activated PhK complex as well. Further, the successive, increased activation (deinhibiton) of the γ subunit[53] through the binding of Ca^{2+} by δ and the phosphorylation of β at its N-terminal region[12] occurs concomitantly with a parallel tier of conformational changes that increase the solvent accessibility of portions of γ.[53] Such an increase in accessibility is corroborated by the preferential binding of γ, as well as β, by subunit-specific mAbs in phospho-activated conformers of PhK[12] and by the increased chemical modification of γ in PhK complexed with Ca^{2+}.[53] Although the structural details of the coupling between β and γ that is

associated with PhK's activation remains largely unknown, we previously demonstrated through chemical crosslinking that Arg18 of β, which is in its N-terminal phosphorylatable region, and Lys303, in the N-CBD of γ, are proximal in the PhK complex.[13] In that same report, we showed that the crosslinking of these two residues within the complex was inhibited by a peptide corresponding to the N-terminal 22 residues of β. Moreover, this same peptide not only crosslinked with γ Lys303 in the complex (i.e., the same residue targeted by its parent β subunit in the PhK complex), it was also phosphorylated by PhK (Ser11 is an autophosphorylation site),[4, 13] consistent with the active site and N-CBD of γ and the phosphorylatable region of β all being relatively proximal. The sum of these results suggests a communication network involving the phosphorylatable N-terminus of β, the γ N-CBD, and δ; and in fact, the phosphorylation of PhK reduces its stringency for activation by Ca^{2+},[49] presumably mediated by the N-CBD.

Chapter 5
CONCLUSIONS

5.1 Summary

Although the structure of the PhK complex has been studied using multiple techniques, most previous studies provided low resolution information or data under non-physiological conditions. In an attempt to improve on previous findings, we have applied three different MS-based techniques that provided peptide to single residue resolution analyzing the entire complex as a whole. These techniques together have confirmed models of two of the subunits of PhK, confirmed previously hypothesized structural locations of different functional domains, provided new hypotheses concerning the orientation and location of three of the subunits within the complex, and provided information on changes that occur to the structure upon activation.

Both partial proteolysis and H/D exchange provide information on the solvent exposure of regions of each subunit. While H/D exchange is more limited in how much can be said about solvent exposure, since hydrogen-bonding and tertiary structure will also impede exchange, regions with high levels of rapid exchange can reasonably be considered surface exposed. Chemical footprinting was also employed as a complementary technique in studies of PhK. Taking information from these three techniques, combined with information gained from previous techniques, such as mAb epitopes, chemical crosslinking, and two-hybrid studies, we were able to identify a region in the γ subunit that is likely buried within the complex and therefore could be a site of inter-subunit contacts (Figure 2.2). One of the three unique inserts (252-255) found in the γ catalytic domain is found in this hypothesized inter-subunit contact site, supporting the hypothesis mentioned in the Introduction that these inserts could be regions of communication with the other subunits. One other insert (196-201) was observed to have low levels of deuteration at initial time points, also suggesting burial within the complex. The other

two unique inserts, the N-terminus and 60-66, were shown to be surface exposed regions by both partial proteolysis and H/D exchange, consistent with the lack of electron density observed for those regions in the crystal structure. Additionally, we have shown a model for the γCRD, providing for the first time a full-length structural model of the γ subunit. While subtle changes are obvious, our H/D exchange work confirms that conclusions from previous work performed on isolated γ apply to the structure of the subunit within the complex as well.

H/D exchange studies were consistent with a model for the α-subunit, presented in this dissertation, which shows a highly helical structure undergoing relatively low levels of exchange, much like that of the β-subunit model. In the partial proteolysis study, the high levels of cleavage for the α subunit indicate that this subunit is peripheral in PhK, an idea that had been previously suggested by prior work using partial proteolysis.

The regions in the α and β subunits that are unique from each other have been hypothesized to be surface exposed regions of communication based on the high hydrophilic residue content. Two-hybrid studies suggested this communication was with GP for one of the regions in α, showing interactions between the two at residues 864-1014 in α. Our partial proteolysis results show that in the intact holoenzyme, this same region (967-1041) is surface exposed, making it available for external interactions even when in complex with the other subunits. Crosslinking studies have shown that the interaction of α with GP occurs in the holoenzyme as well (Personal Communication). Taken together, these results suggest this particular region is the site of interaction and communication of PhK with GP, warranting further exploration of this site. Additionally on the α subunit, we have observed low levels of exchange on a loop in the model (373-384 and 386-406) on the face of the GHL domain, which suggests

that this region is also a region of inter-subunit contacts. This suggestion is consistent with crosslinking and other known interactions of α within the complex.

Incomplete post-translational modification was observed on the α-subunit, as the typically farnesylated Cys was found to be carboxymethylated. While this does not explain the frequency or physiological relevance of this PTM, it does provide evidence that these subunits are not always farnesylated. As PhK purifies water soluble, this has been a question since farnesylation was reported to be found on the α and β subunits. We have thus raised questions that will require further study.

The β subunit has been shown to undergo conformational changes upon activation, particularly within the region of the mAb epitope, which becomes more exposed upon phosphorylation. In our partial proteolysis results, we were able to narrow this region that undergoes changes by identifying a new loop (713-725) that becomes more exposed upon phosphorylation.

Using the data from partial proteolysis, chemical footprinting, and H/D exchange, we have been able to learn more about the regions of exposure in three of the four subunits within the complex. This has provided more information about the disposition of the subunits within the structure, to confirm and improve previously determined information about these subunits. We have also provided two new experimentally confirmed models, and provided evidence that the communication network shown via Ca^{2+} activation is present in the phospho-activated complex as well, although likely not undergoing the same conformational change.

5.2 Future Directions and Preliminary Data

As described in the introduction to this dissertation, changes in the structure and conformation of the PhK complex have been observed via various methods upon activation, by both Ca^{2+} and

phosphorylation. We have performed the partial proteolysis and the H/D exchange on the phospho-activated and pH-activated complex, respectively, and the non-activated complex, to further study these changes. The results from the partial proteolysis on the phosphorylated, activated complex are in Chapter 3. The same experiment was performed on the pH-activated complex as on the non-activated complex, but with an increased buffer pH from pH 6.8 to 8.2. This *in vitro* activation mimics the physiological activation of PhK by phosphorylation. These data will allow us to compare the solvent exposure and dynamics of the activated complex with the non-activated complex, giving a global and specific view of the effects activation has on the entire complex and individual subunits. As the partial proteolysis results on the phospho-activated complex resulted in several additional exposed loops, it is reasonable to expect that the H/D exchange results will show higher exposure in select regions. Preliminary analyses of the results seem to support this hypothesis. The communication network that was previously modeled, showing communication from the tips of the wings down through the lobes and back up, via the γCRD, will provide a basis for the connecting of all data together, and H/D exchange results will provide a more clear and resolved picture of this communications network.

5.3 Author Contributions

Mary Ashley Rimmer, Antonio Artigues, and Gerald M. Carlson designed the partial proteolysis (Chapter 2) and H/D exchange experiments (Chapters 3 and 4), which were performed by M.A.R. M.A.R. analyzed the partial proteolysis data, and Owen W. Nadeau and M.A.R. analyzed the H/D exchange. A.A., O.W.N., G.M.C. designed the carboxymethylation experiments (Chapter 2), which were performed by Victor Vasquez-Montes and analyzed by Maite Villar. Jianyi Yang and Yang Zhang at the Department of Computation Medicine and Bioinformatics, University of Michigan, performed and analyzed the α protein modeling (Chapter 3). O.W.N performed and analyzed the γCRD protein modeling. M.A.R., O.W.N. and G.M.C wrote the manuscripts.

REFERENCES

[1] Bossemeyer, D. (1995) Protein kinases--structure and function, *FEBS Lett. 369*, 57-61.

[2] Brushia, R. J., and Walsh, D. A. (1999) Phosphorylase kinase: the complexity of its regulation is reflected in the complexity of its structure, *Front. Biosci. 4*, D618-641.

[3] Jeyasingham, M. D., Artigues, A., Nadeau, O. W., and Carlson, G. M. (2008) Structural evidence for co-evolution of the regulation of contraction and energy production in skeletal muscle, *J. Mol. Biol. 377*, 623-629.

[4] Kilimann, M. W., Zander, N. F., Kuhn, C. C., Crabb, J. W., Meyer, H. E., and Heilmeyer, L. M., Jr. (1988) The α and β subunits of phosphorylase kinase are homologous: cDNA cloning and primary structure of the β subunit, *Proc. Natl. Acad. Sci. U. S. A. 85*, 9381-9385.

[5] Ramachandran, C., Goris, J., Waelkens, E., Merlevede, W., and Walsh, D. A. (1987) The interrelationship between cAMP-dependent α and β subunit phosphorylation in the regulation of phosphorylase kinase activity. Studies using subunit specific phosphatases, *J. Biol. Chem. 262*, 3210-3218.

[6] Pallen, M. J. (2003) Glucoamylase-like domains in the α- and β-subunits of phosphorylase kinase, *Protein Sci. 12*, 1804-1807.

[7] Carriere, C., Jonic, S., Mornon, J. P., and Callebaut, I. (2008) 3D mapping of glycogenosis-causing mutations in the large regulatory α subunit of phosphorylase kinase, *Biochim. Biophys. Acta 1782*, 664-670.

[8] Nadeau, O. W., Lane, L. A., Xu, D., Sage, J., Priddy, T. S., Artigues, A., Villar, M. T., Yang, Q., Robinson, C. V., Zhang, Y., and Carlson, G. M. (2012) Structure and location of the regulatory β subunits in the (αβγδ)4 phosphorylase kinase complex, *J. Biol. Chem. 287*, 36651-36661.

[9] Nadeau, O. W., Liu, W., Boulatnikov, I. G., Sage, J. M., Peters, J. L., and Carlson, G. M. (2010) The glucoamylase inhibitor acarbose is a direct activator of phosphorylase kinase, *Biochemistry. 49*, 6505-6507.

[10] Carriere, C., Mornon, J. P., Venien-Bryan, C., Boisset, N., and Callebaut, I. (2008) Calcineurin B-like domains in the large regulatory α/β subunits of phosphorylase kinase, *Proteins 71*, 1597-1606.

[11] Wilkinson, D. A., Marion, T. N., Tillman, D. M., Norcum, M. T., Hainfeld, J. F., Seyer, J. M., and Carlson, G. M. (1994) An epitope proximal to the carboxyl terminus of the α-subunit is located near the lobe tips of the phosphorylase kinase hexadecamer, *J. Mol. Biol. 235*, 974-982.

[12] Wilkinson, D. A., Norcum, M. T., Fizgerald, T. J., Marion, T. N., Tillman, D. M., and Carlson, G. M. (1997) Proximal regions of the catalytic γ and regulatory β subunits on the interior lobe face of phosphorylase kinase are structurally coupled to each other and with enzyme activation, *J. Mol. Biol. 265*, 319-329.

[13] Nadeau, O. W., Anderson, D. W., Yang, Q., Artigues, A., Paschall, J. E., Wyckoff, G. J., McClintock, J. L., and Carlson, G. M. (2007) Evidence for the location of the allosteric activation switch in the multisubunit phosphorylase kinase complex from mass spectrometric identification of chemically crosslinked peptides, *J. Mol. Biol. 365*, 1429-1445.

[14] Heilmeyer, L. M., Jr., Serwe, M., Weber, C., Metzger, J., Hoffmann-Posorske, E., and Meyer, H. E. (1992) Farnesylcysteine, a constituent of the α and β subunits of rabbit

skeletal muscle phosphorylase kinase: localization by conversion to S-ethylcysteine and by tandem mass spectrometry, *Proc. Natl. Acad. Sci. U. S. A. 89*, 9554-9558.
[15] Wang, M., and Casey, P. J. (2016) Protein prenylation: unique fats make their mark on biology, *Nat Rev Mol Cell Biol 17*, 110-122.
[16] Rimmer, M. A., Artigues, A., Nadeau, O. W., Villar, M. T., Vasquez-Montes, V., and Carlson, G. M. (2015) Mass Spectrometric Analysis of Surface-Exposed Regions in the Hexadecameric Phosphorylase Kinase Complex, *Biochemistry. 54*, 6887-6895.
[17] Yeaman, S. J., and Cohen, P. (1975) The hormonal control of activity of skeletal muscle phosphorylase kinase. Phosphorylation of the enzyme at two sites in vivo in response to adrenalin, *Eur. J. Biochem. 51*, 93-104.
[18] Cohen, P., Burchell, A., Foulkes, J. G., and Cohen, P. T. (1978) Identification of the Ca^{2+}-dependent modulator protein as the fourth subunit of rabbit skeletal muscle phosphorylase kinase, *FEBS Lett. 92*, 287-293.
[19] Paudel, H. K., and Carlson, G. M. (1990) The quaternary structure of phosphorylase kinase as influenced by low concentrations of urea. Evidence suggesting a structural role for calmodulin, *Biochem. J. 268*, 393-399.
[20] James, P., Cohen, P., and Carafoli, E. (1991) Identification and primary structure of calmodulin binding domains in the phosphorylase kinase holoenzyme, *J. Biol. Chem. 266*, 7087-7091.
[21] Reimann, E. M., Titani, K., Ericsson, L. H., Wade, R. D., Fischer, E. H., and Walsh, K. A. (1984) Homology of the γ subunit of phosphorylase b kinase with cAMP-dependent protein kinase, *Biochemistry. 23*, 4185-4192.
[22] Owen, D. J., Noble, M. E., Garman, E. F., Papageorgiou, A. C., and Johnson, L. N. (1995) Two structures of the catalytic domain of phosphorylase kinase: an active protein kinase complexed with substrate analogue and product, *Structure 3*, 467-482.
[23] Zander, N. F., Meyer, H. E., Hoffmann-Posorske, E., Crabb, J. W., Heilmeyer, L. M., Jr., and Kilimann, M. W. (1988) cDNA cloning and complete primary structure of skeletal muscle phosphorylase kinase (α subunit), *Proc. Natl. Acad. Sci. U. S. A. 85*, 2929-2933.
[24] Harmann, B., Zander, N. F., and Kilimann, M. W. (1991) Isoform diversity of phosphorylase kinase α and β subunits generated by alternative RNA splicing, *J. Biol. Chem. 266*, 15631-15637.
[25] Bender, P. K., and Emerson, C. P., Jr. (1987) Skeletal muscle phosphorylase kinase catalytic subunit mRNAs are expressed in heart tissue but not in liver, *J. Biol. Chem. 262*, 8799-8805.
[26] Wehner, M., and Kilimann, M. W. (1995) Human cDNA encoding the muscle isoform of the phosphorylase kinase γ subunit (PHKG1), *Hum. Genet. 96*, 616-618.
[27] Burwinkel, B., Shiomi, S., Al Zaben, A., and Kilimann, M. W. (1998) Liver glycogenosis due to phosphorylase kinase deficiency: PHKG2 gene structure and mutations associated with cirrhosis, *Hum. Mol. Genet. 7*, 149-154.
[28] Calalb, M. B., Fox, D. T., and Hanks, S. K. (1992) Molecular cloning and enzymatic analysis of the rat homolog of "PhK-γ T," an isoform of phosphorylase kinase catalytic subunit, *J. Biol. Chem. 267*, 1455-1463.
[29] Maichele, A. J., Burwinkel, B., Maire, I., Sovik, O., and Kilimann, M. W. (1996) Mutations in the testis/liver isoform of the phosphorylase kinase γ subunit (PHKG2) cause autosomal liver glycogenosis in the gsd rat and in humans, *Nat. Genet. 14*, 337-340.

[30] Grand, R. J., Shenolikar, S., and Cohen, P. (1981) The amino acid sequence of the δ subunit (calmodulin) of rabbit skeletal muscle phosphorylase kinase, *Eur. J. Biochem. 113*, 359-367.

[31] Nadeau, O. W., Traxler, K. W., and Carlson, G. M. (1998) Zero-length crosslinking of the β subunit of phosphorylase kinase to the N-terminal half of its regulatory α subunit, *Biochem. Biophys. Res. Commun. 251*, 637-641.

[32] Rice, N. A., Nadeau, O. W., Yang, Q., and Carlson, G. M. (2002) The calmodulin-binding domain of the catalytic γ subunit of phosphorylase kinase interacts with its inhibitory α subunit: evidence for a Ca^{2+} sensitive network of quaternary interactions, *J. Biol. Chem. 277*, 14681-14687.

[33] Ayers, N. A., Wilkinson, D. A., Fitzgerald, T. J., and Carlson, G. M. (1999) Self-association of the α subunit of phosphorylase kinase as determined by two-hybrid screening, *J. Biol. Chem. 274*, 35583-35590.

[34] Nadeau, O. W., and Carlson, G. M. (1994) Zero length conformation-dependent cross-linking of phosphorylase kinase subunits by transglutaminase, *J. Biol. Chem. 269*, 29670-29676.

[35] Ayers, N. A., Nadeau, O. W., Read, M. W., Ray, P., and Carlson, G. M. (1998) Effector-sensitive cross-linking of phosphorylase b kinase by the novel cross-linker 4-phenyl-1,2,4-triazoline-3,5-dione, *Biochem. J. 331 (Pt 1)*, 137-141.

[36] Nadeau, O. W., Traxler, K. W., Fee, L. R., Baldwin, B. A., and Carlson, G. M. (1999) Activators of phosphorylase kinase alter the cross-linking of its catalytic subunit to the C-terminal one-sixth of its regulatory α subunit, *Biochemistry. 38*, 2551-2559.

[37] Fitzgerald, T. J., and Carlson, G. M. (1984) Activated states of phosphorylase kinase as detected by the chemical cross-linker 1,5-difluoro-2,4-dinitrobenzene, *J. Biol. Chem. 259*, 3266-3274.

[38] Nadeau, O. W., Sacks, D. B., and Carlson, G. M. (1997) Differential affinity cross-linking of phosphorylase kinase conformers by the geometric isomers of phenylenedimaleimide, *J. Biol. Chem. 272*, 26196-26201.

[39] Cohen, P. (1974) The role of phosphorylase kinase in the nervous and hormonal control of glycogenolysis in muscle, *Biochem. Soc. Symp.*, 51-73.

[40] Schramm, H. J., and Jennissen, H. P. (1985) Two-dimensional electron microscopic analysis of the chalice form of phosphorylase kinase, *J. Mol. Biol. 181*, 503-516.

[41] Trempe, M. R., Carlson, G. M., Hainfeld, J. F., Furcinitti, P. S., and Wall, J. S. (1986) Analyses of phosphorylase kinase by transmission and scanning transmission electron microscopy, *J. Biol. Chem. 261*, 2882-2889.

[42] Edstrom, R. D., Meinke, M. H., Yang, X., Yang, R., and Evans, D. F. (1989) Direct observation of phosphorylase kinase and phosphorylase b by scanning tunneling microscopy, *Biochemistry. 28*, 4939-4942.

[43] Norcum, M. T., Wilkinson, D. A., Carlson, M. C., Hainfeld, J. F., and Carlson, G. M. (1994) Structure of phosphorylase kinase. A three-dimensional model derived from stained and unstained electron micrographs, *J. Mol. Biol. 241*, 94-102.

[44] Nadeau, O. W., Carlson, G. M., and Gogol, E. P. (2002) A Ca^{2+}-dependent global conformational change in the 3D structure of phosphorylase kinase obtained from electron microscopy, *Structure 10*, 23-32.

[45] Nadeau, O. W., Gogol, E. P., and Carlson, G. M. (2005) Cryoelectron microscopy reveals new features in the three-dimensional structure of phosphorylase kinase, *Protein Sci. 14*, 914-920.

[46] Priddy, T. S., MacDonald, B. A., Heller, W. T., Nadeau, O. W., Trewhella, J., and Carlson, G. M. (2005) Ca^{2+}-induced structural changes in phosphorylase kinase detected by small-angle X-ray scattering, *Protein Sci. 14*, 1039-1048.

[47] Lane, L. A., Nadeau, O. W., Carlson, G. M., and Robinson, C. V. (2012) Mass spectrometry reveals differences in stability and subunit interactions between activated and nonactivated conformers of the $(\alpha\beta\gamma\delta)_4$ phosphorylase kinase complex, *Mol Cell Proteomics 11*, 1768-1776.

[48] Traxler, K. W., Norcum, M. T., Hainfeld, J. F., and Carlson, G. M. (2001) Direct visualization of the calmodulin subunit of phosphorylase kinase via electron microscopy following subunit exchange, *J. Struct. Biol. 135*, 231-238.

[49] Brostrom, C. O., Hunkeler, F. L., and Krebs, E. G. (1971) The regulation of skeletal muscle phosphorylase kinase by Ca^{2+}, *J. Biol. Chem. 246*, 1961-1967.

[50] Burger, D., Cox, J. A., Fischer, E. H., and Stein, E. A. (1982) The activation of rabbit skeletal muscle phosphorylase kinase requires the binding of 3 Ca^{2+} per δ subunit, *Biochem. Biophys. Res. Commun. 105*, 632-638.

[51] Heilmeyer, L. M., Jr., Meyer, F., Haschke, R. H., and Fischer, E. H. (1970) Control of phosphorylase activity in a muscle glycogen particle. II. Activation by calcium, *J. Biol. Chem. 245*, 6649-6656.

[52] Ozawa, E., Hosoi, K., and Ebashi, S. (1967) Reversible stimulation of muscle phosphorylase b kinase by low concentrations of calcium ions, *J. Biochem. (Tokyo). 61*, 531-533.

[53] Nadeau, O. W., Sacks, D. B., and Carlson, G. M. (1997) The structural effects of endogenous and exogenous Ca^{2+}/calmodulin on phosphorylase kinase, *J. Biol. Chem. 272*, 26202-26209.

[54] Liu, W., Priddy, T. S., and Carlson, G. M. (2008) Physicochemical Changes in Phosphorylase Kinase Associated with Its Activation, *Protein Sci.*

[55] Paudel, H. K., and Carlson, G. M. (1990) Functional and structural similarities between the inhibitory region of troponin I coded by exon VII and the calmodulin-binding regulatory region of the catalytic subunit of phosphorylase kinase, *Proc. Natl. Acad. Sci. U. S. A. 87*, 7285-7289.

[56] Kastenschmidt, L. L., Kastenschmidt, J., and Helmreich, E. (1968) Subunit interactions and their relationship to the allosteric properties of rabbit skeletal muscle phosphorylase b, *Biochemistry. 7*, 3590-3608.

[57] King, M. M., and Carlson, G. M. (1981) Synergistic activation by Ca^{2+} and Mg^{2+} as the primary cause for hysteresis in the phosphorylase kinase reactions, *J. Biol. Chem. 256*, 11058-11064.

[58] Priddy, T. S., Middaugh, C. R., and Carlson, G. M. (2007) Electrostatic changes in phosphorylase kinase induced by its obligatory allosteric activator Ca^{2+}, *Protein Sci. 16*, 517-527.

[59] Cohen, P., Picton, C., and Klee, C. B. (1979) Activation of phosphorylase kinase from rabbit skeletal muscle by calmodulin and troponin, *FEBS Lett. 104*, 25-30.

[60] Fontana, A., de Laureto, P. P., Spolaore, B., Frare, E., Picotti, P., and Zambonin, M. (2004) Probing protein structure by limited proteolysis, *Acta Biochim. Pol. 51*, 299-321.

[61] Monti, M., and Pucci, P. (2006) Limited Proteolysis Mass Spectrometry of Protein Complexes, In *Mass Spectrometry of Protein Interactions*, pp 63-82, John Wiley & Sons, Inc.
[62] Hvidt, A. (1964) A DISCUSSION OF THE PH DEPENDENCE OF THE HYDROGEN-DEUTERIUM EXCHANGE OF PROTEINS, *C. R. Trav. Lab. Carlsberg 34*, 299-317.
[63] Hvidt, A., and Nielsen, S. O. (1966) Hydrogen exchange in proteins, *Adv. Protein Chem. 21*, 287-386.
[64] Englander, S. W., Downer, N. W., and Teitelbaum, H. (1972) Hydrogen exchange, *Annu. Rev. Biochem. 41*, 903-924.
[65] Bai, Y., Milne, J. S., Mayne, L., and Englander, S. W. (1993) Primary structure effects on peptide group hydrogen exchange, *Proteins 17*, 75-86.
[66] Konermann, L., Pan, J., and Liu, Y. H. (2011) Hydrogen exchange mass spectrometry for studying protein structure and dynamics, *Chem Soc Rev 40*, 1224-1234.
[67] Truhlar, S. M., Croy, C. H., Torpey, J. W., Koeppe, J. R., and Komives, E. A. (2006) Solvent accessibility of protein surfaces by amide H/2H exchange MALDI-TOF mass spectrometry, *J. Am. Soc. Mass Spectrom. 17*, 1490-1497.
[68] Hoofnagle, A. N., Resing, K. A., and Ahn, N. G. (2003) Protein analysis by hydrogen exchange mass spectrometry, *Annu. Rev. Biophys. Biomol. Struct. 32*, 1-25.
[69] Engen, J. R. (2009) Analysis of protein conformation and dynamics by hydrogen/deuterium exchange MS, *Anal. Chem. 81*, 7870-7875.
[70] Paudel, H. K., and Carlson, G. M. (1987) Inhibition of the catalytic subunit of phosphorylase kinase by its α/β subunits, *J. Biol. Chem. 262*, 11912-11915.
[71] Meyer, W. L., Fischer, E. H., and Krebs, E. G. (1964) Activation of Skeletal Muscle Phosphorylase B Kinase by Ca, *Biochemistry. 3*, 1033-1039.
[72] Venien-Bryan, C., Lowe, E. M., Boisset, N., Traxler, K. W., Johnson, L. N., and Carlson, G. M. (2002) Three-dimensional structure of phosphorylase kinase at 22 Å resolution and its complex with glycogen phosphorylase b, *Structure 10*, 33-41.
[73] Venien-Bryan, C., Jonic, S., Skamnaki, V., Brown, N., Bischler, N., Oikonomakos, N. G., Boisset, N., and Johnson, L. N. (2009) The structure of phosphorylase kinase holoenzyme at 9.9 Å resolution and location of the catalytic subunit and the substrate glycogen phosphorylase, *Structure 17*, 117-127.
[74] Dasgupta, M., Honeycutt, T., and Blumenthal, D. K. (1989) The γ-subunit of skeletal muscle phosphorylase kinase contains two noncontiguous domains that act in concert to bind calmodulin, *J. Biol. Chem. 264*, 17156-17163.
[75] Harris, W. R., Malencik, D. A., Johnson, C. M., Carr, S. A., Roberts, G. D., Byles, C. A., Anderson, S. R., Heilmeyer, L. M., Jr., Fischer, E. H., and Crabb, J. W. (1990) Purification and characterization of catalytic fragments of phosphorylase kinase γ subunit missing a calmodulin-binding domain, *J. Biol. Chem. 265*, 11740-11745.
[76] Babu, Y. S., Bugg, C. E., and Cook, W. J. (1988) Structure of calmodulin refined at 2.2 Å resolution, *J. Mol. Biol. 204*, 191-204.
[77] Trempe, M. R., and Carlson, G. M. (1987) Phosphorylase kinase conformers. Detection by proteases, *J. Biol. Chem. 262*, 4333-4340.
[78] Cohen, S. L., Ferre-D'Amare, A. R., Burley, S. K., and Chait, B. T. (1995) Probing the solution structure of the DNA-binding protein Max by a combination of proteolysis and mass spectrometry, *Protein Sci. 4*, 1088-1099.

[79] Orru, S., Dal Piaz, F., Casbarra, A., Biasiol, G., De Francesco, R., Steinkuhler, C., and Pucci, P. (1999) Conformational changes in the NS3 protease from hepatitis C virus strain Bk monitored by limited proteolysis and mass spectrometry, *Protein Sci. 8*, 1445-1454.

[80] Hubbard, S. J. (1998) The structural aspects of limited proteolysis of native proteins, *Biochim. Biophys. Acta 1382*, 191-206.

[81] Neurath, H. (1980) Limited Proteolysis, Protein Folding and Physiological Regulation, In *Protein Folding* (Jaenicke, R., Ed.), pp 501-523, Elsevier/North-Holland Biomedical Press, Amsterdam.

[82] Cohen, P. (1973) The subunit structure of rabbit-skeletal-muscle phosphorylase kinase, and the molecular basis of its activation reactions, *Eur. J. Biochem. 34*, 1-14.

[83] Cohen, P., Watson, D. C., and Dixon, G. H. (1975) The hormonal control of activity of skeletal muscle phosphorylase kinase. Amino-acid sequences at the two sites of action of adenosine-3':5'-monophosphate-dependent protein kinase, *Eur. J. Biochem. 51*, 79-92.

[84] Daube, H., Billich, A., Mann, K., and Schramm, H. J. (1991) Cleavage of phosphorylase kinase and calcium-free calmodulin by HIV-1 protease, *Biochem. Biophys. Res. Commun. 178*, 892-898.

[85] Davidson, J. J., Ozcelik, T., Hamacher, C., Willems, P. J., Francke, U., and Kilimann, M. W. (1992) cDNA cloning of a liver isoform of the phosphorylase kinase α subunit and mapping of the gene to Xp22.2-p22.1, the region of human X-linked liver glycogenosis, *Proc. Natl. Acad. Sci. U. S. A. 89*, 2096-2100.

[86] Wullrich, A., Hamacher, C., Schneider, A., and Kilimann, M. W. (1993) The multiphosphorylation domain of the phosphorylase kinase α M and α L subunits is a hotspot of differential mRNA processing and of molecular evolution, *J. Biol. Chem. 268*, 23208-23214.

[87] Andreeva, I. E., Rice, N. A., and Carlson, G. M. (2002) The regulatory α subunit of phosphorylase kinase may directly participate in the binding of glycogen phosphorylase, *Biochemistry. 67*, 1197-1202.

[88] Sotiroudis, T. G., and Xenakis, A. (1990) PEST sequences present in the subunits of phosphorylase kinase, *Biochem. Int. 21*, 941-947.

[89] Rogers, S., Wells, R., and Rechsteiner, M. (1986) Amino acid sequences common to rapidly degraded proteins: the PEST hypothesis, *Science 234*, 364-368.

[90] Newsholme, P., Angelos, K. L., and Walsh, D. A. (1992) High and intermediate affinity calmodulin binding domains of the α and β subunits of phosphorylase kinase and their potential role in phosphorylation-dependent activation of the holoenzyme, *J. Biol. Chem. 267*, 810-818.

[91] Wotske, M., Wu, Y., and Wolters, D. A. (2012) Liquid chromatographic analysis and mass spectrometric identification of farnesylated peptides, *Anal. Chem. 84*, 6848-6855.

[92] Wangsgard, W. P., Meixell, G. E., Dasgupta, M., and Blumenthal, D. K. (1996) Activation and inhibition of phosphorylase kinase by monospecific antibodies raised against peptides from the regulatory domain of the γ-subunit, *J. Biol. Chem. 271*, 21126-21133.

[93] Lowe, E. D., Noble, M. E., Skamnaki, V. T., Oikonomakos, N. G., Owen, D. J., and Johnson, L. N. (1997) The crystal structure of a phosphorylase kinase peptide substrate complex: kinase substrate recognition, *EMBO J. 16*, 6646-6658.

[94] Pettersen EF, G. T., Huang CC, Couch GS, Greenblatt DM, Meng EC, Ferrin TE. (supported by NIGMS P41-GM103311). (2004) UCSF chimera-a visualization system

for exploratory research and analysis, J Comput Chem. 13, 1605-1612.1, In *UCSF Chimera package* (1PHK, I. o., Ed.), (Owen, D. J., Noble, M. E., Garman, E. F., Papageorgiou, A. C., and Johnson, L. N. (1995), Two structures of the catalytic domain of phosphorylase kinase: an active protein kinase complexed with substrate analogue and product, Structure 3, 467-482.

[95] Hilder, T. L., Carlson, G. M., Haystead, T. A., Krebs, E. G., and Graves, L. M. (2005) Caspase-3 dependent cleavage and activation of skeletal muscle phosphorylase b kinase, *Mol. Cell. Biochem. 275*, 233-242.

[96] Cohen, P. (1980) The role of calcium ions, calmodulin and troponin in the regulation of phosphorylase kinase from rabbit skeletal muscle, *Eur. J. Biochem. 111*, 563-574.

[97] Ozawa, E., and Ebashi, S. (1967) Requirement of Ca ion for the stimulating effect of cyclic 3',5'-AMP on muscle phosphorylase b kinase, *J. Biochem. (Tokyo). 62*, 285-286.

[98] Bott, R., Saldajeno, M., Cuevas, W., Ward, D., Scheffers, M., Aehle, W., Karkehabadi, S., Sandgren, M., and Hansson, H. (2008) Three-dimensional structure of an intact glycoside hydrolase family 15 glucoamylase from Hypocrea jecorina, *Biochemistry. 47*, 5746-5754.

[99] Villar, M. T., Miller, D. E., Fenton, A. W., and Artigues, A. (2010) SAIDE: A Semi-Automated Interface for Hydrogen/Deuterium Exchange Mass Spectrometry, *Proteomica 6*, 63-69.

[100] Prasannan, C. B., Villar, M. T., Artigues, A., and Fenton, A. W. (2013) Identification of regions of rabbit muscle pyruvate kinase important for allosteric regulation by phenylalanine, detected by H/D exchange mass spectrometry, *Biochemistry. 52*, 1998-2006.

[101] Yang, J., Yan, R., Roy, A., Xu, D., Poisson, J., and Zhang, Y. (2015) The I-TASSER Suite: protein structure and function prediction, *Nature methods 12*, 7-8.

[102] Zhang, Y. (2008) I-TASSER server for protein 3D structure prediction, *BMC bioinformatics 9*, 40.

[103] Wu, S., and Zhang, Y. (2007) LOMETS: a local meta-threading-server for protein structure prediction, *Nucleic Acids Res 35*, 3375-3382.

[104] Xue, Z., Xu, D., Wang, Y., and Zhang, Y. (2013) ThreaDom: extracting protein domain boundary information from multiple threading alignments, *Bioinformatics 29*, i247-256.

[105] Zhang, Y., and Skolnick, J. (2004) SPICKER: a clustering approach to identify near-native protein folds, *Journal of computational chemistry 25*, 865-871.

[106] Li, Y., and Zhang, Y. (2009) REMO: A new protocol to refine full atomic protein models from C-alpha traces by optimizing hydrogen-bonding networks, *Proteins 76*, 665-676.

[107] Maertens, G. N., Cook, N. J., Wang, W., Hare, S., Gupta, S. S., Oztop, I., Lee, K., Pye, V. E., Cosnefroy, O., Snijders, A. P., KewalRamani, V. N., Fassati, A., Engelman, A., and Cherepanov, P. (2014) Structural basis for nuclear import of splicing factors by human Transportin 3, *Proc. Natl. Acad. Sci. U. S. A. 111*, 2728-2733.

[108] Strom, A. C., and Weis, K. (2001) Importin-β-like nuclear transport receptors, *Genome Biol 2*, REVIEWS3008.

[109] Mizuno, M., Tonozuka, T., Suzuki, S., Uotsu-Tomita, R., Kamitori, S., Nishikawa, A., and Sakano, Y. (2004) Structural insights into substrate specificity and function of glucodextranase, *J. Biol. Chem. 279*, 10575-10583.

[110] Pascal, B. D., Chalmers, M. J., Busby, S. A., and Griffin, P. R. (2009) HD desktop: an integrated platform for the analysis and visualization of H/D exchange data, *J. Am. Soc. Mass Spectrom. 20*, 601-610.

[111] Xu, J., and Zhang, Y. (2010) How significant is a protein structure similarity with TM-score = 0.5?, *Bioinformatics 26*, 889-895.
[112] Svensson, B., and Sierks, M. R. (1992) Roles of the aromatic side chains in the binding of substrates, inhibitors, and cyclomalto-oligosaccharides to the glucoamylase from Aspergillus niger probed by perturbation difference spectroscopy, chemical modification, and mutagenesis, *Carbohydr. Res. 227*, 29-44.
[113] Liu, H. L., and Wang, W. C. (2003) Predicted unfolding order of the 13 α-helices in the catalytic domain of glucoamylase from Aspergillus awamori var. X100 by molecular dynamics simulations, *Biotechnol. Prog. 19*, 1583-1590.
[114] Forwood, J. K., Lonhienne, T. G., Marfori, M., Robin, G., Meng, W., Guncar, G., Liu, S. M., Stewart, M., Carroll, B. J., and Kobe, B. (2008) Kap95p binding induces the switch loops of RanGDP to adopt the GTP-bound conformation: implications for nuclear import complex assembly dynamics, *J. Mol. Biol. 383*, 772-782.
[115] Ozawa, E. (1973) Activation of phosphorylase kinase from brain by small amounts of calcium ion, *J. Neurochem. 20*, 1487-1488.
[116] Thompson, J. A., Nadeau, O. W., and Carlson, G. M. (2015) A model for activation of the hexadecameric phosphorylase kinase complex deduced from zero-length oxidative crosslinking, *Protein Sci. 24*, 1956-1963.
[117] Chattopadhyaya, R., Meador, W. E., Means, A. R., and Quiocho, F. A. (1992) Calmodulin structure refined at 1.7 Å resolution, *J. Mol. Biol. 228*, 1177-1192.
[118] Roy, A., Kucukural, A., and Zhang, Y. (2010) I-TASSER: a unified platform for automated protein structure and function prediction, *Nature protocols 5*, 725-738.
[119] Thompson, J. A. a. C., G.M. (2016) Unpublished results.
[120] Hook, S. S., and Means, A. R. (2001) Ca^{2+}/CaM-dependent kinases: from activation to function, *Annu. Rev. Pharmacol. Toxicol. 41*, 471-505.
[121] Manning, G., Whyte, D. B., Martinez, R., Hunter, T., and Sudarsanam, S. (2002) The protein kinase complement of the human genome, *Science 298*, 1912-1934.
[122] de Diego, I., Kuper, J., Bakalova, N., Kursula, P., and Wilmanns, M. (2010) Molecular basis of the death-associated protein kinase-calcium/calmodulin regulator complex, *Sci Signal 3*, ra6.
[123] Rellos, P., Pike, A. C., Niesen, F. H., Salah, E., Lee, W. H., von Delft, F., and Knapp, S. (2010) Structure of the CaMKIIδ/calmodulin complex reveals the molecular mechanism of CaMKII kinase activation, *PLoS Biol 8*, e1000426.
[124] Kornev, A. P., and Taylor, S. S. (2015) Dynamics-Driven Allostery in Protein Kinases, *Trends Biochem. Sci. 40*, 628-647.
[125] Kornev, A. P., Haste, N. M., Taylor, S. S., and Eyck, L. F. (2006) Surface comparison of active and inactive protein kinases identifies a conserved activation mechanism, *Proc. Natl. Acad. Sci. U. S. A. 103*, 17783-17788.
[126] Kornev, A. P., Taylor, S. S., and Ten Eyck, L. F. (2008) A helix scaffold for the assembly of active protein kinases, *Proc. Natl. Acad. Sci. U. S. A. 105*, 14377-14382.
[127] Taylor, S. S., and Kornev, A. P. (2011) Protein kinases: evolution of dynamic regulatory proteins, *Trends Biochem. Sci. 36*, 65-77.
[128] Meharena, H. S., Chang, P., Keshwani, M. M., Oruganty, K., Nene, A. K., Kannan, N., Taylor, S. S., and Kornev, A. P. (2013) Deciphering the structural basis of eukaryotic protein kinase regulation, *PLoS Biol 11*, e1001680.

[129] Azam, M., Seeliger, M. A., Gray, N. S., Kuriyan, J., and Daley, G. Q. (2008) Activation of tyrosine kinases by mutation of the gatekeeper threonine, *Nature structural & molecular biology 15*, 1109-1118.
[130] Yang, J., Wu, J., Steichen, J. M., Kornev, A. P., Deal, M. S., Li, S., Sankaran, B., Woods, V. L., Jr., and Taylor, S. S. (2012) A conserved Glu-Arg salt bridge connects coevolved motifs that define the eukaryotic protein kinase fold, *J. Mol. Biol. 415*, 666-679.
[131] Taylor, S. S., Yang, J., Wu, J., Haste, N. M., Radzio-Andzelm, E., and Anand, G. (2004) PKA: a portrait of protein kinase dynamics, *Biochim. Biophys. Acta 1697*, 259-269.
[132] Kannan, N., and Neuwald, A. F. (2005) Did protein kinase regulatory mechanisms evolve through elaboration of a simple structural component?, *J. Mol. Biol. 351*, 956-972.
[133] Cox, S., and Johnson, L. N. (1992) Expression of the phosphorylase kinase γ subunit catalytic domain in Escherichia coli, *Protein Eng. 5*, 811-819.
[134] Priddy, T. S., Price, E. S., Johnson, C. K., and Carlson, G. M. (2007) Single molecule analyses of the conformational substates of calmodulin bound to the phosphorylase kinase complex, *Protein Sci. 16*, 1017-1023.
[135] Schumacher, M. A., Rivard, A. F., Bachinger, H. P., and Adelman, J. P. (2001) Structure of the gating domain of a Ca^{2+}-activated K^+ channel complexed with Ca^{2+}/calmodulin, *Nature 410*, 1120-1124.
[136] Vlach, J., Samal, A. B., and Saad, J. S. (2014) Solution structure of calmodulin bound to the binding domain of the HIV-1 matrix protein, *J. Biol. Chem. 289*, 8697-8705.
[137] Ledoux, J., Bonev, A. D., and Nelson, M. T. (2008) Ca^{2+}-activated K^+ channels in murine endothelial cells: block by intracellular calcium and magnesium, *J. Gen. Physiol. 131*, 125-135.

APPENDIX A

Supplementary Data: Chapter 2

Table A.1 Complete List of Partial Proteolysis Peptides

Phospho-activated PhK: Chymotrypsin Number of runs: 3	**Position**	**MH+**	**m/z**	**z**	**XCorr**	**# runs obs.**
Alpha						
VTKAKEL	703-709	788.49	788.49	1	1.57	3
LPTKLF	718-723	718.45	718.45	1	1.81	3
KSEIKQVEF	1006-1014	1107.60	554.30	2	3.49	3
LSKAATY*	1217-1224	824.45	824.45	1	2.11	2
Beta						
aGATGLMAEVSWKVL	1-15	1574.82	1574.82	1	2.90	3
GAAFTQKFSSIAPHITTF	784-802	2011.03	1006.01	2	4.20	2
LVHGKQVTL*	803-811	994.61	994.61	1	1.94	2
Gamma						
TRDAALPGSHSTHGFY	1-16	1716.81	858.90	2	4.35	3
TAEEALAHPF	277-286	1085.52	1085.52	1	2.50	2
TAEEALAHPF	277-286	1085.53	543.26	2	3.64	1
FQQYVVEEVRHF	287-298	1580.79	790.89	2	3.90	2
ENTPKAVLF	371-379	1018.56	509.78	2	2.30	3
SLAEDDY	380-386	812.33	812.33	1	1.85	3
Non-Activated PhK: Chymotrypsin Number of runs: 5	**Position**	**MH+**	**m/z**	**z**	**Xcorr**	**# runs obs.**
Alpha						
LPTKLF	718-723	718.45	718.45	1	1.94	5
KSEIKQVEF	1006-1014	1107.61	554.31	2	3.57	5
KSEIKQVEFRRL	1006-1017	1532.89	766.95	2	2.16	4
Beta						
aGATGLMAEVSWKVL	1-15	1574.83	1574.83	1	2.78	5
LAVRYGAAF	779-787	967.54	967.54	1	1.72	3
TQKFSSSIAPHITTF	788-802	1664.87	832.94	2	4.08	4
LVHGKQVTL	803-811	994.60	994.60	1	2.41	2
Gamma						
TAEEALAHPF	277-286	1085.53	1085.53	1	1.91	3
FQQYVVEEVRHF	287-298	1580.79	790.90	2	3.68	4
ENTPKAVLF	371-379	1018.56	1018.56	1	1.72	3
SLAEDDY	380-386	812.33	812.33	1	2.02	2
Phospho-activated PhK: Lys C Number of runs: 3	**Position**	**MH+**	**m/z**	**z**	**XCorr**	**# runs obs.**
Alpha						
LAPASQK	677-683	714.42	714.42	1	1.63	3
ELHVQNVHMYLPTK	708-721	1708.88	854.94	2	4.45	3
TERTGIMQLK	997-1006	1176.64	588.82	2	3.03	2
Beta						
aGATGLMAEVSWK	1-13	1362.67	1362.67	2	3.57	2
SFEELEPPKHSK	683-694	1427.72	714.36	2	2.82	2
Non-activated PhK: Lys C Number of runs: 6	**Position**	**MH+**	**m/z**	**z**	**XCorr**	**# runs obs.**
Alpha						
LAPASQK	677-683	714.43	714.43	1	1.73	2
GGLNRFRAAVQTTCDLMSLVTKAK	684-707	2580.42	645.86	4	3.15	2
GGLNRFRAAVQTTCDLMSLVTKAK	684-707	2580.38	860.80	3	4.68	2
AKELHVQNVHMYLPTK	706-721	1908.01	636.68	3	5.38	2
AKELHVQNVHMYLPTK	706-721	1908.01	954.51	2	5.38	1
TERTGIMQLKSEIK	997-1010	1633.89	545.30	3	3.61	1
TERTGIMQLKSEIK	997-1010	1633.89	817.45	2	3.74	2
Beta						
aGATGLMAEVSWKVLERRARTK	1-22	2472.37	824.79	3	3.42	3
RSGSVYEPLK	23-32	1135.61	568.31	2	3.14	3
SFEELEPPKHSKVK	683-696	1654.88	827.94	2	3.35	3
FSSSIAPHITTFLVHGK	791-807	1841.99	921.50	2	3.16	

Gamma						
KGQQQNRAALFENTPKAVLFSLAEDDY	360-386	3053.54	1018.52	3	4.48	3
Non-activated PhK: Thermolysin Number of runs: 3	**Position**	**MH+**	**m/z**	**z**	**XCorr**	**# runs obs.**
Alpha						
LAPASQKGGLNR	677-688	1211.69	1211.69	1	2.74	3
LMSLVTKAKE	699-708	1119.64	1119.64	1	2.51	3
LVTKAKELHVQNVHMYLPTKL	702-722	2462.40	821.47	3	3.99	
FQASRPSLNLLDSSHPSQEDQVPT	723-746	2653.28	1327.15	2	3.06	3
ISIHEIGAVGATKTERTGIMQ	984-1004	2212.18	1106.59	2	5.69	3
LKSEIKQVE	1005-1013	1073.62	1073.62	1	2.18	1
LKSEIKQVE	1005-1013	1073.62	537.31	2	2.24	2
LSISTESQPNGGHSLGADLMSPSF	1017-1040	2432.14	1216.57	2	3.87	3
IHSIGSIIAVEKIVH	1156-1170	1615.92	808.47	2	2.24	3
Beta						
aGATGLMAEVSWKVLERRARTK	1-22	2472.35	824.79	3	3.01	3
Gamma						
TRDAALPGSHSTHGFYENYEPKE	1-23	2606.20	869.40	3	3.37	3
Phospho-activated PhK: Protease V8 Number of runs: 4	**Position**	**MH+**	**m/z**	**z**	**XCorr**	**# runs obs.**
Alpha						
LMSLVTKAKE	699-708	1119.64	1119.64	1	2.53	1
LMSLVTKAKE	699-708	1119.64	560.33	2	3.27	3
LHVQNVHMYLPTKLFQASRPSLNLLDSSHPSQE	709-741	3786.95	947.49	4	5.92	4
FGVERSVRPTDSNVSPAISIHE	967-988	2397.22	799.74	3	3.64	4
IGAVGATKTERTGIMQLKSEIKQVE	989-1013	2687.47	896.50	3	3.47	1
IGAVGATKTERTGIMQLKSEIKQVE	989-1013	2687.47	1352.23	3	5.22	3
GFVLPSSTTRE	1103-1113	1193.62	1193.62	1	2.11	4
Beta						
aGATGLMAE	1-9	862.40	862.40	1	1.78	4
VSVTEWRNKPTHE	713-725	1582.80	791.90	2	2.78	4
Gamma						
TRDAALPGSHSTHGFYE	1-17	1845.84	923.43	2	4.45	4
NYEPKE	18-23	779.36	779.26	1	2.03	4
YAVKIIDVTGGGSFSAEE	45-62	1842.91	921.96	2	4.65	2
VQELRE	63-68	773.42	773.42	1	1.88	4
LREATLKE	66-73	959.55	959.55	1	2.02	4
VCGTPSYLAPEIIE	184-196	1491.74	1491.74	1	2.56	3
EALAHPFFQQYVVEE	280-294	1806.87	903.94	2	2.51	4
Non-activated PhK: Protease V8 Number of runs: 5	**Position**	**MH+**	**m/z**	**z**	**XCorr**	**# runs obs.**
Alpha						
LMSLVTKAKE	699-708	1119.65	1119.65	1	2.36	1
LMSLVTKAKE	699-708	1119.65	560.33	2	3.49	4
LHVQNVHMYLPTKLFQASRPSLNLLDSSHPSQE	709-741	3786.96	1262.99	3	5.47	1
LHVQNVHMYLPTKLFQASRPSLNLLDSSHPSQE	709-741	3786.96	947.49	4	5.91	4
FGVERSVRPTDSNVSPAISIHE*	967-988	2397.22	799.75	3	4.01	4
IGAVGATKTERTGIMQLKSEIKQVE	989-1013	2687.48	896.50	3	5.38	3
IGAVGATKTERTGIMQLKSEIKQVE	989-1013	2687.48	672.63	4	5.46	2
Beta						
aGATGLMAE	1-9	862.40	862.40	1	1.83	5
VSWKVLE	10-16	860.49	860.49	1	1.74	5
Gamma						
TRDAALPGSHSTHGFYE	1-17	1845.85	923.43	2	4.32	5
YAVKIIDVTGGGSFSAEE	45-62	1842.91	921.96	2	3.73	3
VQELRE	63-68	773.42	773.42	1	1.55	3
ALAHPFFQQYVVEE	281-294	1677.83	839.42	2	3.05	5
Phospho-activated PhK: Trypsin Number of runs: 6	**Position**	**MH+**	**m/z**	**z**	**XCorr**	**# runs obs.**
Alpha						
LYSEDYDDNYDELESGDQMDGYNSTSTAR	627-655	3411.33	1706.17	2	4.15	4
CGDEVAR	656-662	749.33	749.33	1	2.37	2
YLDHLLAHTAPHPK	663-676	1612.86	806.93	2	4.87	5
LAPASQKGGLNRFR	677-690	1514.86	757.93	2	2.77	5
AAVQTTCDLMSLVTKAK	691-707	1779.93	890.47	2	3.99	2
ELHVQNVHMYLPTK	708-721	1708.88	854.95	2	4.64	5

LFQASRPSLNLLDSSHPSQEDQVPTVR	722-748	3021.54	1007.85	3	5.48	5
TGIMQLKSEIKQVEFR	1000-1015	1907.05	954.03	2	5.61	5
Beta						
aGATGLMAEVSQKVLERR	1-18	2016.07	1008.54	2	4.17	5
SGsVYEPLK	24-32	1059.48	1059.48	1	2.13	5
Gamma						
TRDAALPGSHSTHGFYENYEPKEILGR	1-27	3045.48	1015.83	3	5.52	2
TRDAALPGSHSTHGFYENYEPKEILGR	1-27	3045.48	762.13	4	5.63	3
EATLKEVDILR	68-78	1286.73		2	3.02	
YTAEEALAHPFFQQYVVEEVR	276-296	2526.22	1263.61	2	4.23	1
YTAEEALAHPFFQQYVVEEVR	276-296	2526.22	842.75	3	3.49	1
AALFENTPKAVLFSLAEDDY	367-386	2214.10	1107.55	2	5.23	5
Non-activated PhK: Trypsin Number of runs: 7	**Position**	**MH+**	**m/z**	**z**	**XCorr**	**# runs obs.**
Alpha						
YLDHLLAHTAPHPKLAPASQKGGLNR	663-688	2805.52	935.85	3	5.22	7
LAPASQKGGLNRFR	677-690	1514.85	757.93	2	2.84	7
ELHVQNVHMYLPTKLFQASRPSLNLLDSSHPSQEDQVPTVR	708-748	4711.43	1178.61	4	5.65	5
ELHVQNVHMYLPTK	708-722	1708.89	854.95	2	4.38	7
LFQASRPSLNLLDSSHPSQEDQVPTVR	722-748	3021.54	1007.85	3	5.75	7
SVRPTDSNVSPAISIHEIGAVGATKTER	972-999	2892.52	964.85	3	6.87	7
TGIMQLKSEIKQVEFR	1000-1015	1907.05	954.03	2	5.73	7
Beta						
aGATGLMAEVSWKVLERR	1-18	2016.08	1008.54	2	4.06	7
SGSVYEPLK	24-32	979.51	979.51	1	2.33	5
SGSVYEPLK	24-32	979.51	490.26	2	2.31	2
SFEELEPPKHSK	683-694	1427.72	714.36	2	3.25	6
Gamma						
TRDAALPGSHSTHGFYENYEPKEILGR	1-27	3045.48	1015.83	3	6.81	7
AALFENTPKAVLFSLAEDDY	367-386	2214.12	1107.56	2	5.11	7
Non-activated PhK: Ficin Number of runs: 3	**Position**	**MH+**	**m/z**	**z**	**XCorr**	**# runs obs.**
Alpha						
ISELNASSVGMAKAALE	194-210	1690.85	845.93	2	2.23	3
LPTKLF	718-723	718.45	718.45	1	1.65	3
LFQASRPSLNLLDSSHPSQEDQVPTVR	722-748	3021.54	1007.85	3	5.06	3
EIGAVGATKTERTGIMQLKSEIKQV	988-1012	2687.48	1344.24	2	2.07	2
EIGAVGATKTERTGIMQLKSEIKQV	988-1012	2687.48	896.50	3	2.59	1
ADLMSPSFL	1033-1041	980.47	980.47	1	1.86	3
Beta						
aGATGLMAEVSWKVLERRARTK	1-22	2472.35	824.79	3	2.62	3
SVYEPLK	26-32	835.46	835.46	1	1.57	3
Gamma						
TRDAALPGSHSTHGFYENYEPKEILG	1-26	2889.38	963.80	3	4.50	3
AALFENTPKAVLFSLAEDDY	367-386	2214.10	1107.55	2	3.58	3
Non-activated PhK: Arg C Number of runs: 3	**Position**	**MH+**	**m/z**	**z**	**XCorr**	**# runs obs.**
Beta						
aGATGLMAEVSQKVLERRAR	1-20	2243.22	748.41	3	2.54	6

Lower case letters denote modification. The N-terminus of β is acetylated and the serine 26 in phospho-activated trypsin samples is phosphorylated where denoted. The number of experiments using each protease is listed next to the protease with the number of times each peptide was observed listed in the far right column. If the same peptide was observed with different modifications or charges, however, these are each listed separately.

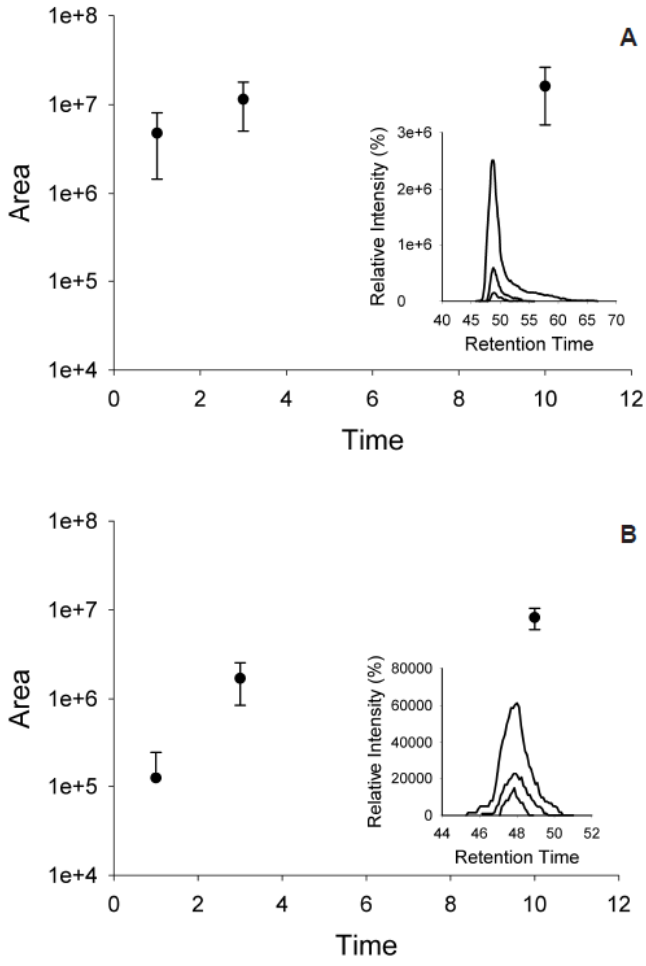

Figure A.1 Quantification of Peptide β1-15

Representative label-free quantification analysis for the release of peptide β1-15 (m/z = 795.91) from the partial proteolysis of PhK by chymotrypsin. This was done by measuring the area under the curve of the base peak from each time point. Insets are chromatograms from a representative time course for reference. Non-activated (A) and phospho-activated (B) conformers are both shown here.

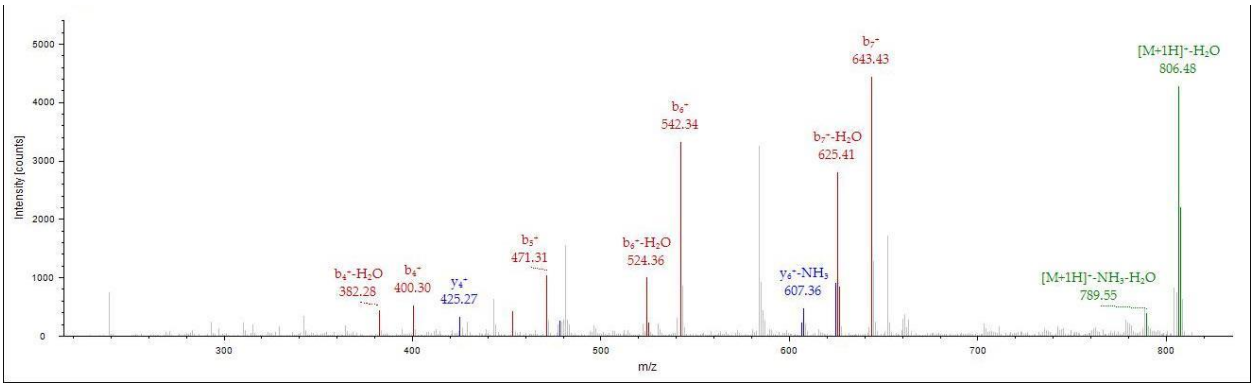

Figure A.2 MS/MS of Peptide 1217-1224 of Phospho-Activated PhK subunit

APPENDIX B

Supplementary Data: Chapter 3

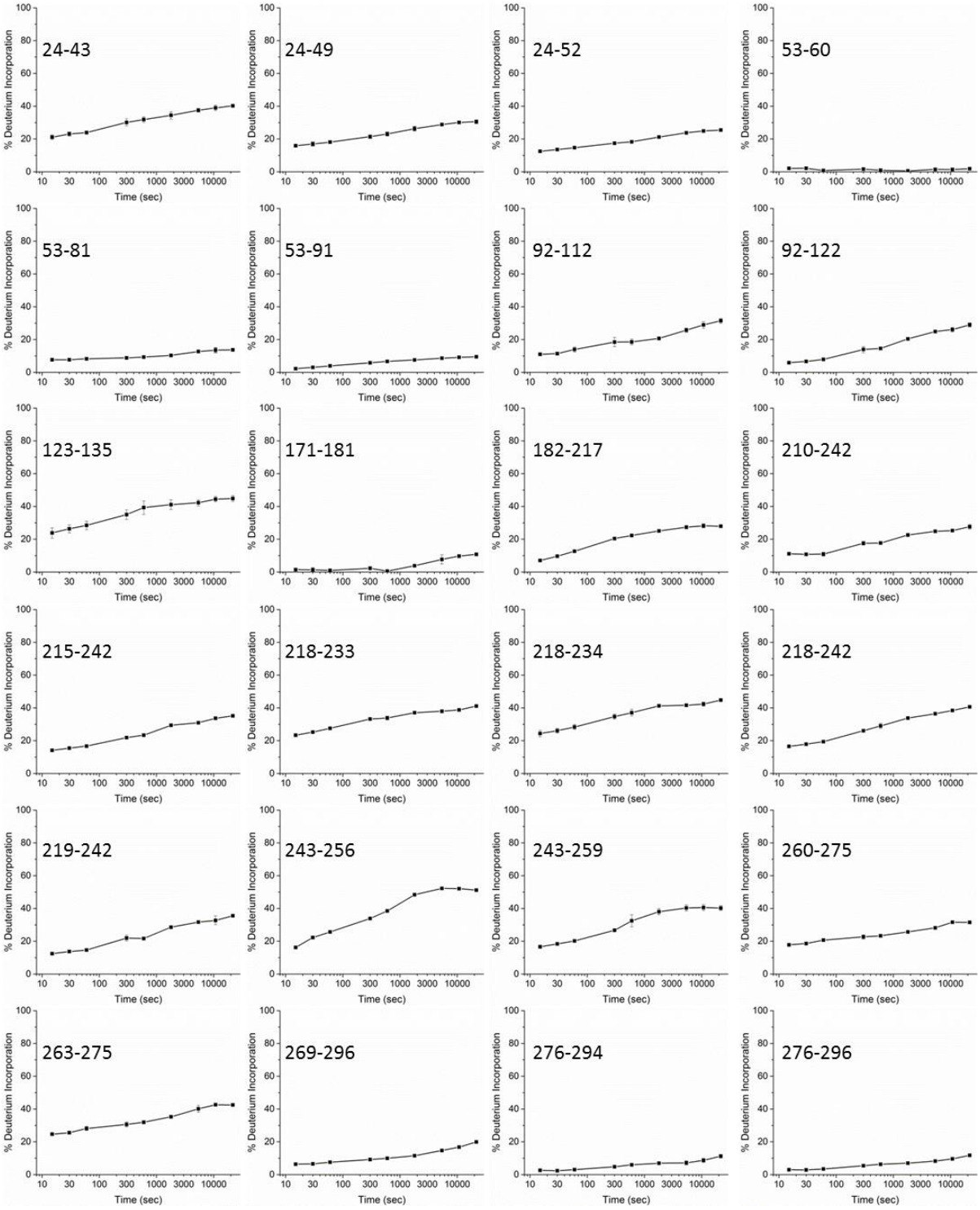

Figure B.1 Percent Deuterium Incorporation Curves for α Peptides

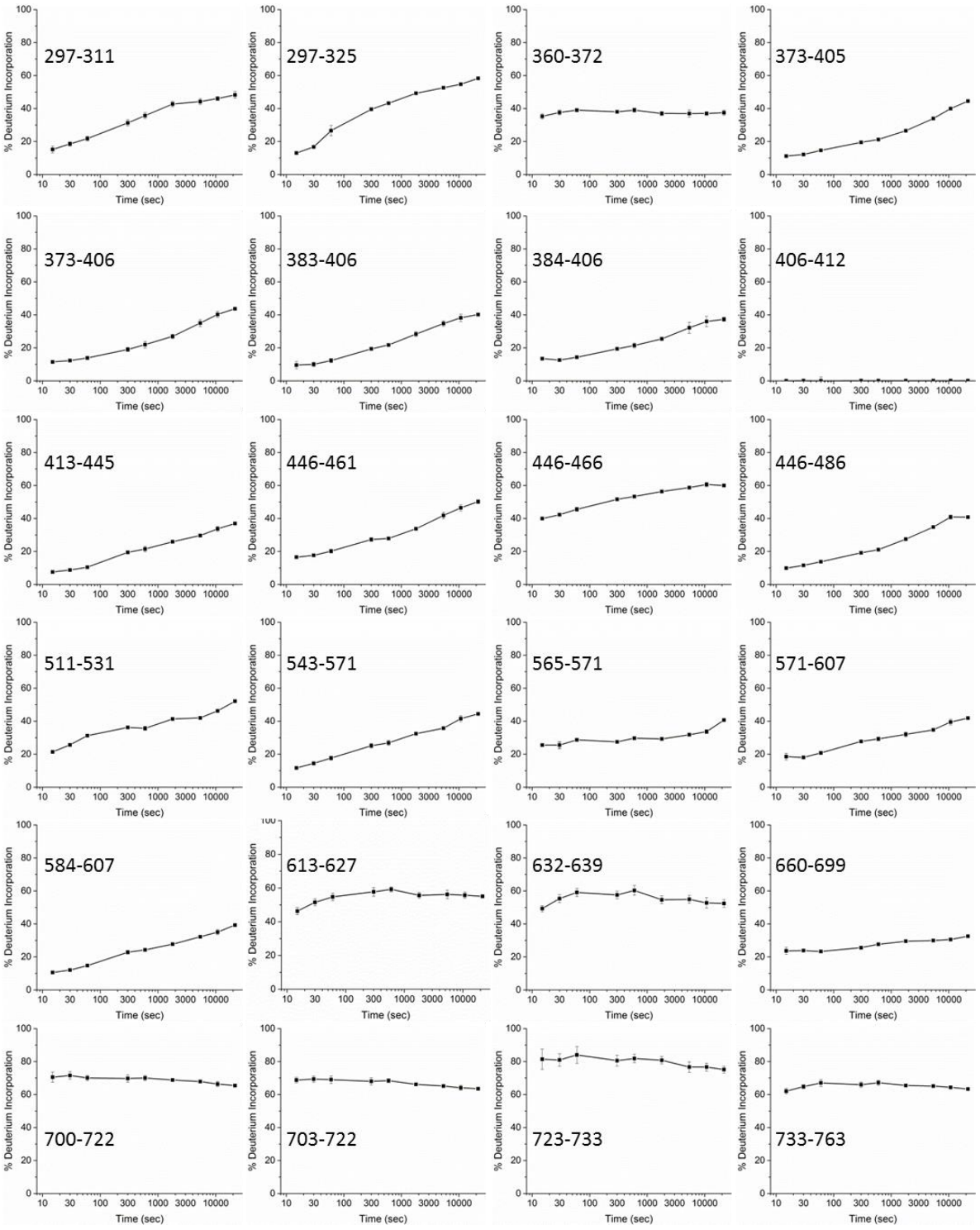

Figure B.1 Percent Deuterium Incorporation Curves for α Peptides

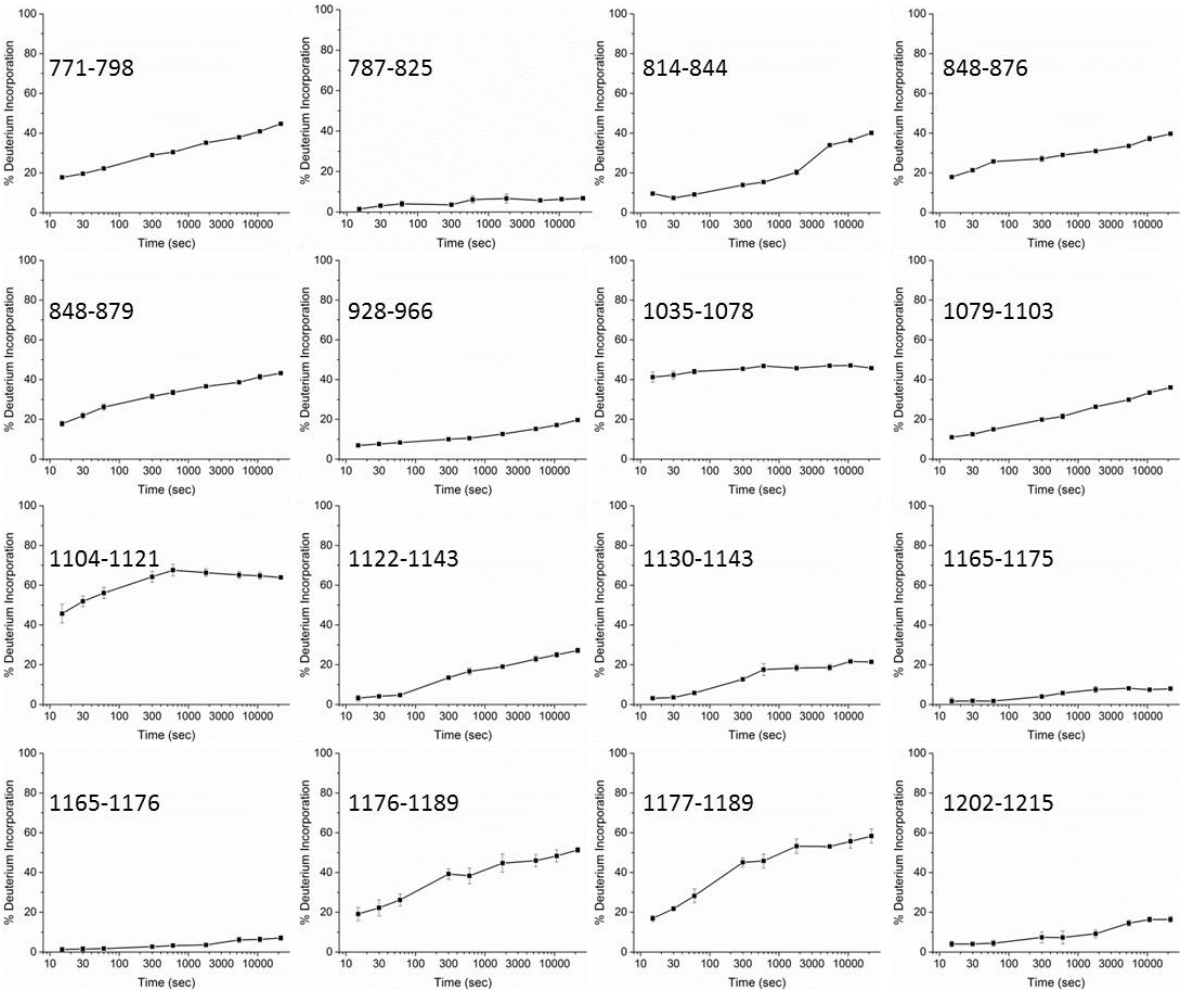

Figure B.1 Percent Deuterium Incorporation Curves for α Peptides

APPENDIX C

Supplementary Data: Chapter 4

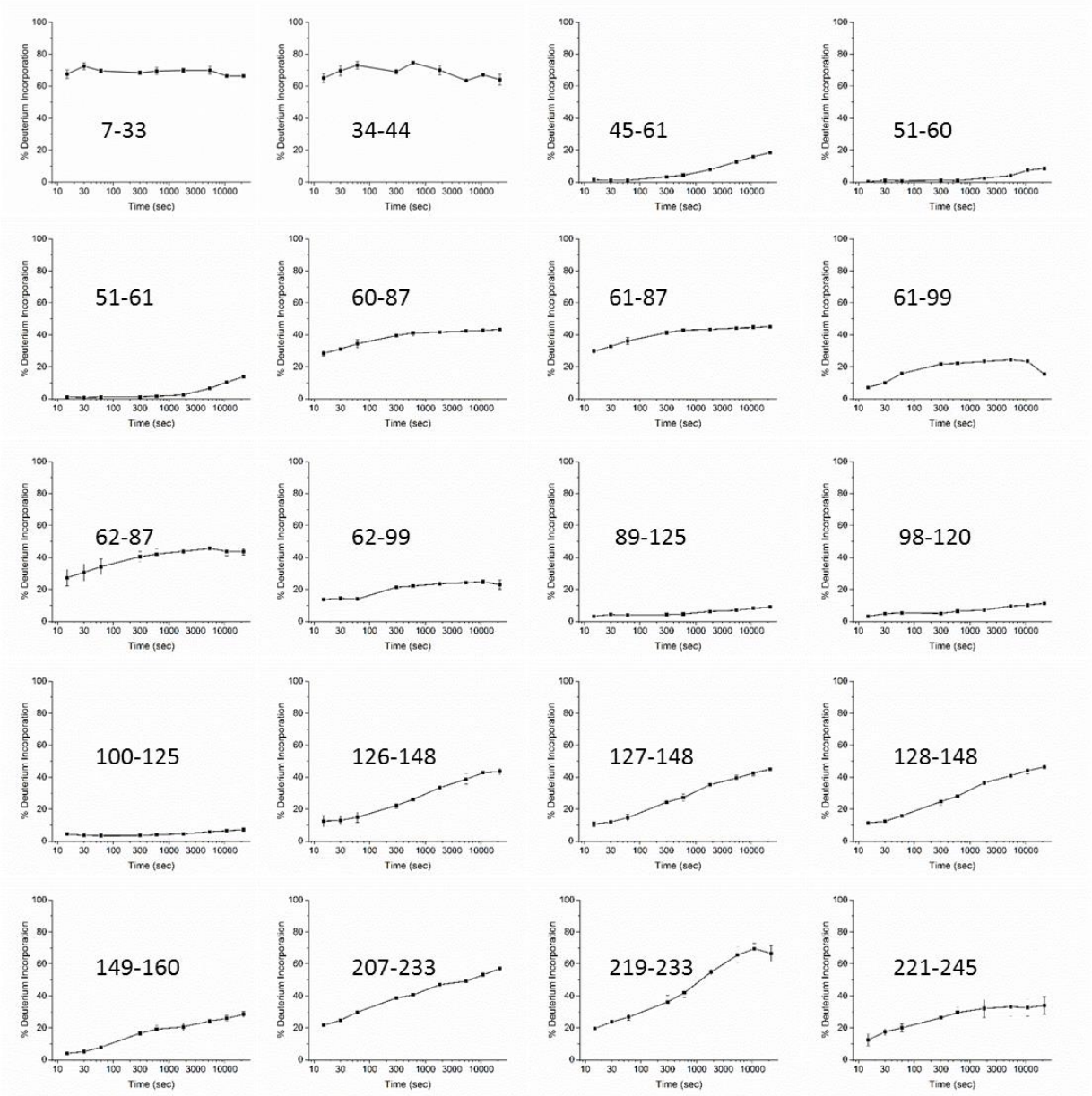

Figure C.1 Percent Deuterium Incorporation Curves for β Peptides

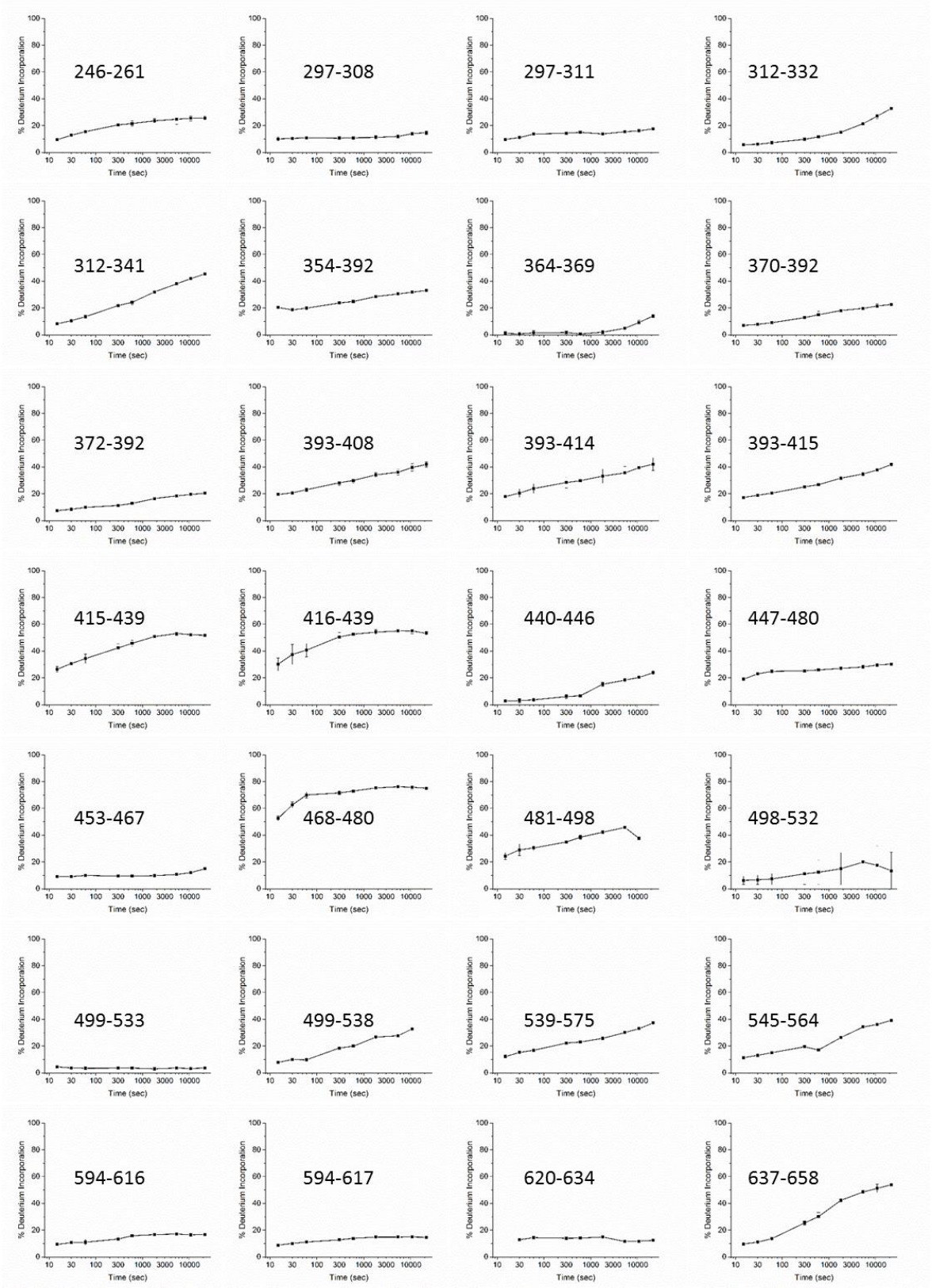

Figure C.1 Percent Deuterium Incorporation Curves for β Peptides

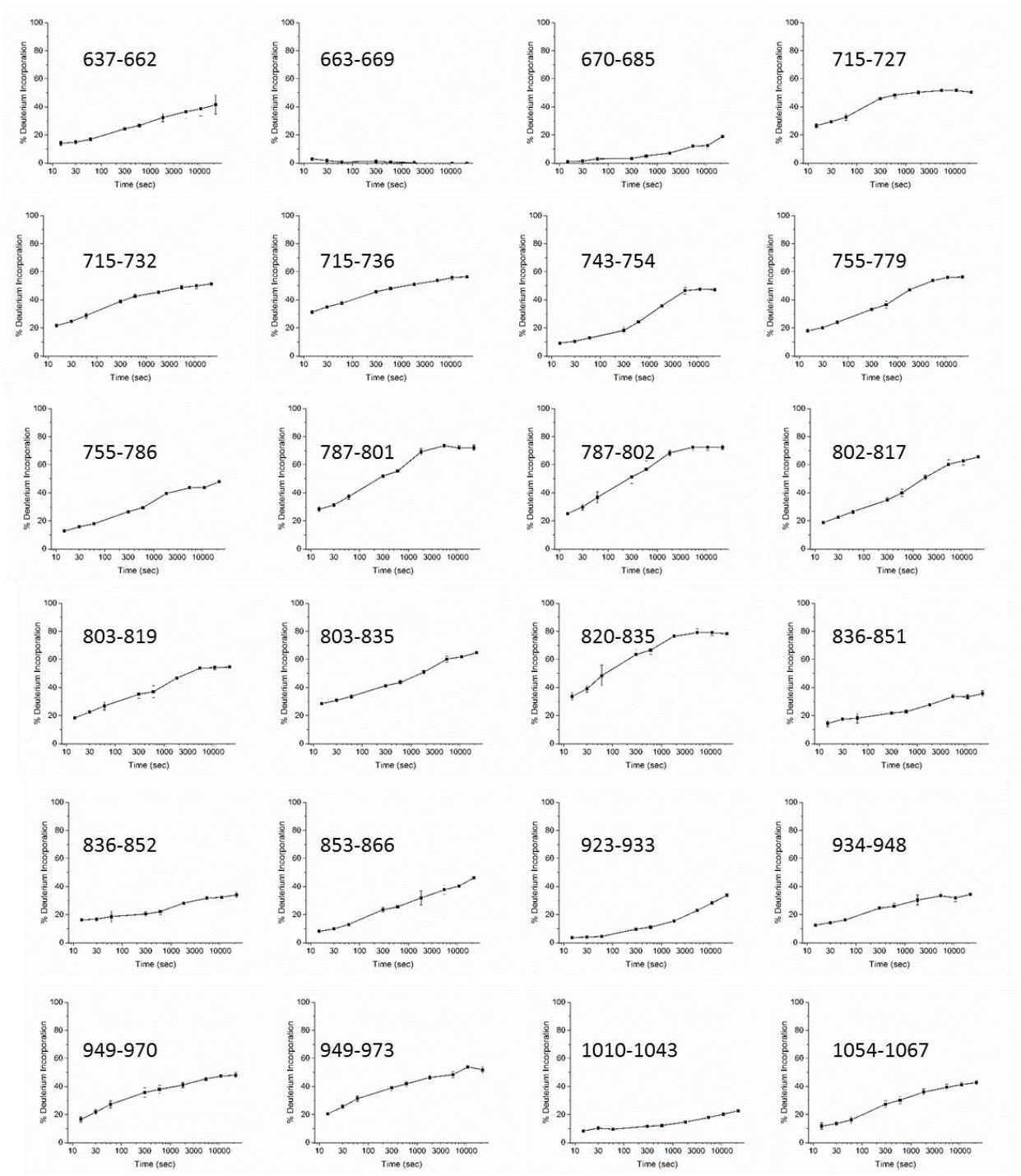

Figure C.1 Percent Deuterium Incorporation Curves for β Peptides

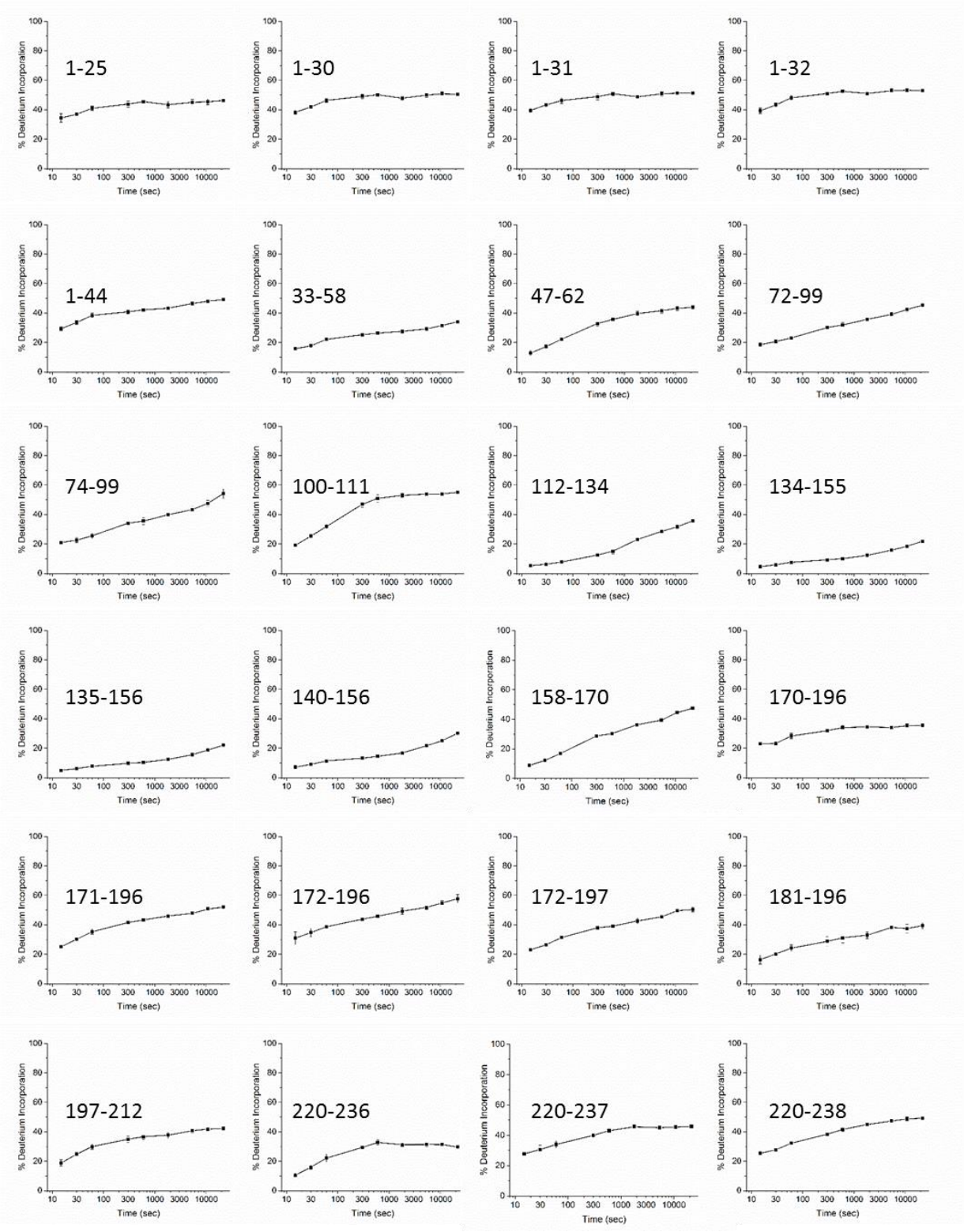

Figure C.2 Percent Deuterium Incorporation Curves for γ Peptides

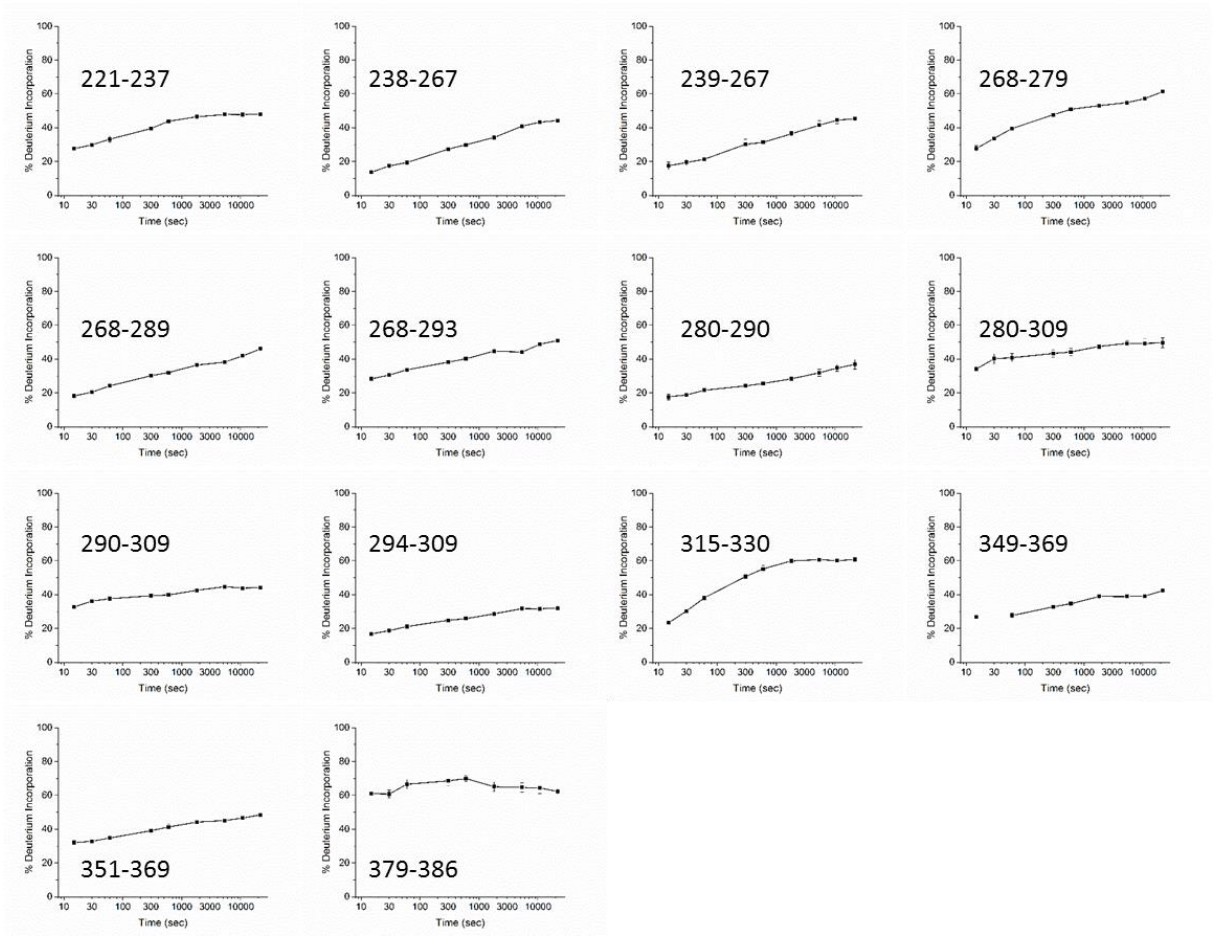

Figure C.2 Percent Deuterium Incorporation Curves for γ Peptides